ORGANISATION
~~SPECTROSCOPIC INVESTIGATIONS OF THE STRUCTURE~~ OF THE PHOTOSYSTEM 2 TWO REACTION CENTRE
AS REVEALED BY SPECTROSCOPY

Thesis submitted for the degree of Doctor of Philosophy
in the University of London

by

William Robert Newell

Department of Pure & Applied Biology,
Imperial College of Science and Technology,
London.

January 1989

SUMMARY

The isolated D1/D2/ Cytochrome b_{559} reaction centre complex of Photosystem 2 from higher plants has been investigated using a number of spectroscopic techniques. Absorption spectroscopy has revealed the presence of Chlorophyll *a*, Pheophytin *a*, and β-carotene in the complex. The absorption properties of the isolated complex are shown to be dependent on temperature and the degree of aggregation of the complex. Circular dichroic spectroscopy has shown the existence of strong dipolar coupling between some of the constituent pigments. Linear dichroic spectroscopy has revealed the occurence of two extreme forms of the particle which exist at different concentrations of detergent, which are interpreted as monomeric and aggregated forms of the reaction centre unit. Comparison of the core complex LD with that of the aggregated reaction centre suggests that PS2 reaction centres exist in an aggregated (possibly dimeric) form in the larger core complex.

Fourier transform infrared spectroscopy and ultraviolet circular dichroic spectroscopy have shown a large proportion of α-helical structure in the Photosystem 2 reaction centre. Exposure of the complex to light causes a change in the protein conformation from α-helical to β-sheet. Computer algorithms predict the presence of membrane-spanning α-helices in all the constituent polypeptides, but it is not possible to predict unequivocally the exact number of helices. Preliminary models of Photosystem 2 are presented that are consistent with the different data, and with data from independent investigations.

ACKNOWLEDGEMENTS

Many people have been involved directly or indirectly in the work presented in this thesis.

I would like to thank all my colleagues in the department of Pure & Applied Biology, Imperial College, London: David Chapman, Shirley Coomber, Kleoniki Gounaris, Wei-zhong He, Neil Hunter, Steve Mayes, Jonathan Marder, Peter Nixon, Alison Telfer, and Steve Zara. In particular, I am grateful to Drs. David Chapman and Niki Gounaris for instruction in the isolation and biochemical characterisation of the Photosystem 2 complexes, to Dr. Alison Telfer for help with fluorescence experiments in my first year of study, to Dr. Steve Zara for help with computing during the last three years, to Drs.Neil Hunter, Shirley Coomber, and Mark Ashby, and Grant Burgess for help in the preparation of the bacterial reaction centres, to John De-Felice, Kenneth Davis, and Jenny Nicolson for expert technical assistance, and to Lyn Barber and Pam Cook. Some of the later CD and FTIR experiments were carried out with the enthusiastic help of Wei-zhong He. I am grateful to Prof. J. Palmer for making available the Aminco UV-VIS spectrophotometer, and to Jill Farmer for assistance in the installation of the cryostat.

I am most grateful to Prof. Dr. Rienk van Grondelle, Department of Biophysics, Physics Laboratory of the Free University, Amsterdam, for a most productive and enjoyable collaboration over the past eighteen months. I would like to thank Drs. Herbert van Amerongen, who taught me the techniques of sample alignment and linear dichroic spectroscopy, and with whose help many of the LD spectra were measured. The models of PS2 presented in Chapter 4 of this thesis were born after long and detailed discussion with Rienk and Herbert.

I am grateful to everyone in the Biophysics department for help in different aspects of the work. I thank Jan-Willem Aalberts, Drs. Barbara Hoebee, Leo van Houte, Maxim Kuil, Stefan Kwa, Frank van Mourik, Dr. Kees Visscher, Ronald Visschers and Ineke Vlaanderen, for assistance in bichemical techniques, the measurement of LD spectra, computer-assisted spectral analysis using the "odp" program (Maxim Kuil), and for general help and advice.

I am particularly grateful to Barbara Hoebee and Willem Oosterbeek for looking after me in illness, and to Truss and Rienk van Grondelle for much hospitality.

CD spectra were measured in the laboratory of Dr Alex Drake, who runs the National CD spectroscopy Service (SERC), Department of Chemistry, Birkbeck College, London. Spectra were measured with the enthusiastic assistance of Drs. Alex Drake and Peter Udvarhelyi.

FTIR spectra were measured in the laboratory of Prof. Denis Chapman, FRS, Department of Biophysics and Protein Structure, School of Medicine, Royal Free Hospital, London, with the continued help of Parvez Haris.

I am most grateful to my parents, Moira and John, for continued support and encouragement during my time in London. I would like to thank my father, Dr. J.A. Newell, Department of Medical Physics, Queen Elizabeth Hospital, Birmingham, for help in the final production of this thesis.

Finally, I am most grateful to my supervisor, Prof. James Barber, for his sustained interest in this work, and for suggesting and making available new techniques and fields of enquiry.

ABBREVIATIONS

APS	ammonium persulphate
(B)Chl	(bacterio)chlorophyll
(B)Pheo	(bacterio)pheophytin
Car	carotene
CD	circular dichroism
Cyt	cytochrome
EDTA	ethylenediaminetetraacetic acid
FTIR	Fourier transform infrared
LD	linear dichroism
LDAO	laurylaminediamineoxide
PAGE	polyacrylamide gel electrophoresis
PS	photosystem
Rb.	*Rhodobacter*
RC	reaction centre
Rps.	*Rhodopseudomonas*
SDS	sodium dodecyl sulphate
SP	special pair
TE	Tris-EDTA (10mM, pH 7.5)
TX-100	Triton X-100
UVCD	ultraviolet circular dichroism

TABLE OF CONTENTS

CHAPTER 1 : INTRODUCTION

1.1. PHOTOSYNTHESIS

1.1.1. Van Niel's hypothesis

1.1.2. The range of Photosynthetic Organisms

1.1.3. Light and Dark Reactions of Photosynthesis

1.1.4. Complexes involved in the "light reactions"

1.1.5. Separability of antenna complex and reaction centre

1.2. REACTION CENTRES

1.2.1. Primary Photochemical Reactions

1.2.2. The classes of reaction centre

1.2.2.1. Purple and filamentous bacteria

1.2.2.2. Green sulphur bacteria

1.2.2.3. Oxygen-evolving photosynthesis

1.2.3. The two universal types of reaction centre

1.2.4. The RC2-type reaction centre

1.2.5. The Reaction Centre of Purple non-sulphur Bacteria

1.2.5.1. Composition

1.2.5.2. Structure

1.2.6. The structure of the *Rps. viridis* reaction centre

1.2.6.1. Pigment organisation

1.2.6.2. Protein organisation

1.2.6.3. The overall structure

1.2.7. The structure of the *Rb. sphaeroides* reaction centre

1.2.8. Orientation of the bacterial reaction centre in the membrane

1.2.9. The reaction centre of Photosystem 2

1.2.9.1. Polypeptides of Photosystem 2

1.2.9.1.1. Proteins of the oxygen-evolving complex

1.2.9.1.2. Proteins of the Photosystem 2 core complex

1.2.9.2. The 47kD protein as the reaction centre of PS2

1.2.9.3. Molecular biology and the isolation of the PS2 RC

1.2.10. The similarity between the reaction centres from purple photosynthetic bacteria and Photosystem 2
1.2.11. Reaction centre triplets and singlet oxygen

1.3. MOLECULAR SPECTROSCOPY IN PHOTOSYNTHESIS RESEARCH

1.3.1. Interaction of light with molecules
1.3.2. Electronic spectra
1.3.3. Electronic spectra of the reaction centre chromophores
1.3.3.1. The porphyrins - chlorophylls, pheophytins, and cytochromes
1.3.3.2. The carotenoid pigments
1.3.4. Sensitivity of electronic transition energies on local environment
1.3.4.1. The effect of the solvent
1.3.4.2. Changes in absorption on polymerisation
1.3.5. Excitons - a coupled chromophore dimer
1.3.5.1. Interaction energy
1.3.5.2. Excited state wavefunctions
1.3.5.3. Energies of the excited states
1.3.5.4. Directions and intensities of the two excited states
1.3.6. Vibrational spectra
1.3.6.1. Infrared spectroscopy of the peptide bond
1.3.6.2. Sensitivity of the band positions to protein conformation
1.3.6.3. Linear dichroism of the peptide bond
1.3.7. Circular dichroism (CD)
1.3.7.1. Monomeric or "intrinsic" CD
1.3.7.2. CD of a dimer of interacting chromophores
1.3.7.3. CD of a polymer
1.3.7.4. Determination of protein secondary structure from ultraviolet circular dichroism (UVCD) spectra
1.3.8. Fluorescence spectroscopy
1.3.9. Rotation of charge - EPR spectroscopy

1.4. SPECTROSCOPIC PROPERTIES OF PURPLE BACTERIAL REACTION CENTRES

1.4.1. Steady-state absorption spectra of purple bacterial reaction centres
1.4.2. Absorption difference spectroscopy of the primary donor

1.4.3. Absorption difference spectroscopy of the primary acceptors
1.4.3.1. Quinone
1.4.3.2. Bacteriopheophytin
1.4.4. Visible circular dichroic spectroscopy
1.4.4.1. Circular dichroism of the unperturbed reaction centre
1.4.4.2. Circular dichroism of the oxidised reaction centre
1.4.4.3. Circular dichroism of the reduced reaction centre
1.4.4.4. Circular dichroism of the reaction centre carotenoid
1.4.4.5. A model of the pigments and their interactions
1.4.4.6. Ultraviolet circular dichroism of the bacterial reaction centre
1.4.5. Linear dichroic spectroscopy
1.4.6. Infrared spectroscopy of the amide bond in bacterial reaction centres
1.4.7. EPR and ENDOR spectroscopy
1.4.7.1. The primary donor
1.4.7.2. Electron acceptors
1.4.7.3. The spin-polarised reaction centre triplet

1.5. SPECTROSCOPIC PROPERTIES OF PHOTOSYSTEM 2

1.5.1. Steady-state absorption spectra of different particles
1.5.1.1. Thylakoid membranes
1.5.1.2. PS2-enriched membranes
1.5.1.3. Purer PS2 samples
1.5.2. Absorption difference spectroscopy of the primary donor
1.5.3. Absorption difference spectroscopy of the primary acceptors
1.5.3.1. Quinone
1.5.3.2. Pheophytin
1.5.3.3. Reaction centre fluorescence and charge recombination
1.5.3.4. Activation energy of fluorescence from Photosystem 2
1.5.3.5. Estimation of the oxidising potential of $P680^{+}$
1.5.4. Circular dichroism of thylakoid particles
1.5.5. Steady-state linear dichroism of thylakoid membranes
1.5.6. Linear dichroism of light-induced absorbance changes
1.5.6.1. Orientation of the primary donor
1.5.6.2. Orientation of the primary acceptor
1.5.7. Infrared spectroscopy of the amide bond in higher plant pigment-protein complexes

1.5.8. EPR signals from Photosystem 2

1.5.8.1. The primary electron acceptors

1.5.8.2. The S2 multiline signal

1.5.8.3. The g=4 component

1.5.8.4. Signal II

1.5.9. Spectroscopic similarities between the reaction centres of purple bacteria and Photosystem 2

CHAPTER 2 : MATERIALS AND METHODS

2.1. PREPARATION OF COMPLEXES FROM HIGHER PLANTS

2.1.1. Thylakoid membranes

2.1.2. PS2-enriched membranes (BBY's)

2.1.3. Oxygen-evolving photosystem 2 core complex

2.1.4. Photosystem 2 reaction centre complex

2.2. PREPARATION OF SAMPLES FROM *RHODOBACTER SPHAEROIDES*

2.2.1. Method of culture of *Rb. sphaeroides*

2.2.2. Preparation of chromatophores

2.2.3. Preparation of reaction centres

2.3. BIOCHEMICAL CHARACTERISATION OF THE SAMPLES

2.3.1. Sodium dodecyl sulphate polyacrylamide gel electrophoresis (SDS-PAGE)

2.3.2. Spectroscopic determination of pigment content

2.3.3. Estimation of Cytochrome b_{559}

2.4. SPECTROSCOPIC APPARATUS AND TECHNIQUES

2.4.1. Absorption spectrophotometry

2.4.2. Absorption difference spectrophotometry

2.4.3. Derivative spectroscopy

2.4.4. Polarised absorption spectrophotometry

2.4.5. Partial alignment of samples

2.4.6. Modifications for measurement at 77K
2.4.7. Fourier transform infrared (FTIR) spectroscopy
2.4.7.1. Measurement of the interferogram
2.4.7.2. Computation of the spectrum
2.4.7.3. Calculation of second derivative spectra
2.4.7.4. Fourier self-deconvolution

CHAPTER 3 : ABSORPTION PROPERTIES OF THE CORE AND REACTION CENTRE OF PHOTOSYSTEM 2

3.1. INTRODUCTION

3.2. RESULTS

3.2.1. Absorption spectra of the constituent pigments
3.2.2. Absorption spectrum of the PS2 oxygen-evolving core complex
3.2.3. Absorption properties of the PS2 reaction centre
3.2.3.1. High detergent, 4°C
3.2.3.2. High detergent, 77K
3.2.3.3. Low detergent, 4°C
3.2.3.4. Low detergent, 77K
3.2.3.5. The Q_y absorption band at 77K
3.2.3.6. Derivative spectra of the aggregated complex
3.2.3.7. Chemically reduced-oxidised spectrum of the reaction centre

3.3. DISCUSSION

3.3.1. Detergent dependence of the absorption spectrum
3.3.2. Carotenoid conformational change on cooling and aggregation
3.3.3. Aggregation and carotenoid excitons
3.3.4. Q_y blue shift in "disaggregated" spectrum
3.3.5. Electron transport activity in relation to aggregation
3.3.6. Conditions for aggregation/disaggregation
3.3.7. Comparison with other published spectra

CHAPTER 4 : LINEAR DICHROISM OF PHOTOSYSTEM 2 PARTICLES

4.1. INTRODUCTION

4.2. RESULTS

4.2.1. LD spectrum of PS2-enriched membranes (BBY's)

4.2.2. LD spectrum of the PS2 core complex

4.2.3. LD spectra of the PS2 reaction centre complex

4.2.3.1. High detergent, 4°C

4.2.3.2. High detergent, 77K

4.2.3.3. Low detergent, 4°C

4.2.3.4. Low detergent, 77K

4.2.3.5. Intermediate spectra

4.3. DISCUSSION

4.3.1. General effects of detergent on linear dichroic properties

4.3.1.1. The shape of the aggregate

4.3.1.2. Exciton formation

4.3.1.3. Conformational changes on aggregation

4.3.2. Detergent dependence of the linear dichroic properties of the isolated PS2 reaction centre.

4.3.1.1. Different shapes and orientation axes of the monomer and aggregates

4.3.1.2. Excitonic interactions between β-carotene pigments in the aggregate

4.3.1.3. Conformational change in β-carotene on aggregation

4.3.3. Comparison of aggregated PS2 RC LD with PS2 core complex LD

4.3.4. Comparison of the reaction centre LD with other published spectra

4.4. IMPLICATIONS AND POSSIBLE MODEL STRUCTURES

4.4.1. The monomeric reaction centre

4.4.2. The dimeric reaction centre

4.4.3. The Photosystem 2 core complex

CHAPTER 5 : CIRCULAR DICHROISM OF THE CORE AND REACTION CENTRE OF PHOTOSYSTEM 2

5.1. INTRODUCTION

5.2. RESULTS

5.2.1. CD spectrum of the PS2 oxygen-evolving core complex

5.2.2. CD spectrum of the PS2 reaction centre complex

5.2.3. CD of the PS2 reaction centre following exposure to light

5.2.4. The effect of aggregation on the PS2 reaction centre CD

5.2.5. CD spectra of monomeric and dimeric chlorophyll *a*

5.2.6. UVCD spectra of the PS2 reaction centre

5.3. DISCUSSION

5.3.1. The PS2 reaction centre CD spectrum

5.3.2. The visible CD spectrum of the PS2 reaction centre following exposure to light

5.3.3. Comparison of the CD spectra of the PS2 reaction centre and chlorophyll *a* dimer

5.3.4. Comparison of the CD spectra of the PS2 reaction centre and core complexes

5.3.5. The effect of aggregation on the reaction centre CD spectrum

5.3.6. Comparison of the PS2 reaction centre CD spectrum with other published spectra

5.3.7.UVCD spectra of the PS2 reaction centre

CHAPTER 6 : FOURIER TRANSFORM INFRARED (FTIR) SPECTROSCOPY OF THE REACTION CENTRES FROM *RHODOBACTER SPHAEROIDES* AND PHOTOSYSTEM 2

6.1 INTRODUCTION

6.2 RESULTS

6.2.1. Absorption spectra

6.2.2. Second derivative spectra

6.2.3. Fourier self-deconvolved spectra

6.2.4. Changes in protein secondary structure following exposure to light and heat

6.3 DISCUSSION

6.3.1. Comparison of the FTIR spectrum of the bacterial reaction centre with previously published spectra

6.3.2. Comparison of the FTIR spectrum of the *Rb. sphaeroides* reaction centre with the X-ray crystallographic data

6.3.3. The quantitative determination of protein secondary structure from FTIR spectra

6.3.4. Comparison of the FTIR spectra of the reaction centres from *Rb. sphaeroides* and Photosystem 2

6.3.5. Photodamage of the PS2 reaction centre

6.4. CONCLUSIONS

CHAPTER 7 : CONCLUSIONS AND GENERAL DISCUSSION

7.1. SUMMARY OF RESULTS

7.2. OTHER EVIDENCE FOR AGGREGATION OF PHOTOSYSTEM 2

7.2.1. Cross-linking and binding experiments

7.2.2. Electron micrographic investigations

7.2.2.1. Morschel *et al*

7.2.2.2. Rogner *et al*

7.2.2.3. Concensus on dimensions from these two studies

7.3. PREDICTIONS OF THE SECONDARY STRUCTURE OF PHOTOSYSTEM 2

7.4. THE DIMENSIONS OF THE MODELS OF THE REACTION CENTRE AND CORE COMPLEXES OF PHOTOSYSTEM 2

7.5. AGGREGATION OF PHOTOSYSTEM 2 *IN VIVO* AND *IN VITRO*

7.6 IMPLICATIONS OF PHOTOSYSTEM 2 AGGREGATION

7.6.1. P680:PS2 stoichiometry

7.6.2. Two pools of Cyt b_{559}, and the stoichiometry of Cyt b_{559} : PS2.

7.6.3. Cytochrome b_{559} and photoinhibition

7.6.4. The composition of the monomeric (one haem) Cyt b_{559}

7.6.5. Photosystem 2 α and β centres

7.7. SUMMARY OF PROPOSED PROPERTIES OF THE MONOMERIC AND DIMERIC PHOTOSYSTEM 2 COMPLEXES

7.8. FUTURE AREAS OF ENQUIRY

CHAPTER 1 - INTRODUCTION

1.1. PHOTOSYNTHESIS

"... the general battle for existence of living organisms is not one for the basic substances - these substances are abundant in the air, in water and on the ground - also not for energy that every body contains abundantly in the form of heat, though unfortunately in a non-available form, but for entropy which becomes available by the transition of energy from the hot sun to the cold earth."
Boltzmann, L. (1886)

For the Earth to sustain life requires the regular input of energy from the Sun. This energy is in the form of the free energy of photons originating from nuclear fusions occurring in the Sun. The process by which the energy of photons is converted to that of chemical bonds is called photosynthesis. The primary reaction of photosynthesis is the production of a charge-separated state following absorption of a photon, and is mediated by the photosynthetic reaction centres. These membrane-bound pigment-protein complexes become excited by the absorption of a photon, accept electrons at a positive redox potential, and release an electron at a potential which is of the order of 1 volt more negative. In this way, light energy is directly converted to electrochemical potential. It is this potential energy that is used to maintain the high degree of order, reproducible structure, and flexible response to the environment that distinguishes life from other processes.

1.1.1. VAN NIEL'S HYPOTHESIS

Van Niel (1941) examined the nett reaction of photosynthesis for green and purple sulphur bacteria, purple non-sulphur bacteria, and oxygen-evolving organisms. He deduced that oxidised and reduced intermediates were formed during the process. Photosynthesis in all organisms could be summarised as:

$2H_2A + CO_2$ ------> $(CH_2O) + H_2O + 2A$.

van Niel proposed that photosynthesis is a process in which carbon dioxide is reduced to carbohydrate at the expense of an oxidisable substrate, H_2A.

1.1.2. THE RANGE OF PHOTOSYNTHETIC ORGANISMS

Photosynthesis occurs in the eukaryotic green plants and algae, and in the prokaryotic cyanobacteria, prochlorophyta, and photosynthetic bacteria. Green plants and algae, the prochlorophyta, and the cyanobacteria evolve oxygen as a photosynthetic product. The photosynthetic bacteria (purple, filamentous, and green sulphur) do not. Below is a summary of the photosynthetic organisms.

photosynthetic prokaryotes
Archaebacteria : Halobacteria
Eubacteria :
cyanobacteria
purple bacteria (Rhodospirillales)
- purple sulphur bacteria (Chromatiaceae)
- purple non-sulphur bacteria (Rhodospirillaceae)
filamentous bacteria (Chloroflexaceae)
green sulphur bacteria (Chlorobiaceae)
gram positive bacteria (Heliobacterium)
Prochlorophyta --------> **photosynthetic eukaryotes**

The halobacteria do not use chlorophyll pigments to convert light into chemical free energy, but the pigment retinal. This pigment is contained in the protein bacteriorhodopsin (related to the visual pigment-protein complex, rhodopsin), which mediates proton pumping across the membrane when illuminated. No reduced intermediate is formed during this reaction. This thesis concerns the chlorophyll-containing organisms, whose photosynthesis involves a light-driven redox reaction.
Van Niel (1941) summarised the nett reaction of photosynthesis for the different classes of organism, and could make the following simple classification, on the basis of the oxidisable substrate, H_2A:
green and purple sulphur and filamentous bacteria:

$$2H_2S + CO_2 \text{ ----> } CH_2O + H_2S + 2S$$

purple non-sulphur bacteria:

$2COOH(CH_2)_2COOH + CO_2 \text{ ----> } CH_2O + H_2O + 2COOH(CH)_2COOH$

oxygen-evolving organisms:

$2H_2O + CO_2 \text{ ----> } CH_2O + H_2O + O_2$

The **purple sulphur and green bacteria** are classified together from their common oxidisable substrate, sulphide, which is normally hydrogen sulphide. They differ in the redox potential of the first stable reduced intermediate; that of green bacteria has a more negative redox potential (by 0.4 V) than that of the purple sulphur bacteria. The **purple non-sulphur bacteria** are more diverse, and can use a variety of oxidisable substrates such as hydrogen sulphide, hydrogen, acetate and pyruvate. The redox potential of the first stable reduced product is the same as for purple sulphur bacteria. **Oxygen-evolving organisms** use water as their electron donor. The reducing potential generated in these organisms is similar to that generated in bacteria. However, the redox span between this acceptor and the ultimate electron donor (water) is much greater. This requires two photochemically active systems (Photosystems 1 and 2) with different redox properties. Photosystem 2 is the major subject of this thesis.

1.1.3. LIGHT AND DARK REACTIONS OF PHOTOSYNTHESIS

The hyperbolic dependences of oxygenic photosynthesis on light intensity, carbon dioxide, and temperature were interpreted by Blackman (1905) as due to a temperature-independent photochemical reaction together with a light-independent or "dark" reaction which is dependent on temperature and carbon dioxide concentration. Emerson & Arnold (1932a, 1932b) studied photosynthesis under flashing illumination and showed that the amount of CO_2 fixed was dependent on not only the intensity of the flash, but also the time interval between flashes, a dark period of 100 msec giving optimal rates. This was interpreted as due to production by the flash of an intermediate that had to be consumed before the photochemical reaction could operate again. In 1940, Hill and Scarisbrook showed that light-dependent oxygen evolution could be restored in isolated chloroplasts by the addition of an artificial reducible substrate (electron acceptor or "Hill oxidant"), e.g. potassium ferricyanide. They thus demonstrated the separability of a light-driven redox reaction mediating the transfer of electrons from water to an electron acceptor, from the light-independent reduction of carbon dioxide.

Van Niel's equation could now be divided into two parts:

(1) $2H_2A$ + substrate (oxidised) -----(light)---> substrate (reduced) + 2A.

(2) substrate (reduced) + CO_2 ---(dark)----> substrate (oxidised) + CH_2O.

The reduction of carbon dioxide is accomplished through a series of enzyme-catalysed reactions, which are collectively termed the Calvin Cycle (review, Robinson & Walker, 1981). Since these reactions do not require the direct intervention of photons but only the final products of the light reactions, ATP and NADPH, they are referred to as the "dark reactions" of photosynthesis.

This thesis concerns only the first, light-driven, part of photosynthesis, which generates electrons with a more negative potential in reduced substrates, using electrons with a more positive potential in an electron donor, and the energy of light.

1.1.4. COMPLEXES INVOLVED IN THE "LIGHT REACTIONS"

The following complexes are always found in photosynthetic organisms:

(1) photochemically active complexes, called "reaction centres",

(2) other pigment-protein complexes ("antenna complexes") that serve to increase the optical cross-section for photon capture,

(3) photochemically inactive oxidoreductases, usually cytochrome complexes, which mediate electron transfer from low potential electron carriers to higher potential electron carriers, and couple this energy-releasing process to energy-requiring reactions (e.g. proton pumping), and

(4) some form of ATP synthase enzyme to generate ATP from a proton gradient, or vice versa.

Most of the complexes comprise electron tranfer cofactors and hydrophobic proteins, which are constarined in a lipid bilayer. The arrangement of these components in purple and green bacteria, and in oxygen-evolving organisms is shown in Fig.1.1.

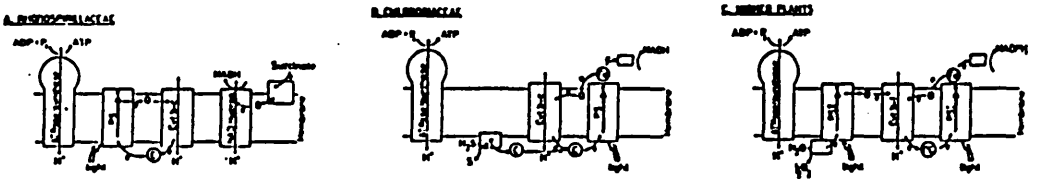


Fig. 1.1. Schemes of electron transport in the purple and green bacteria (Rhodospirillaceae and Chlorobiaceae) and oxygenic organisms (from Packham & Barber, 1987). Q - quinone; PS - photosystem; e - electron; C - soluble cytochrome c; PC - plastocyanin; Fd - ferredoxin.

1.1.5. SEPARABILITY OF ANTENNA COMPLEX AND REACTION CENTRE

That only a fraction of the total chlorophyll directly participates in the primary photochemical reaction was first indicated from the experiments of Emerson & Arnold (1932a, 1932b). Duysens (1951) found that light energy brings about the primary reaction in bacteria only after transfer through a large number of "antenna" pigments. Similar experiments on algae led to the same conclusion, that excitation energy is transferred between a large number of pigments before initiating the photochemical reaction, at a "reaction centre".

Several experiments indicated that this complex was a distinct particle which could in principle be isolated. Clayton (1963) observed that photochemical activity could be amplified (with respect to the total chlorophyll concentration) in the carotenoidless strain R-26 of *Rps. sphaeroides* by damaging (by pheophytinising) the "antenna" chlorophyll *in vivo* or by illuminating isolated chromatophres in the presence of detergent (Triton X-100). A similar result was acheived (Loach *et al*, 1963) by treating chromatophores of several wild-type species of purple bacteria with the oxidant K_2IrCl_6. 95% of the antenna pigment could be destroyed without affecting the bleaching of a pigment at 870nm (denoted P870) associated with photochemistry (estimated from the enhancement of the bleach relative to the total absorbance). Both of these results suggested that the antenna could be selectively destroyed, because the reaction centre pigments occur in a special environment. Moreover, mutants of *Rps. sphaeroides* which lack the 870 signal were found to be photosynthetically inactive (Sistrom & Clayton, 1964), providing further evidence that the photooxidation of P870 is an essential reaction in the photosynthetic process.

To summarise, the primary reactions of photosynthesis comprise:

(1) the conversion of the electromagnetic field energy of a photon to the excited state energy of a pigment molecule,

(2) transfer of this molecular excited state energy among a large number of peripheral "antenna" pigment molecules (see van Grondelle, 1985), and

(3) final transfer of the excitation to the reaction centre, which

(4) converts the excited state energy to redox potential energy in the form of a reduced intermediate.

Van Niel (1941) predicted that photosynthesis gives rise to reduced and oxidised components. Emerson & Arnold (1932a, 1932b) showed the equivalence of the light-dependent reactions of photosynthesis with the generation of this redox potential. This photochemical activity is located completely within the photosynthetic reaction centres.

1.2. REACTION CENTRES

1.2.1. PRIMARY PHOTOCHEMICAL REACTIONS

The primary photochemical reaction is a light-induced separation of charges that occurs in the reaction centre. The resulting oxidised component is known as the primary electron donor. The first reduced molecule is the primary electron acceptor. No charge transfer reactions occur between any of the antenna pigments. Thus a reaction centre is defined as that minimal unit which is capable of mediating a light-driven separation of charges.

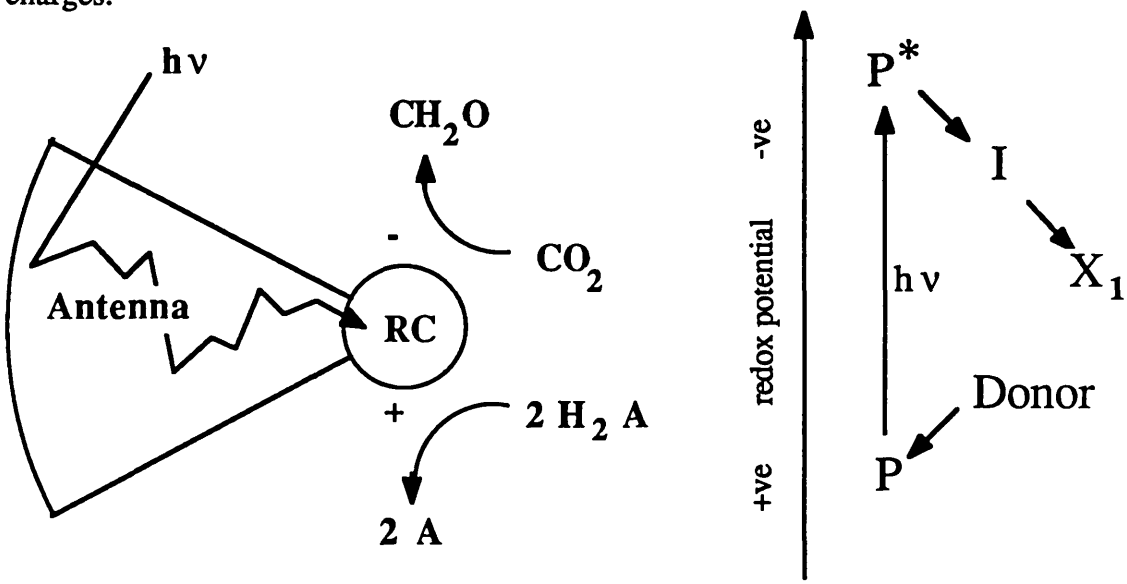


Fig. 1.2. Transfer of excitation through antenna pigments to the reaction centre, where charge separation gives rise to an oxidised (+) and a reduced (-) intermediate. P* - excited state of the primary electron donor, P. For other nomenclature, see Table 1.1.

Subsequent charge separations in the reaction centre are not possible until the oxidised primary donor and reduced primary acceptor have returned to their uncharged states. This requires an electron from outside the reaction centre to reduce the primary donor, and other electron acceptors to oxidise the primary electron acceptor.

Depending on the origin of the electron that reduces the primary electron donor, the reaction centre can perform either cyclic or non-cyclic electron transport. During non-cyclic electron transport, the oxidised primary donor is reduced by an electron donor from outside the reaction centre, e.g. water, sulphide, acetate, pyruvate etc. Cyclic electron transport occurs when the reduced intermediate formed as a result of the primary charge separation is passed back through a series of electron carriers to reduce the oxidised primary donor. The electron cycles round the reaction centre. Its exergonic transfer through the components between the primary electron acceptor and the primary donor is usually coupled to proton pumping *via* cytochromes.

1.2.2. THE CLASSES OF REACTION CENTRE

Different classes of reaction centre can be distinguished, differing in their primary and secondary electron donors and acceptors. Photosynthetic bacteria contain only one sort of reaction centre, while oxygenic organsims contain two. Table 1.1 summarises the characteristics of the reaction centres from different organisms.

1.2.2.1. Purple and filamentous bacteria (Rhodospirillales and Chloroflexaceae)

All purple and filamentous bacterial reaction centres generate a mildly reducing potential in their first stable acceptor (X_1), with an operating midpoint potential of between -0.0 and -0.2 V, and a relatively oxidising potential (0.45 - 0.55 V) in their oxidised primary donor. The reaction centres can drive both cyclic and non-cyclic electron transport. Cyclic electron transport generates ATP (photophosphorylation). Non-cyclic electron transport uses low potential donors, such as H_2S or succinate, to reduce a variety of acceptors, including NAD^+ and CO_2. The low potentials required for reducing NAD^+ ($E_{m,7}$ = -0.32V) are not generated directly but by an additional process requiring ATP ("reverse electron flow", reviewed by Knaff & Kampf, 1987). Purple sulphur bacteria (Chromatiaceae) are obligate anaerobes, using sulphide as their electron donor. Purple non-sulphur bacteria (Rhodospirillaceae) are more diverse, and can perform anaerobic photosynthesis and aerobic respiration. The range of electron donors is large and includes hydrogen sulphide, hydrogen, acetate and pyruvate.

1.2.2.2. Green sulphur bacteria (Chlorobiaceae)

Green bacteria differ considerably from the purple and filamentous bacteria in their photochemistry and their intracellular structure. The photochemistry generates a strong reductant ($E_{m,7}$ = -0.55 V) that can reduce NAD^+ directly, using H_2S as an electron donor. ATP is therefore not required directly for this process. Reduction of NAD^+ is via a water-soluble ferredoxin, as in the higher plant Photosystem I. The potential generated in the primary donor is not as oxidising as in purple bacteria (0.25-0.35 V).

1.2.2.3. Oxygen-evolving Photosynthesis

Photosynthesis that results in the evolution of oxygen is carried out by the cyanobacteria and all eukaryotic photosynthetic organisms. It is a considerably more complex process than in bacteria, requiring the cooperation of two photosystems with different redox properties. They act in series (Hill & Bendall, 1960) to raise the energy of an electron from that in water ($E_{m,7}$ = +0.82 V) to that in NADPH ($E_{m,7}$ = -0.32V).

Photosystem 2 generates a sufficiently oxidising potential (+1.12 V) when excited by a 680 nm photon (1.82 V) to remove electrons from water (+0.82 V), and a reducing potential (-0.61 V) sufficient to reduce a quinone (Q_a = -0.13 V). Photosystem 1 when excited by a 700 nm photon (1.77 eV) generates a strong reducing potential (-0.9 V) to reduce NADP ($E_{m,7}$ = -0.32V) via ferredoxin ($E_{m,7}$ = -0.53V), and becomes reduced by the copper-containing protein, plastocyanin (+0.37V).

The electron transport chain requires intermediate complexes to mediate electron flow between the two photosystems. The only membrane-bound multipeptide complex catalysing electron flow between Photosystems 2 and 1 is the Cyt b_6-f complex, which functions as a plastoquinol / plastocyanin oxidoreductase. Oxidation of the lipid-soluble plastoquinol (Q_bH_2, $E_{m,7}$ = 0.0 V) occurs at the inner surface of the thylakoid membrane. The electron passes through a series of carriers to the plastocyanin ($E_{m,7}$ = +0.37 V). The free energy available through electron transfer (0.37 eV) may be coupled to vectorial proton pumping to the inner face of the thylakoid membrane via a 'Q' cycle (see Rich & Moss, 1987; Cramer *et al*, 1987). This mechanism involves the one-electron reduction of cytochromes b and f by plastoquinol, coupled to the vectorial release of the two protons on the luminal face of the thylakoid membrane.

Table 1.1 - Reaction centre primary electron donors and acceptors
Nomenclature: P - primary donor (the number after the P is the position of the long wavelength bleach of the primary donor); I is an intermediary acceptor which becomes rapidly oxidised by X_1, the primary electron acceptor (Q_a in purple bacteria, PS2), which is itself oxised by X_2, the secondary electron acceptor (Q_b in purple bacteria, PS2). Other abbreviations: (B)Chl - (bacterio) chlorophyll; (B)Pheo - (bacterio) pheophytin; SP - special pair; MQ - menaquinone; PQ - plastoquinone; UQ - ubiquinone; Fe-S - iron-sulphur centre. The information in this table is from several sources: Clayton, 1980; Barber, 1987a; Pierson & Olson, 1987.

reaction centre	**P/I/X**	**molecular species**	**$E_{m,7.0}$ (V)**
PURPLE BACTERIA			
Rb. sphaeroides	P (P870)	SP (BChl*a*)	+0.45
	I	BPheo	-0.55
	X_1	UQ_a.Fe	-0.02
	X_2	UQ_b	+0.04
Rps. viridis	P (P960)	SP (BChl*b*)	+0.53
	I	BPheo	-0.55
	X_1	MQ_a.Fe	-0.10
	X_2	UQ_b	+0.04
FILAMENTOUS BACTERIA			
Chl. aurantiacus	P (P860)	SP (BChl*a*)	+0.36
	I	BPheo*c*	-0.54
	X_1	MQ_a	-0.08
	X_2	MQ_b	-0.05
GREEN BACTERIA			
Chlorobium limicola	P (P840)	BChl dimer ?	+0.25
	I	BPheo*c*	?
	X_1	Fe-S	-0.54
OXYGENIC ORGANISMS			
Photosystem 2	P (P680)	SP? (Chl*a*)	+1.12
	I	Pheo*a*	-0.61
	X_1	PQ_a.Fe	-0.05
	X_2	PQ_b	+0.035
Photosystem 1	P (P700)	SP?	+0.45
	I_0	Chl monomer	-0.90
	I_1	phylloquinone	?
	X_1 ($Fe\text{-}S_X$)	4Fe-4S	-0.73
	X_2 ($Fe\text{-}S_B$)	4Fe-4S	-0.59
	X_3 ($Fe\text{-}S_A$)	4Fe-4S	-0.53

1.2.3. TWO UNIVERSAL TYPES OF REACTION CENTRE

From the summary above, we can distinguish two types of reaction centre (Pierson & Olson, 1987): RC1-type, in which the initial electron acceptor (I) is a (B)Chl molecule and the first stable acceptor (X_1) is an Fe-S centre (a strong reductant), and RC2-type, in which I is a (B)Pheo molecule and X_1 is a quinone (a mild reductant). RC1-type reaction centres occur in the green sulphur bacteria, and in Photosystem 1 of oxygenic organisms. RC2-type reaction centres occur in the filamentous bacteria, purple bacteria, and in the reaction centre of Photosystem 2 of oxygenic organisms. The BChl pigment employed in bacterial RC-2 type reaction centres is either BChl*a* or *b*. Filamentous, green sulphur, and purple bacteria use BChl*a*; some purple bacteria use BChl*b*. Photosystem 2 employs Chl*a*.

No Fe-S centres have been found in RC2-type reaction centres, but there is evidence for a low-potential quinone in PS1 (RC1-type) (Rutherford & Heathcote, 1985). Van Gorkom (1987) suggests on the basis of this observation that the quinone-reducing reaction centres (RC2) are primordial, from which the RC1-type reaction centre evolved.

1.2.4. THE RC2-TYPE REACTION CENTRE

There is much current interest in the RC2-type reaction centre, following the recent crystallisation and X-ray analysis of reaction centres from the purple bacteria *Rps. viridis* (Deisenhofer *et al*, 1984, 1985) and *Rb. sphaeroides* (Allen *et al*, 1987a, 1987b). The distinction between RC1 and RC2 is made from functional differences in their redox properties and the nature of the cofactors involved in the primary charge separation. Only recently, with more extensive amino acid sequencing of the protein subunits have structural similarities in the proteins between different RC2-type reaction centres been observed. Thus it now seems possible that the RC2-type reaction centre is a well-defined pigment-protein in structure and function in a wide range of phylogenetic groups. We return to these important discoveries when discussing Photosystem 2 (section 1.2.9.).

1.2.5. THE REACTION CENTRE OF PURPLE NON-SULPHUR BACTERIA

1.2.5.1. Composition

All reaction centres isolated so far from different species of photosynthetic purple bacteria have a similar composition (review, Gingras, 1978; Feher & Okamura, 1978). They consist of three protein subunits as shown by SDS-PAGE, which are called H (heavy), M (medium), and L (light), and occur in a 1:1:1 stoichiometry. Reaction centres

from some species (e.g. *Rps. viridis*) contain an additional strongly-bound c-type cytochrome containing four haem groups. The L, M and H subunits migrate with apparent molecular masses of 21,000, 24,000, and 28,000, respectively. Sequencing of the three genes encoding L,M,H reveal actual molecular masses of 31, 34, and 28 kD, respectively. They contain 281, 307, and 207 amino acids, respectively. The amino acid composition of the L/M/H subunit shows that 68% of the residues are hydrophobic. The L, M, and H subunits individually contain 71%, 70% and 62% hydrophobic residues, respectively. Thus L and M seem to have a closer association with the membrane. The difference in hydrophobicity between H and the other subunits explains the misleading molecular masses estimated from their electrophoretic mobilities (Feher & Okamura, 1978). The L/M/H complex contains four BChl (*a* or *b*) molecules, two BPheo (*a* or *b*), one non-haem iron atom, and probably two quinones (1 menaquinone, 1 ubiquinone) (see for example Jolchine & Reiss-Husson, 1974). The H subunit can be removed leaving an intact L/M complex that has an identical absorption spectrum to the L/M/H complex. Thus all the pigments are associated with the L/M dimer and do not seem to be disrupted by removal of the H subunit.

1.2.5.2. Structure

The many spectroscopic experiments performed on these preparations have yielded much information concerning their structure. These data will be discussed below. In this section, I discuss the model derived from X-ray crystallography. The Rhodospirillaceae is the only class of photosynthetic organism from which reaction centre crystals, of sufficient quality and size to obtain X-ray diffraction patterns, have been obtained. The detailed molecular structure computed from such patterns has been published for two organisms to date: *Rps. viridis* (Deisenhofer *et al,* 1984, 1985) and *Rb. sphaeroides* (Allen *et al*, 1987a, 1987b).

1.2.6. THE STRUCTURE OF THE *RPS. VIRIDIS* REACTION CENTRE (Deisenhofer *et al*, 1984, 1985)

Johann Deisenhofer, Hartmut Michel, and Robert Huber have recently been awarded the 1988 Nobel Prize for Chemistry for solving the structure of this membrane-bound reaction centre complex. The structure of the reaction centres from *Rps. viridis* and *Rb. sphaeroides* are presented in Figs. 1.3 and 1.4.

1.2.6.1. Pigment Organisation

The constituent pigments (4 BChl's, 2BPheo's, and two quinones) are arranged along an approximate two-fold rotationally symmetric axis (Fig.1.5). The axis runs along the

line connecting two closely adjacent BChl molecules (the "special pair" arrangement of the primary electron donor predicted from spectroscopic measurements), and the ferrous non-haem iron atom. This atom lies between the two quinones on the cytoplasmic side of the membrane. From the crystal structure, it appears that there are two equivalent paths for electron transport from the special pair to either of the two pheophytins. From spectroscopic data, it is clear that only one of the paths is actually employed (L branch). A carotenoid molecule lies close to one of the monomeric BChl molecules (on the M arm, which is inoperative in electron transport). This is proposed to be the quencher of the primary donor triplet. The four haem groups of the fixed cytochrome form a linear chain ending in the vicinity of the primary donor.

1.2.6.2. Protein Organisation

The two polypeptides L and M form the central part of the reaction centre. This region is composed of highly hydrophobic residues in stretches of 19 or more amino acids, which are therefore predicted to span the membrane. It has a cylindrical form, 50Å in length with an elliptical cross-section (30Å x 70Å). Both L and M have five roughly parallel α-helices and are related by the same rotational symmetry axis as the pigments (75% of the C_α carbon atoms coincide after rotation of the complex through 180°; see review of Parson, 1987). Despite the high degree of sequence homology between L and M, there are slight structural differences between the two polypeptides: the L and M subunits show differences in folding at the N- and C-termini, and in the connections of the first and second, and fourth and fifth main helices. The M subunit is longer in each case. All end regions and the segments connecting the main helices form flat parallel surfaces.
The H subunit occupies a globular domain on one of the flat faces of the complex. It has one N-terminal α-helix which lies approximately parallel to the L and M main helices. The cytochrome is bound to the opposite face of the L/M complex, close to the special pair. The distribution of charged residues is asymmetric either side of the central hydrophobic region. One side of the complex has four positive charges from M and two from L; the other side has four negative charges from M and four from L. Thus there is a net dipole moment along the symmetry axis of the reaction centre.

1.2.6.3. The Overall Structure

The pigments lie in the hydrophobic pocket between the L and M subunits. L and M provide histidine ligands for binding the central magnesium atom of the two bacteriochlorophyll molecules comprising the special pair, and the two monomeric BChls. The primary quinone (Q_a) is bound by a tryptophan on M, which is also very close to the bacteriopheophytin on the M branch. The ferrous non-haem iron atom is bound by four histidine residues, two on the L subunit and two on the M subunit, and

by an glutamic acid residue on M. The unidirectionality of charge transfer along the L branch exclusively is perhaps controlled electrostatically by the asymmtric distribution of polar amino acids on the two branches. This has been explored in a recent theoretical paper (Michel-Beyerle *et al*, 1988).

1.2.7. THE STRUCTURE OF THE *RB. SPHAEROIDES* REACTION CENTRE (Allen *et al*, 1987a, 1987b)

The reaction centre of *Rb. sphaeroides* has a very similar composition to that from *Rps. viridis* (see Gingras, 1978). The central part is composed of the three proteins L, M, and H. It differs from *Rps. viridis* in having a cytochrome which is not firmly attached to the membrane, and is therefore not retained during isolation of the reaction centre. The M subunit from *Rps. viridis* has 18 more residues in its carboxy end region, which may be involved in the tighter binding of the cytochrome.

The structures of the two reaction centres are essentially the same in the following respects: the L and M proteins have five main helices each; the H subunit has one transmembrane helix (Fig.1.4); the relative positions of the prosthetic groups (special pair, accessory chlorophylls, pheophytins, Q_a, and non-haem iron) are the same (Fig.1.5). The overall homology between three different species, *Rb. sphaeroides*, *Rb. capsulata*, and *Rps. viridis*, is 53% for L, 46% for M, and 31% for H (Feher & Okamura, 1978). The most strongly conserved amino acids are those that ligate the cofactors. Thus this structure may be universal in the purple photosynthetic bacteria. Fine details of the spatial arrangement of pigments and polar amino acids may affect the precise path of electron transfer in different species.

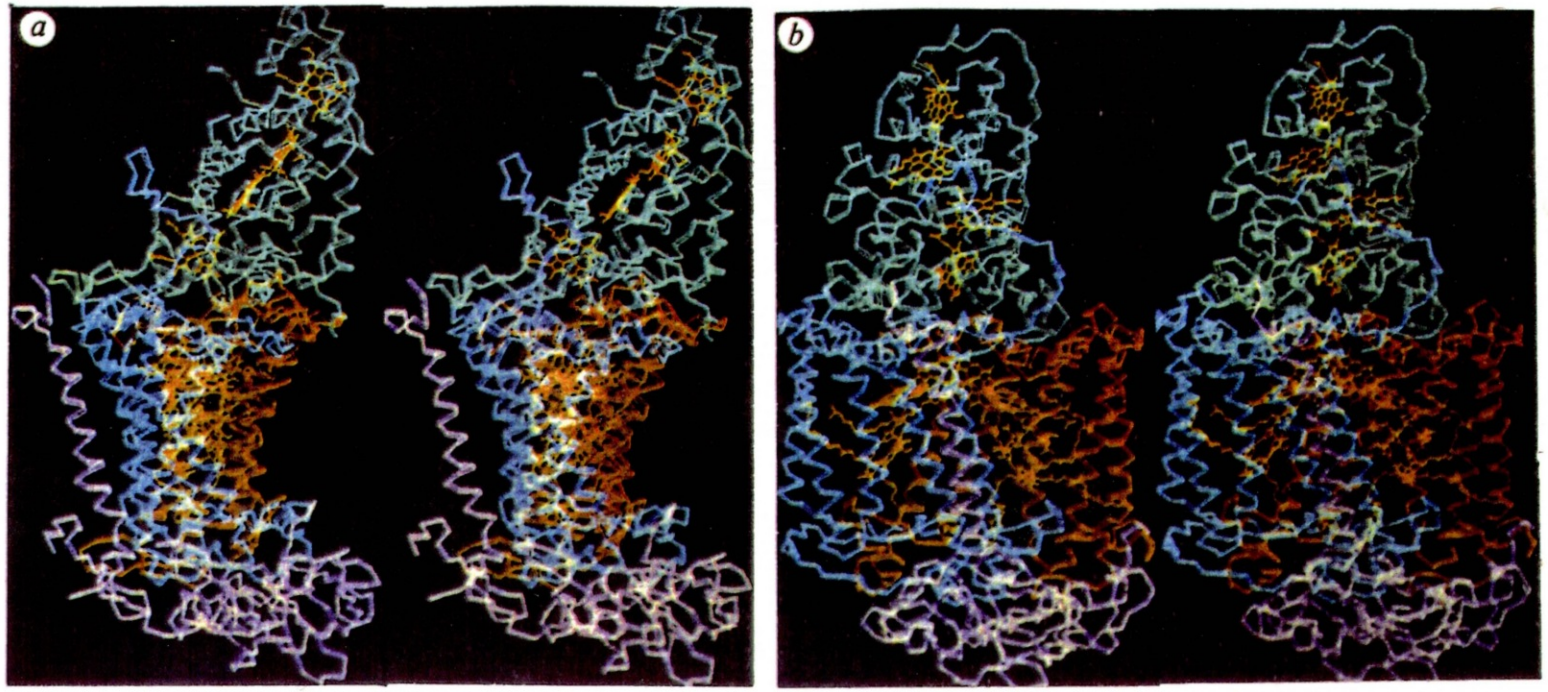
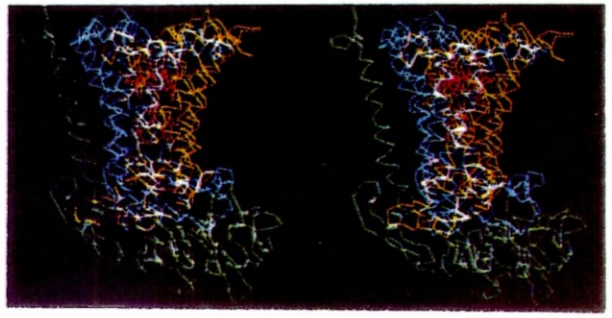


Fig 1.3. The reaction centre of *Rps. viridis* at 3Å resolution. 1.3.(b) is rotated with respect to 1.3.(a) by 90° about the vertical C_2 axis of symmetry. Green - cytochrome; orange - L subunit; blue - M subunit; purple - H subunit; yellow - cofactors.
(from Deisenhofer *et al*, 1985).

(a)



(b)

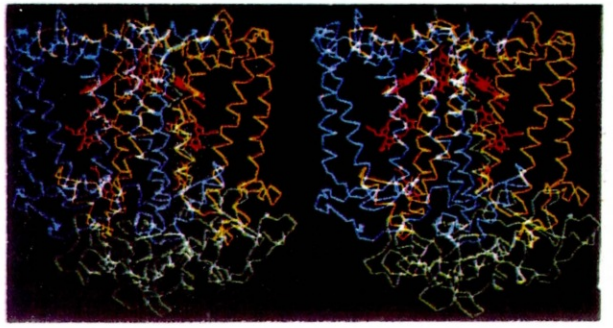


Fig. 1.4. The reaction centre of *Rb. sphaeroides* at 2.8Å resolution. 1.4.(b) is rotated with respect to 1.4.(a) by 90° about the vertical C_2 axis of symmetry. Yellow - L subunit; blue - M subunit; green - H subunit; green - H subunit; red - cofactors.
(from Allen *et al*, 1987b).

1.2.8. ORIENTATION OF THE BACTERIAL REACTION CENTRE IN THE MEMBRANE

X-ray analysis of membrane-derived particles can only be performed on crystals of proteins that have been extracted from the membrane by detergent treatment. Any conclusions from X-ray data on the orientation of the native protein in the membrane must therefore inferred using data from other experiments, e.g. hydropathy plots of the primary sequences (Kyte & Doolittle, 1982), predictive computer algorithms for secondary structure (Rao & Argos, 1986; Eisenberg *et al*, 1984), minimisation of the hydrophobic energy (Eisenberg & McLachlan, 1986) of the crystal structure in different regions of the membrane/water matrix, and UVCD, IR and optical absorption spectroscopic data (Nabedryk *et al*, 1982). Such measurements and calculations have led to the following conclusions:

(1) The approximate 2-fold symmetric axis of the proteins and cofactors lies perpendicular to the plane of the membrane.

(2) The five main helices of L and M, and the one helix of the H subunit are perpendicular to the plane of the membrane.

(3) Radio-labelling of the L subunit has located its amino terminal at the cytoplasmic side of the membrane (Brunisholz *et al*, 1984). Thus the globular domain of the H subunit lies at the cytoplasmic membrane face, and the cytochrome sits on the periplasmic side of the membrane.

(4) The asymmetric distribution of charged amino acids across the membrane plane results in a net negative charge on the periplasmic side. This asymmetry is thermodynamically preferred, given the net negative charge inside the cells.

(5) The primary donor, P, lies close to one membrane face (periplasmic) and close to the cytochrome. Light-activated electron transfer through the reaction centre occurs from the periplasmic face to the quinone located nearer the opposite (cytoplasmic) face of the membrane.

The position of the reaction centre of *Rb. sphaeroides* in the membrane, as determined from minimising the hydrophobic energy (Yeates *et al*, 1987), is shown in Fig.1.6.

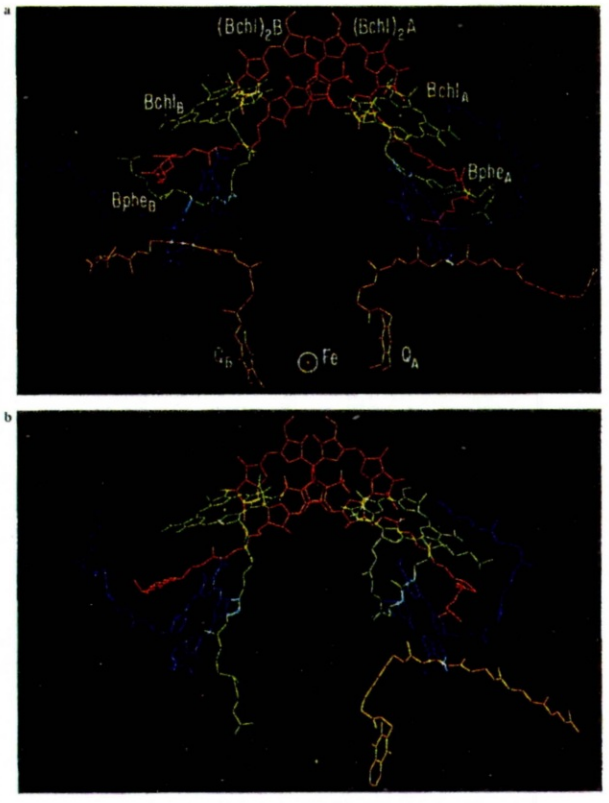


Fig. 1.5. Arrangement of the cofactors in the reaction centres of (a) *Rb. sphaeroides* (Allen *et al*, 1987a), and (b) *Rps. viridis* (Michel *et al*, 1986). The special pair is at the top of the complex, and electron transfer occurs along the A branch.

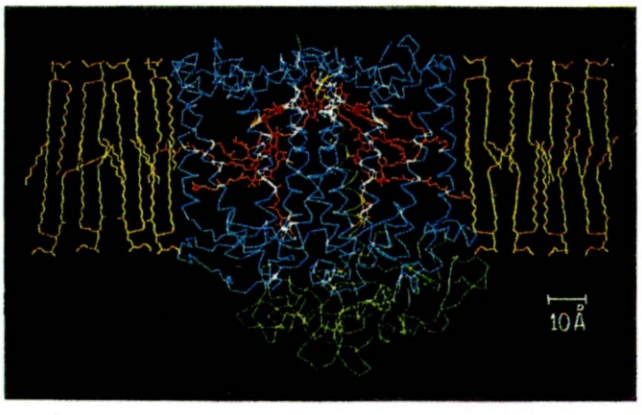


Fig. 1.6. Position of the *Rb. sphaeroides* reaction centre in the lipid bilayer. (from Yeates *et al* , 1987).

1.2.9. THE REACTION CENTRE OF PHOTOSYSTEM 2

Photosystem 2 is a multi-protein complex comprising the reaction centre, the tightly coupled antenna complex, the water-splitting (or oxygen-evolving) complex (WSC or OEC), and other components whose functions have not been identified (e.g. cytochrome b_{559}) (see Velthuys, 1987). The core of photosystem 2 contains all the PS2 proteins except those of the OEC. The reaction centre has long been known to be RC2-type, i.e. I is a pheophytin and X_1 is a quinone (plastoquinone). Below, I discuss some of the biochemical and functional properties of the Photosystem 2 complex.

1.2.9.1. Polypeptides of Photosystem 2

There are three main functional components of an active oxygen-evolving Photosystem 2 unit, besides the LHC2 complex which is often closely associated with it: (1) the reaction centre, in which the light-driven production of oxidised and reduced intermediates occurs; (2) the core polypeptides which bind the "antenna" chlorophyll and carotenoid pigments; (3) The extrinsic oxygen-evolving complex (OEC) associated with the membrane-bound core and reaction centre on the luminal face of the thylakoid membrane.

1.2.9.1.1. Proteins of the oxygen-evolving complex

Because of the relative ease of separation and rebinding of the OEC from and to the thylakoid membrane, its components and their functions are quite well-defined. It consists of possibly five proteins of relative molecular mass 33, 23, 16, 10 and 5 kD (see Andersson & Akerlund, 1987). The 33 kD particle lies closest to the membrane, and the 16 kD furthest from it, with the 23 kD protein lying between them. The 23 and 16 kD polypeptides serve to maintain a high concentration of calcium and chloride ions near the site of water oxidation, while the 33 kD protein is involved in stabilising the manganese cluster, whose redox activity results in the oxidation of water to yield molecular oxygen. It is thought (see Barber, 1987b) that the 33kD protein protects, but does not actually contain, the manganese cluster. The precise location of the manganese in a specific protein subunit is not known. The 10 kD protein appears to be less extrinsic than the 33, 23, and 16 kD particles, since it cannot be removed by high salt alone, but requires some Triton X-100 in addition.

1.2.9.1.2. Proteins of the Photosystem 2 core complex

At present, there are estimated to be at least nine polypeptides associated with the core of Photosystem 2 (reaction centre and tightly bound antenna components), with RMM of 47, 43, 32, 30, 28, 22, 9, and 4 kD. The product of gene psbI (Ikeuchi & Inoue, 1988; Webber *et al*, 1989) lies between the 9 and 4 kD particles in SDS-PAGE. PS2 thus has

many more protein components than the purple bacterial reaction centre, and it was thought unlikely that all these components are involved in primary charge separation. Rather, this activity should be located in a smaller part of the complex, the other components binding "antenna" pigments, or having other functions.

1.2.9.2. The 47kD protein as the reaction centre of Photosystem 2

It had been proposed that the 47 kD protein contained all the reaction centre cofactors, i.e. P680, pheophytin, and quinone (Nakatani *et al*, 1984). This conclusion was based on correlations between signals thought to be characteristic of the PS2 reaction centre, notably a light induced absorption bleach at 680nm and a fluorescence emission at 695nm (Breton, 1982), and the presence of the 47kD protein. However, these results have not proved to be conclusive. Yamaghishi and Katoh (1984, 1985) obtained two complexes from PS2 after solubilisation of *Synechococcus* membranes with the detergent LDAO. One was photochemically inactive, and consisted of mostly the 43 kD protein. The other, photochemically active, component contained the 47 kD protein, but in addition the 30 and 32 kD proteins. Therefore, the primary photochemical activity had not been located exclusively in the 47 kD particle. Indeed, when this protein was further purified (Tang and Satoh, 1984), it showed no photochemical activity.

1.2.9.3. Molecular biology and the isolation of the PS2 reaction centre

Molecular biological techniques for the rapid sequencing of DNA have resolved the question of the location of the PS2 reaction centre.

The sequence of the M subunit of the *Rb. sphaeroides* reaction centre was reported by Williams *et al* (1983). Following the sequencing of the L subunit, homologies were observed between L and M (Williams *et al* ,1984). Youvan *et al* (1984) noted homologous regions in the L and M subunits of reaction centres from *Rb. capsulata.* Both groups noted homologies between these two subunits and the Q_b or quinone-binding protein (D1) from Photosystem 2, which had been sequenced by Zurawski *et al* (1982). Both the L subunit from *Rb. sphaeroides* and the Q_b protein bind the herbicide azidoatrazine (DeVitry and Diner, 1984; Pfister *et al*, 1981). The homologous region was proposed to be involved in quinone binding (Hearst and Sauer, 1984), the quinone acceptor being a common feature distinguishing the RC2-type reaction centre from the RC1-type. Publication of the sequence of another Photosystem 2 polypeptide called D2 (Rasmussen *et al*, 1984; Rochaix *et al*, 1984) revealed sequence similarities to D1, and further between D1 and D2, and the L and M subunits of *Rb. sphaeroides*. Recently, the sequencing of the L and M subunits of the reaction centre from the filamentous bacterium *Chloroflexus aurantiacus* (Ovchinnikov *et al*, 1988a, 1988b), has strengthened the idea that the RC2-type reaction centre is a distinct entity in

structure as well as function.

Following the crystallisation of the reaction centre form *Rps. viridis*, the regions of homology were found to be in the binding regions (in the bacterial reaction centre) for BChl, BPheo, the non-haem ferrous iron atom, in addition to the quinone binding region. It was thus proposed (Deisenhofer *et al*, 1985; Michel & Deisenhofer, 1986; Trebst, 1986) that D1 and D2 exclusively bind the cofactors involved in primary charge separation. These would comprise a similar heterodimer in PS2 as the L and M subunits in the purple bacterial reaction centre. The protein folding models proposed on the basis of the homologies have been further discussed and developed (Barber, 1987c).

The proposal that D1 and D2 together comprise the reaction centre of Photosystem 2 has recently received experimental support from the isolation of a PS2 subfraction containing D1, D2 (both 30-32 kD), and the two polypeptides of the cyt-b_{559} (9kD and 4kD) (Satoh & Nanba, 1987; Nanba & Satoh, 1987; Barber *et al*, 1987). This complex exhibits photoreduction of Pheo (Satoh & Nanba, 1987), a photoinduced radical pair (Takahashi *et al*, 1987; Danielius *et al*, 1987), an EPR signal characteristic of a spin-polarised triplet (Okamura *et al*, 1987; Telfer *et al*, 1988), a light-induced bleaching at 680nm in the presence of an electron acceptor (Barber *et al*, 1987), and light-driven electron transport in the presence of exogenous electron donors and acceptors (Chapman *et al*, 1988). The 47 and 43 kD proteins are thus thought to bind the antenna pigments. The table below summarises the polypeptides of Photosystem 2 and their functions.

Table 1.2. Polypeptides of Photosystem 2

PS2 function	**RMM (kDa)**
reaction centre	32 (D1), 30 (D2), 9 ($Cytb_{559}$), 4 ($Cytb_{559}$), 4.8 (psbI)
core antenna	47, 43
oxygen-evolving complex	33, 23, 16, (10), (5)
unknown function	28, 22, 9, 6, 4.5, 4, 2

A current model for the organisation of the polypeptides in the core of Photosystem 2 is reproduced below (Fig. 1.7).

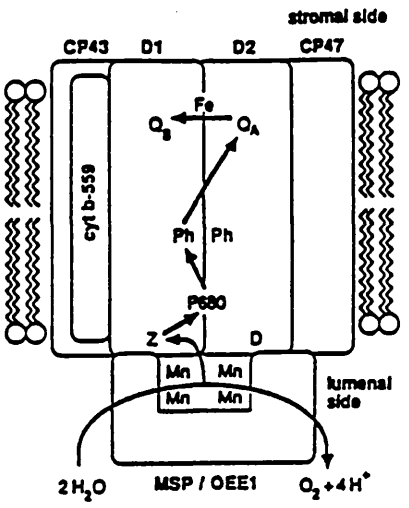


Fig. 1.7. Schematic organisation of the Photosystem 2 core complex in the thylakoid membrane. (from Vermaas, 1989). MSP/OEE1 - manganese-stabilising protein (33kD); Z, D - donors to P680; Ph - pheophytin; $Q_{A,B}$ - quinone electron acceptors.

1.2.10. THE SIMILARITY BETWEEN THE REACTION CENTRES FROM PURPLE BACTERIA AND PHOTOSYSTEM 2

The sequence homologies between D1 and D2, and L and M, the identification of the homologous regions with cofactor binding regions, and the isolation of a photoactive PS2 particle containing the D1 and D2 polypeptides have resulted in a much deeper understanding of the RC-2-type reaction centre. However, despite the many similarities between the oxygenic PS2 and anoxygenic bacterial systems on the electron acceptor side of the reaction centre, there remain several important differences. Perhaps the most significant dissimilarity is the oxidising potential generated by charge separation in the two types of reaction centre. Photosystem 2 generates a potential of greater than 1.1 V, whereas purple bacterial reaction centres generate 0.55 V. As bacterial photosynthesis progressed, so the reserves of oxidisable substrate diminished. This problem was circumvented with the evolution of Photosystem 2. The potential generated in this system is sufficiently oxidising to remove electrons from water, and water was abundant as an oxidisable substrate. The reaction required in addition the development of the molecular components to catalyse this reaction. The difference in the oxidising potential of the reaction centre primary donor, and the close association of the manganese-containing oxygen-evolving complex with the PS2 reaction centre must be reflected in structural differences between the higher plant and bacterial systems.

1.2.11. REACTION CENTRE TRIPLETS AND SINGLET OXYGEN

When reaction centres are exposed to high light intensities, the rate of charge separation can exceed the rate of electron transfer to the secondary electron acceptors. In such cases, the radical pair can recombine to form a triplet state that probably resides on the primary donor. Triplet states are potentially damaging, since they can excite ground state oxygen to its singlet state. Singlet oxygen is damaging, since it readily oxidises lipids and other components. Following the appearance of Photosystem 2, the level of atmospheric oxygen rose, and the triplet state of reaction centres became a source of damage to photosynthetic organisms. Carotenoid molecules are quenchers of a variety of triplet states (see Halliwell & Gutteridge, 1985). The reaction centres of purple bacteria and photosystem 2 contain carotenoid, and the formation of carotenoid triplets has been observed in these systems.

In sections 1.4. and 1.5, I examine the extent of the similarities between the two systems as determined from a variety of spectroscopic measurements. Before examining these data, I review briefly the areas of molecular spectroscopy relevant to the discussion and to work presented in later chapters. Particular attention is paid to the exciton model, which is encountered frequently in the spectroscopic study of reaction centres.

1.3. MOLECULAR SPECTROSCOPY OF REACTION CENTRES

In this section, I briefly review the molecular origins of the phenomena observed in photosynthetic reaction centres by spectroscopic techniques. Many of the results of quantum mechanical calculations are stated without proof or detailed comment. For derivations see Cantor & Schimmel, Vol. II (1980), Campbell & Dwek (1982), or Harada & Nakanishi (1982).

1.3.1 INTERACTION OF LIGHT WITH MOLECULES

Light can induce changes in the total energy of a molecule by displacing charge. This displacement can be linear, induced by interaction of the molecular electrons with the electric component of the radiation, which can result in changes in the electronic or vibrational energy of the molecule. A rotational displacement of charge, induced by interaction of the molecule with the magnetic component of the radiation, can induce changes in the electron or nuclear spin energy of the molecule.

The preferred directions of the charge displacement are fixed with respect to the molecular axes, and are decribed by the transition dipole moment.

1.3.2. ELECTRONIC SPECTRA

Absorption of a photon causes promotion of one of a pair of electrons from an occupied (bonding) orbital of relatively low energy to a previously unoccupied (anti-bonding) orbital of higher energy.

Small polyatomic molecules in general have filled σ-bonding, π-bonding, and non-bonding (n) orbitals. The longest wavelength (i.e. lowest energy) absorption band often corresponds to an n -> π^* transition with the more intense π -> π^* and σ -> σ^* absorptions occurring at shorter wavelengths.

Highly conjugated molecules have as many π-type orbitals as there are conjugated atoms, and the orbitals of both the π and π^* orbitals are spread over a range of energies, as are those of the σ and σ^* sets. The result is a lowering of the energy of the lowest-energy transition, i.e. a red-shift of the lowest-energy absorption. The degree of conjugation thus allows the same class of pigment to have different absorption spectra. Porphyrins and carotenoids have extended conjugated systems.

The absorption of light is a fast process occurring in femtoseconds, and the original spin

of the electron is retained in the excited state. However, spin reversal can occur from the excited (singlet) state by a process known as intersystem crossing to a lower energy excited triplet state. Several triplet states have been observed in photosynthetic systems.

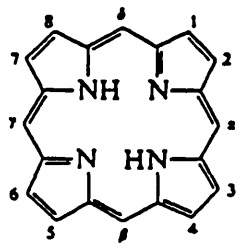
1.3.3. ELECTRONIC SPECTRA OF THE REACTION CENTRE CHROMOPHORES

All the electronic transitions under investigation in this work are those to π^* molecular orbitals. Measurable parameters of the spectra are the energy, magnitude, and direction of the transition. The amide bond has strong electronic absorption in the UV, but we consider mainly one class of molecule: highly conjugated systems (containing alternating double and single bonds) e.g. the porphyrin ring in chlorophylls, pheophytins, and cytochromes, and the conjugated hydrocarbon chain of carotenoids.

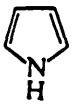
1.3.3.1 The Porphyrins - Chlorophylls, pheophytins, and cytochromes

The basic porphyrin skeleton consists of four pyrrole rings, conjugated together through four extra carbon atoms (Fig. 1.8.). They can bind divalent metal cations (e.g. Fe^{2+}, Mg^{2+}), when they are known as metalloporphyrins. Each conjugated atom is regarded as a source of a p-orbital available for π overlap.

All porphyrins have two main absorption bands, one in the red or near infrared region (Q band), the other in the blue or near ultraviolet region (B band). The theory of porphin and chlorin absorption spectra has been a subject of much discussion (Weiss, 1972, Gouterman, 1961) and is not discussed in detail here, beyond the simplest theory. Gouterman interpreted the visible and near-ultraviolet absorption bands as arising from electronic excitation from the two highest occupied molecular orbitals (HOMO) to the two lowest unoccupied molecular orbitals (LUMO). The interaction between the transitions gives rise to an intense B transition and a weaker Q transition. Polarised fluorescence spectroscopy has identified some of the bands as vibrational sub-bands of one or the other principle electronic transition (Gouterman & Stryer, 1962). It has also allowed assignment of the transition direction (x or y). The directions of the x and y axes with respect to the molecular axes are shown in the diagram of (B)Chl*a* and *b* (Fig. 1.9). Assymetry in the ring structure caused by side groups may result in different magnitudes for the different vibrational bands. The absorption spectra of Chl*a* and Pheo*a* are shown in Chapter 3.

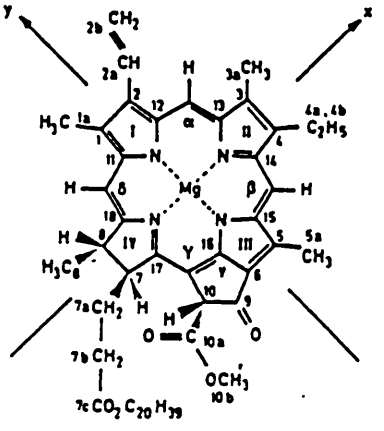


1 porphyrin skeleton

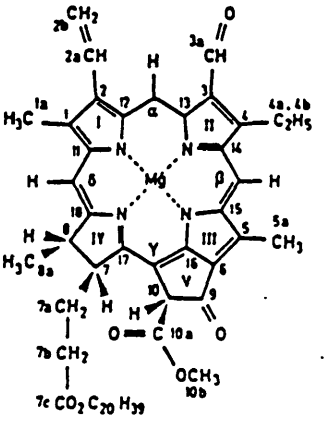


2 pyrrole

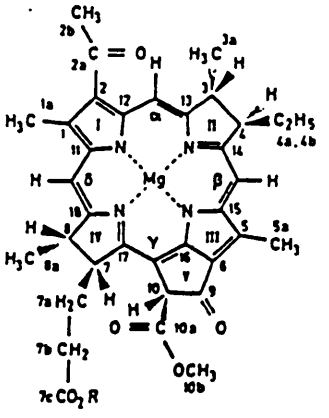
Fig. 1.8. Structure of the porphyrin skeleton, consisting of four pyrrole rings conjugated through four additional carbon atoms.



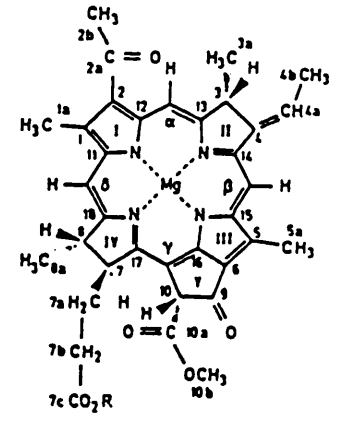
chlorophyll a



chlorophyll b



bacteriochlorophyll a



bacteriochlorophyll b

Fig. 1.9. Molecular formulae of (B)Chls *a* and *b*, showing the X and Y axes along which the electronic transitions are polarised, and the asymmetric carbon atoms on the porphyrin ring.

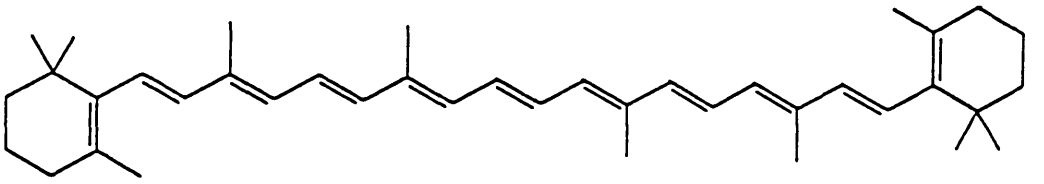


Fig. 1.10. Molecular structure of β-carotene.

1.3.3.2. The Carotenoid Pigments

Two major classes of carotenoid can be distinguished : carotenes which contain only hydrogen and carbon and are hydrophobic, and xanthophylls which contain in addition some oxygen atoms and are thus more hydrophilic. The majority of carotenes and xanthopylls have the same general structure - two six-membered rings separated by a conjugated hydrocarbon chain of variable length. The structure of β-carotene is shown in Fig.1.10. As for the porphyrins, each p-orbital on a constituent atom of the conjugated system is available for overlap to form a π-orbital.

Carotenoids typically have a high energy singlet state and a low energy triplet state, thus enabling them to have a dual role as donors of singlet state energy, and quenchers (acceptors) of triplet state energy. The energy of the both the singlet and the triplet states is lowered relative to the ground state with increasing number of conjugated carbon atoms.

All carotenoids have three major absorption bands in the region 400-500nm. These are all vibrational sub-levels of the same electronic transition, and therefore have the same polarisation, which lies on the long axis. *Cis*- or *trans*-isomers can be detected by resonance Raman spectroscopy. The absorption spectrum of β-carotene in hexane is shown in Chapter 3.

1.3.4. SENSITIVITY OF ELECTRONIC TRANSITION ENERGIES ON LOCAL ENVIRONMENT

The absorption properties of a chromophore are affected by its immediate environment in several ways.

1.3.4.1. The effect of the solvent

A solvent will generally alter the spectroscopic properties of a pigment by hydrogen bond or electrostatic interactions. A different interaction is expected between the ground and first excited singlet states of the molecule and the solvent, since the excited non-bonding orbital is much more extended and will be more affected by the polarity of the solvent. This different interaction will cause a change in the energy separation, and a net shift in the absorption frequency.

A special case of solvent interaction is the binding of pigment to a solid substrate, e.g. chlorophyll and other biological pigments bound to protein. The lowest-energy Q_y transition of Chl*a* is red-shifted when the chlorophyll molecule is bound to protein, relative to the same transition when in organic solvent. This may be due to polar amino acids near to the chlorophylls, which stabilise the transition dipole of the excited state of the chlorophyll in the protein, with respect to the excited state in organic solvents.

1.3.4.2. Changes in absorption on polymerisation

As well as ground and excited states interacting with their solvent or with protein ligands, dipolar interactions are also possible between neighbouring pigments. The simplest polymer whose properties can be altered by such interactions is a dimer. Spectral properties are also different in larger polymers with respect to the component monomers. Dipolar interactions can occur between adjacent nucleotides in nucleic acids, and between amino acids and amide bonds in polypeptides. I now summarise the properties of a dimer coupled by a dipolar interaction.

1.3.5. EXCITONS - A COUPLED CHROMOPHORE DIMER

Two chromophores may be close enough for electronic perturbations in one of the monomers to be felt by the electrons of the other monomer, through a dipolar coupling. In such a case, the spectroscopic properties of the coupled dimer differ from those of the uncoupled monomers. The excitation oscillates between the two monomers, and the absorption properties of the dimer show different characteristics to the absorption properties of the two individual monomers. The excitation in such a case is called an "exciton" (see Cantor & Schimmell, 1980, pp.391-395).

1.3.5.1. Interaction energy

For two monomeric transition moments, μ_1 and μ_2, separated by a distance R_{12}, the dipole-dipole interaction is:

$$V_{12} = (\mu_1 \mu_2).(|R_{12}|)^{-3} - 3(\mu_1 R_{12})(\mu_2 R_{12}).(|R_{12}|)^{-5}$$

Thus, the magnitude of the dipolar interaction is inversely proportional to the cube of the distance between them (i.e. decreases rapidly with distance).

1.3.5.2. Excited state wavefunctions

For each transition in a monomeric pigment, there are two transitions in the coupled dimer, which correspond to the in-phase or out-of-phase excitation of the two locally excited monomer states. These are described by the two excited state exciton wavefuctions ((+),(-)), respectively.

1.3.5.3. Energies of the excited states

The energies of the (+) and (-) exciton states are calculated from the Schrodinger equation, using the excitonic excited state wavefunctions, and the Hamiltonian operator which contains in addition to the two monomer Hamiltonian operators the dipolar interaction energy operator. The result of such a calculation yields the energies of the two

excited states:

$$E_{(+),(-)} = E_o \pm V_{12},$$

where E_o is the monomeric absorption frequency.

The energy of each excited state lies either above or below the monomer transition energy. V_{12} can be positive or negative or zero (no coupling). Thus, the (+) exciton transition can lie above or below the (-) transition, depending on the sign of V_{12}.

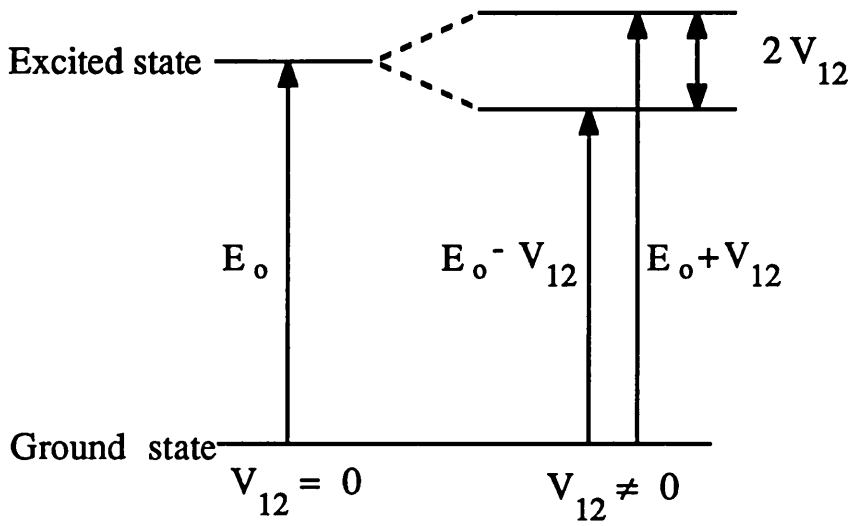


Fig.1.11. The degeneracy of monomeric transitions is lifted in a dimer of chromophores coupled by a dipolar interaction.

1.3.5.4. Directions and intensities of the two excited states

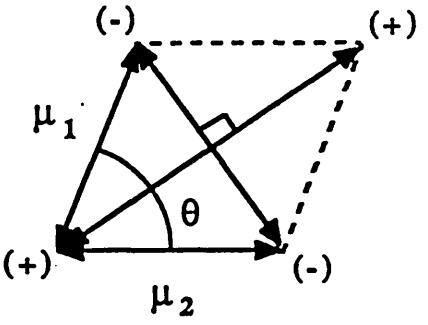
The directions and intensities of the two transitions (+) and (-) are determined by the vector sum and difference of the monomer transitions, respectively. The excitonic electric transition dipoles are therefore mutually perpendicular. The relative magnitude of the two bands is:

$$D_{0A\,(+/-)} = D_{0A} \pm D_{0A} \cos\theta$$

where D_{0A} is the dipole strength of the monomer transition, and θ is the angle between the monomeric transition dipoles μ_1 and μ_2.

Fig.1.12. The directions and intensities of the (+) and (-) exciton states are determined by the vector sum and difference, respectively, of the monomeric transitions, μ_1 and μ_2. The (+) and (-) transitions are therefore always mutually orthogonal.

Fig.1.12. The excitonic transitions (+),(-) are the vector sum and difference respectively of the monomeric transitions μ_1 and μ_2.



The total integrated spectral intensity is always twice the monomer intensity, for all mutual orientations of the two dipoles.A head-to-tail parallel arrangement of the two dipoles results in a negative dipolar interaction energy, and a red-shift in the absorption band due to mutual attraction of the monomers. A side-to-side arrangement results in a positive interaction energy, and a blue-shift of the band, due to mutual repulsion of the monomers. For other orientations, two bands may be seen (Fig1.13).

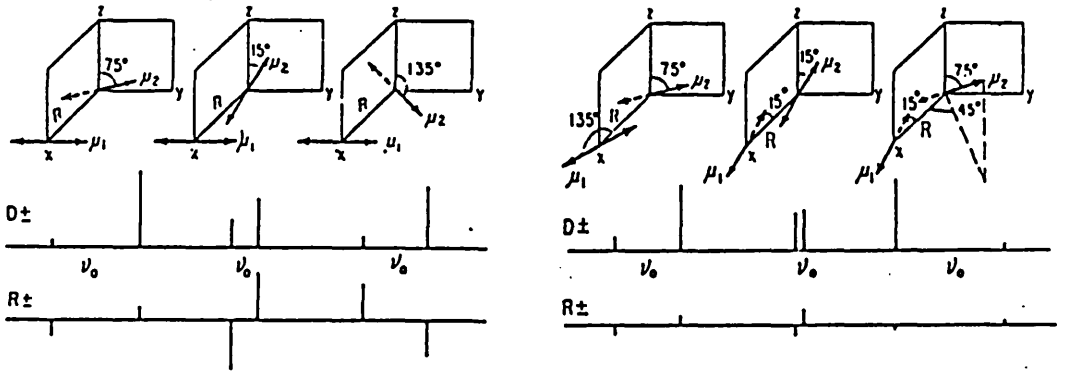


Fig.1.13. The absorption frequencies, dipole strengths, and rotational strengths (see Section 1.3.7) for six model dimers with different geometries. (from Tinoco, 1963).

Chl*a* exists as dimers in CCl_4, and two Q_y transitions can be seen in the second derivative of the absorption spectrum: a major transition at 664nm, and a smaller transition at 683nm, where in the monomeric spectrum, only one transition occurs (see Chapter 5 for discussion of Chl aggregates in different solvents).

Oligomers of identical chromophores will show analogous splittings. For a trimer, three bands are predicted for each single monomer band (Tinoco, 1963, Pearlstein, 1982); four interacting chromophores may show four bands, and so on.

Excitonically coupled dimers show strong optical activity. This property facilitates the identification of such dimers, when the two absorption bands are not sufficiently well-resolved. This is discussed below.

1.3.6. VIBRATIONAL SPECTRA

The energy of most molecular vibrations corresponds to that of the infrared region of the electromagnetic spectrum, in the range 1400-4000 cm^{-1}. The transitions induced by the radiation involve changes in the energy of the molecule associated with the simple harmonic motion of stretching and contraction of a bond between two atoms. Quantum mechanics predict that only certain values of the energy of the vibration are allowed, and that the transition has a fixed direction relative to the molecular geometry as for electronic spectra. The transitions considered in this thesis are those associated with the amide bond between two amino acids in a peptide.

1.3.6.1. Infrared spectroscopy of the peptide bond

The peptide bond has three main vibrational transitions: (1) The Amide A band (N-H stretch) at 3300 cm^{-1}, (2) The Amide I band (C=O stretch) at 1630 - 1660 cm^{-1}, and (3) The Amide II band (N-H bend and C-N stretch) at 1520 - 1550 cm^{-1}. The C=O stretch and the N-H stretch are polarised parallel to the C=O and N-H bonds. The Amide II band is polarised nearly parallel to the C-N peptide bond, and nearly perpendicular to the N-H bond; the vibrations leading to this band are approximately equal contributions from a C-N stretch and an N-H bend.

The two stretching vibrations (C=O stretch and N-H stretch) are shifted to lower energy when they are part of a hydrogen bond, since this interaction makes it easier for the carbonyl oxygen to move towards the electron donor, and for the amide nitrogen to move towards the electron acceptor. The Amide II band is moved to higher energy, since the linear hydrogen bond makes the N-H bend more difficult.

1.3.6.2. Sensitivity of the band positions to protein conformation

Hydrogen bonding between the C=O and N-H groups on different amide groups of a polypeptide are responsible for determining the type of secondary structure that the peptide may adopt (e.g. α-helix, β-sheet, β-turn etc.). The conformation of hydrogen bonds between amide groups differs depending on which type of secondary structure is being stabilised, and therefore have slightly different vibrational frequencies. Thus the frequencies of the Amide I and Amide II vibrations are diagnostic of the type of protein secondary structure being measured (see Yang *et al*, 1985, for a brief historical review). A table of absorption frequencies for the amide bond in different structures is presented in Table 6.1 (Chapter 6). Therefore, infrared spectroscopy can be a powerful analytical tool for investigating protein secondary structure.

1.3.6.3. Linear dichroism of the peptide bond

In the α-helix, N-H···O=C peptide hydrogen bonds are oriented parallel to the long axis of the molecule. Thus the Amide I transition is polarised parallel to the helix axis, and the Amide II perpendicular to it. In β-sheets, the transitions have the opposite polarisation with respect to the axis of the peptide chains. Infrared dichroism can thus determine the orientation of different secondary structures with respect to a macroscopic orientation axis.

1.3.7. CIRCULAR DICROISM (CD)

The majority of molecules synthesised by living cells are optically active. The most commonly measured property of an optically active sample (with modern instrumentation) is its Circular Dichroism (CD). This is defined as the differential absorption of right and left circularly polarised light. The intensity of a CD band is determined by a quantity known as "rotational strength". Rosenfeld (1928) derived an expression for the rotational strength from quantum mechanical principles:

$$R_{oa} = \text{imag} \left(\langle \psi_o | \mu | \psi_a \rangle \, . \, \langle \psi_a | \mathbf{m} | \psi_o \rangle \right)$$

where R_{oa} is the rotational strength of the transition, ψ_o, ψ_a are the wavefunctions of the ground and excited states of the molecule, respectively, μ is an electric dipole operator, **m** is a magnetic dipole operator, and "imag" means the imaginary part of the expression that follows.

1.3.7.1. "Intrinsic" or monomeric CD

For the dot (scalar) product between the electric and magnetic dipole moments to be non-zero for a monomeric chromophore, there must be a component of μ parallel to **m**. Electronic absorption results in an induced dipole that is linear; magnetic absorption results in a circulation of charge. Therefore, observable CD from a monomeric pigment must arise from a helical displacement of charge induced by passage of light through the optically active sample. Only assymetric centres, e.g. asymmetric carbon atoms, will produce this effect. Chl*a* contains 5 asymmetric carbon atoms. Three of these asymmetric centres are on the porphyrin ring (see Fig. 1.9.); the other two are on the phytyl side-chain.

1.3.7.2. CD of a dimer of interacting chromophores

The most powerful application of circular dichroism spectroscopy as an analytical tool is to examine aggregates of chromophores which are coupled by a dipolar interaction. The

same wavefunctions ((+) and (-)) as are used in the calculation of absorption properties, are used to calculate the rotational strength of the dimer using Rosenfeld's equation. The result (see Harada & Nakanishi, 1982, or Cantor & Schimmel, 1980, pp. 418-425) is a complex expression containing contributions to the circular dichroism from three distinct sources:

(1) The sum of the intrinsic CD of the two monomers. In the case of a chlorophyll dimer, this is the CD arising from the internal magnetic moments associated with the asymmetric centres on each of the two chlorophyll monomers.

(2) Electric-magnetic Coupling. This is significant when one of the monomers has a small magnetic transition dipole and the other has a small electric transition dipole. Since the most commonly encountered chromophores (including all those considered in this work) have much larger electric transition dipoles than magnetic transition dipoles, this term is not appreciable.

(3) Coupled oscillator, or Exciton CD. This is usually the dominant term in chromophore aggregates. Its magnitude depends on the distance between the two chromophores, and on the geometry of the aggregate.

Excitonic CD of a coupled dimer has two characteristic properties:

(a) The CD of the two exciton states ((+) and (-)) have identical rotational strengths of opposite sign. Thus, the entire CD is "conservative", i.e. sums to zero, over the region of CD absorption.

(b) The CD is proportional to the product of the dipolar interaction and the triple scalar product of interchromophoric distance and electric transition moments of each of the two monomers:

$$CD_{+/-} = \pm V_{12} \cdot R_{12} \cdot (\mu_1 \times \mu_2)$$

where $CD_{+/-}$ is the CD of the two exciton states (CD is related to rotational strength by a constant of proportionality), R_{12} is the interchromophoric distance, and μ_1, μ_2 are the dipole moments of the excited states of chromophores 1 and 2.

The magnitude of a triple scalar product is equal to the volume of a parellelipiped using the three vectors as three intersecting edges. Thus for any two of the three vectors (R_{12}, μ_1, μ_2) identical (e.g. parallel identical transition dipoles), the value of the triple product is zero. Further, for coplanar dipoles (no component of R_{12} parallel to the dipole vector product), the rotational strength of the exciton dimer is zero. The rotational strengths of the two excitonic transitions of some model dimers are shown in Fig.1.13.

Exciton splitting is more easily observed as CD than as ordinary absorption, since it is accentuated by the opposite signs of the two spectral bands. Thus CD spectra are always

measured when then the presence of exciton coupling in a sample is suspected.

1.3.7.3. CD of a polymer

A coupled aggregate of N chromophores has potentially N excitonic transitions for every monomeric transition depending on orientation restrictions, so the CD of an N-mer may have up to N CD bands (see Pearlstein, 1982). The calculation of the expected polymer CD is complex, so the analytical use of CD the of polymers is usually semiempirical.

1.3.7.4. Determination of protein secondary structure from UVCD spectra

The CD spectrum of the protein is dominated by the peptide backbone. The CD spectrum is sensitive to the conformation of the backbone, as shown from measurements of model polypeptides composed of just one type of amino acid which are made to adopt different conformations by careful adjustment of the conditions (Greenfield & Fasman, 1967). The UVCD spectra of poly-L-lysine in α-helical, β-sheet, and random coil conformations are shown in Fig.1.14. The α-helix shows a typical double minimum at 208nm and 223nm, and a maximum at 193nm; β-sheet structures have a single minimum at 215nm. The UVCD spectroscopic properties of a protein are considered most simply as the sum of the UVCD properties of the constituent backbone stretches in different pure conformations : α-helical, β-sheet, or random coil. The amounts of different secondary structures in a protein can be estimated by a linear least squares fit of the measured spectrum with the standard spectra of poly-L-lysine.

A different method of generating standard UVCD spectra for protein in one pure conformation (e.g. α-helix, β-sheet, random coil) uses the experimental UVCD data for proteins whose structures are known from X-ray diffraction studies (Saxena & Wetlaufer, 1971). From the amounts of the different conformations in each protein comprising the basis set, as seen in the X-ray structure, standard UVCD spectra for the pure conformations (e.g. α-helix, β-sheet, random coil) can be generated by a least-squares fit. These spectra are shown in Fig.1.15, and are similar to those of the model homopolypeptides in different conformations. They are used in the analysis of experimental CD spectra of proteins whose structure is not known from X-ray crystallography. Estimates are made of the relative amounts of the three pure conformations which will give the closest spectrum to that measured. The best fit is obtained by least squares methods. The optical activity is expressed in Figs. 1.14 and 1.15 in terms of molar ellipticity, [θ], which is related to CD (A_l - A_r) by a constant of proportionality (see Cantor & Schimmell, 1980, pp. 411-413).

An inherent problem in this method is the assumption that the protein basis set is applicable to the protein being investigated, i.e. that the structure of the unknown protein

is composed of similar structures to those present in the reference proteins. This may cause errors in the determination of the structure of membrane-bound proteins using a basis set comprising exclusively aqueous globular proteins. Moreover, there are twenty possible conformations for the peptide bond, of which three are α, β, and random form. The β-turn is an example of another possible conformation, and a correction for this in CD spectra has been made (Chang *et al*, 1978). Other conformations are the β-bend, 3_{10}-bend, hairpin bend, β-loop, 1-4 bend, reverse turn, and others (see Yang *et al*, 1986). Also, the CD of an α-helix or β-sheet is a function of its length. The model compounds used e.g. poly-L-lysine) consist of much more extended structures than the helices and sheets encountered in physiological proteins. This can be corrected for in the calculation, but this requires more parameters (Chen *et al*, 1978). Another assumption is that the individual stretches of a particular secondary structure do not interact to give composite CD. Although the interaction falls of as the square of the distance, it is likely that use of extended helical or sheet homopolypeptides will not adequately describe the complete CD of a physiological protein.

A comprehensive review of protein secondary structure predictions from UVCD spectra is provided by Yang *et al* (1986).

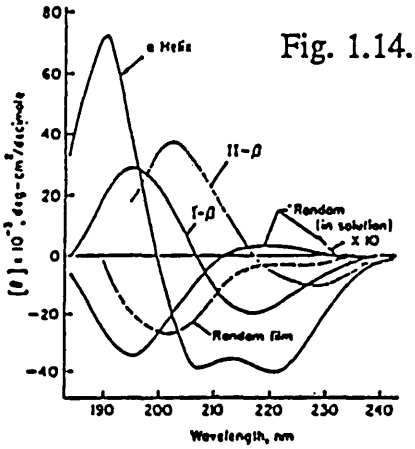


Fig. 1.14.

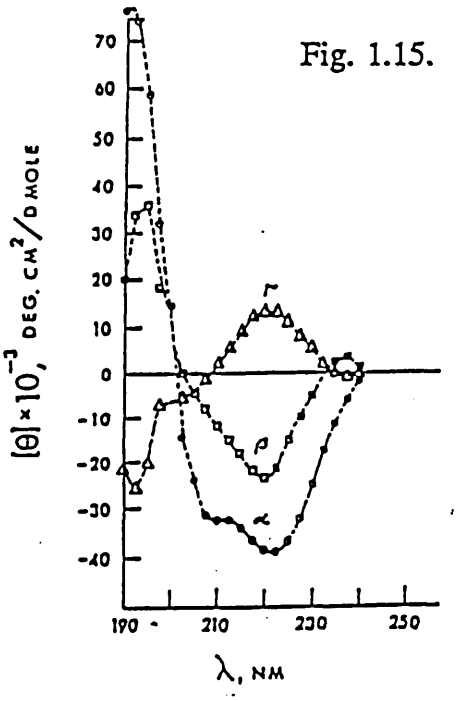


Fig. 1.15.

Fig. 1.14. Circular dichroism spectra of polypeptides in various conformations: α-helix, β-sheet, and random coil. (from Tinoco & Cantor, 1970).

1.3.8. FLUORESCENCE SPECTROSCOPY

Fluorescence is the emission of radiation that occurs when a molecule in an excited state returns to its ground state. It involves excitation (10^{-15}s) followed by emission. The molecule is in its excited state for a finite time (10^{-6}-10^{-9}s).

The measurable parameters for fluorescence are its excitation and emission spectra, and its intensity, lifetime and polarisation.

The fluorescence intensity and wavelength of maximum emission, λ_{max}, are very sensitive to environment. When the absorption of a chromophore is red-shifted (e.g. chlorophyll bound to protein), the fluorescence emission maximum is correspondingly red-shifted. Pigments in solvent generally have a much higher fluorescence yield then pigments in photosynthetic systems, since they have fewer paths of de-excitation other than emission. These two properties can be used as a measure of the intactness of a photosynthetic pigment-protein complex.

1.3.9. ROTATION OF CHARGE

The magnetic component of electromagnetic radiation can induce rotation of charge in a molecule leading to a reversal in the spin of the electrons or nuclei. NMR spectroscopy examines the nuclei, but EPR spectroscopy, which is used to investigate electron spin, is used much more frequently in photosynthesis research. This technique is useful in detecting and characterising unpaired electrons in a molecule, and has particular application in photosynthesis research to detect the various radicals and triplets formed by different reactions in the first stages of energy conversion. Resonance between the two electron spin orientations and the applied magnetic field occur when

$$h\nu = g\beta H, \quad g = h\nu / \beta H$$

where h is Planck's constant, ν is the frequency of the radiation inducing the transitions, β is the Bohr magneton, and H is the magnitude of the external magnetic field.

The g-value is used to characterise the position of a resonance, and is characteristic of the electronic (molecular) environment of the unpaired electron. The g-value is thus diagnostic for the molecular nature of the paramagnetic species. The occurence of EPR signals with diagnostic g-values can be correlated with other processes, allowing identification of novel EPR signals with known phenomena.

I now review the results from the application of these techniques to the study of some photosynthetic reaction centres.

1.4. SPECTROSCOPIC PROPERTIES OF PURPLE BACTERIAL REACTION CENTRES

The identification and characterisation of the primary donor and acceptor components of bacterial reaction centres was greatly accelerated by the isolation of a minimal reaction centre unit. This was achieved independently by Reed and Clayton (1968), who isolated a reaction centre complex from a carotenoidless strain (R-26) of *Rhodobacter sphaeroides*, and by Gingras & Jolchine (1969) who obtained a reaction centre particle from the carotenoidless mutant (G-9) of *Rhodospirillum rubrum*. The spectroscopic signals diagnostic of a reaction centre were amplified in these particles, free from contaminating antenna pigments. Previous attempts to obtain such a sample involved selective oxidation of antenna pigments by light or chemical oxidants (see above). Reed and Clayton, and Gingras and Jolchine, used the detergent Triton X-100 to obtain a particle of molecular weight 200,000 containing the photobleachable pigment P870, ubiquinone (Q), b- and c-type cytochromes, non-haem iron, and copper. Clayton and Wang (1971) and Feher (1971) obtained purer preparations of molecular weight less than 100,000 using lauryl dimethylamine oxide (LDAO) as detergent. The method of Jolchine and Reiss-Husson (1974) also uses LDAO to obtain reaction centres from wild-type strains of *Rb. sphaeroides*, which retain the reaction centre carotenoid. The solubilisation is followed by sucrose density gradient centrifugation and fractionation through ammonium sulphate precipitation of the protein, and a particle of molecular weight 70,000 is routinely obtained. Gingras (1978) provides a comprehensive historical review of the different isolation procedures. Below I describe the results of spectroscopic experiments on this minimal reaction centre unit.

1.4.1. STEADY-STATE ABSORPTION SPECTRA OF PURPLE BACTERIAL REACTION CENTRES

The room temperature absorption spectrum of reaction centres from *Rb. sphaeroides* is shown in Fig. 1.16 (Reed & Ke, 1973). At 77K, greater resolution of the bands is obtained: the 535 nm band splits into two, with peaks at 533 and 545nm, indicating the presence of two pheophytins in slightly different environments (see Parson, 1987). The 865nm absorption shifts to 895nm at 77K, and the 802nm band is clearly composite indicating the presence of more than one transition, as had been shown previously from the second derivative of the low temperature absorption spectrum (Feher, 1971). Comparison of the reaction centre absorption spectrum with the spectra of purified BChl

and BPheo in organic solvent (Reed & Peters, 1972), allowed assignment of the bands at 533 and 545nm to the Q_X transitions of the two pheophytin molecules, and the 597nm to the Q_X transition of BChl.

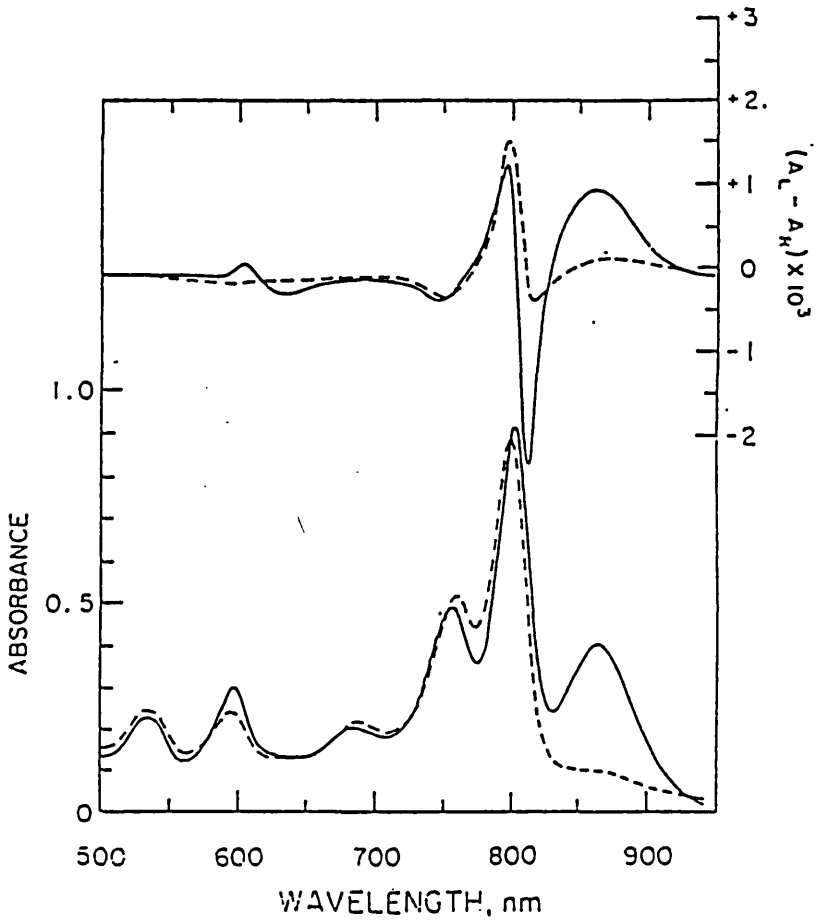


Fig. 1.16. Absorption and circular dichroism spectra of neutral (———) and chemically oxidised (- - - - -) reaction centres from *Rb. sphaeroides* R-26 (Reed & Ke, 1973).

Reed & Ke (1973) assigned other bands from the fluorescence excitation and emission spectra. The 757nm absorption is due to BPheo Q_y, since it emits strongly at 774nm, and is more effectively excited at 533nm, an absorption band of BPheo. The absorption band at 802nm is assigned to a BChl Q_y transition, since the 823nm emission is more effectively excited at 598nm (BChl Q_x). Similarly, the band at 870nm is assigned to BChla.

The room temperature absorption spectrum of reaction centres from *Rps. viridis* is better resolved than the spectrum of *Rb. sphaeroides*, due to the wider absorption range of BChl*b* and BPheo*b* with respect to BChl*a* and BPheo*a*, but the two spectra are qualitatively very similar. The two BPheo*b* molecules have Q_x transitions at 530 and 545nm, and Q_y transitions at 790 and 810nm. The four bacteriochlorophylls absorb at 600, 830, 850 and 960nm (1000 nm at 4K). A theoretical analysis of the absorption spectrum of Rps. viridis, employing model molecular orbital calculations, has been presented recently by Eccles *et al* (1988).

1.4.2. ABSORPTION DIFFERENCE SPECTROSCOPY OF THE PRIMARY DONOR

After addition of excess potassium ferricyanide at room temperature to reaction centres of *Rb. sphaeroides*, the 865nm (895nm at 77K) absorption bleaches completely (Fig. 1.16) and the magnitude of the 597nm band also decreases (by 30%) (Reed & Ke, 1973). The difference spectrum has maxima for these changes at 862 and 600nm. The 802nm band shifts to 799nm, with no change in intensity. The same difference spectrum in the near infrared can be obtained by illuminating the reaction centres at ambient redox potential (+100 mV to +300 mV), thus assigning the 870nm transition to the primary donor. The 870nm bleach was first observed by Duysens (1951) when whole cells were illuminated. Redox titrations of the 865 nm bleach reveal E_m for the primary donor P870 of between 440 to 500 mV (Loach *et al*, 1963). The E_m is pH-independent indicating that the oxidation of P870 is a one-electron step which does not involve a proton (Jackson *et al*, 1973).

Similarly, the oxidation of reaction centres from *Rps. viridis* following the addition of potassium ferricyanide results in the complete bleaching of the 960nm absorption band. The BChl bands at 833 and 850 nm shift to the blue, and a new band appears at 808 nm (Shuvalov & Asadov, 1978, 1979). Redox titrations of the 960nm bleach yielded an $E_{m,7}$ for the primary donor (960nm bleach) of value of 515mV (Klimov *et al*, 1977a). The oxidised vs. non-oxidised absorption difference spectrum shows a peak at 1245nm. This long wavelength absorption band had been predicted for the cation of chlorophyll pigments (Otten, 1971). Analogous long wavelength transitions are seen in the oxidised reaction centres of *Rb. sphaeroides* (at 1025nm) due to the BChl*a* cation, and in Photosystems 1 and 2 in the range 820-830 nm due to the cation of Chl*a*.

1.4.3. ABSORPTION DIFFERENCE SPECTROSCOPY OF THE PRIMARY ACCEPTORS

1.4.3.1. Quinone

Incubation of reaction centres in a mildly reducing medium (-200 mV) in the presence of herbicide (o-phenanthroline) gives rise to a characteristic reduced-oxidised absorption difference spectrum (Strayley & Clayton, 1973; Okamura *et al*, 1975), with a bleach at 270nm, and transitions at 325nm and 450nm, and a shoulder at 430nm. This was similar to the spectrum of reduced quinone, leading to the conclusion that quinone is an electron acceptor in bacterial reaction centres. In the absence of herbicide, the same difference spectrum is obtained following one actinic flash, but disappears after a second flash. It reappears after a third flash, and so on. This indicated the presence of two quinones, the first being a one-electron acceptor (Q_a), and the second a two-electron acceptor (Q_b) (Wraight, 1977).

1.4.3.2. Bacteriopheophytin

When chromatophores of various purple sulphur bacteria were illuminated in a medium of lower redox potential (-400mV), the yield of fluorescence decreased (Klimov *et al*, 1976). The absorption difference spectra (Shuvalov *et al*, 1976; Tiede *et al*, 1976; van Grondelle *et al*, 1976; Dutton *et al*, 1977; Klimov *et al*, 1977a) show bleaching of absorption bands at 545 nm (not 533nm) and 800 nm, and appearance of bands at 680 and 430 nm. These changes were attributed to photoreduction of bacteriopheophytin. Since the mid-point redox potential of this pheophytin is more negative than that of the quinone, it was concluded that pheophytin was an intermediary electron acceptor between the primary donor and the quinone. Of the two pheophytins observed in the absorption spectrum with transitions at 545nm and 533nm, only the pheophytin absorbing at 545nm is bleached.

Further evidence concerning the nature of the primary electron donors and acceptors has been obtained through EPR spectroscopy (see below, section 1.4.8.).

1.4.4. VISIBLE CIRCULAR DICHROIC SPECTROSCOPY

The nature of the dipolar interactions between the reaction centre pigments has been partly revealed through circular dichroic spectroscopy. Of particular value has been the measurement of the CD when the reaction centre is poised in different redox states.

1.4.4.1. The circular dichroism of the unperturbed reaction centre

The circular dichroism spectrum of a reaction centre was first measured by Sauer *et al* (1968), using the recently isolated reaction centre particle from *Rb. sphaeroides* R-26. Intense CD bands were observed and ascribed to dipolar (excitonic) interactions between the reaction centre pigments. The CD spectrum of reaction centres from several different species of BChl*a*-containing purple photosynthetic bacteria is well-represented by the CD spectrum of *Rb. sphaeroides* (Fig. 1.16).

Sauer *et al* (1968) interpreted the CD spectrum as arising from a primary donor composed of a trimer of strongly interacting molecules. In contrast, Reed & Ke (1973) conclude that the primary donor is a dimer of BChl molecules located centrally within the complex so as to interact with the largest number of pigments. Similar features are present in the CD spectrum of reaction centres from *Rps. viridis*, but shifted to longer wavelength.

1.4.4.2. The circular dichroism of the oxidised reaction centre

Chemical oxidation of the *Rb. sphaeroides* reaction centre leads to complete bleaching of the 865 nm transition, and of the negative CD band at 811 nm. The positive CD band at 797 nm increases slightly (Sauer *et al*, 1968, Reed & Ke, 1973). These results were interpreted as arising from large changes in pigment interaction produced by oxidation of the reaction centre, and confirmed the assignment of the 870 nm transition to the primary donor.

Chemical oxidation of *Rps. viridis* reaction centres causes bleaching of the absorption and CD bands at 980nm (confirming the assignment of this transition to the primary donor) and 849nm, and a slight decrease in the magnitude of the 830nm CD band. The intensity of the 787 nm CD band was unaltered after oxidation (Shuvalov & Asadov, 1979). Considering all the changes in the photooxidised CD spectrum, these authors conclude that the primary donor interacts mainly with the BChl molecule absorbing at 850nm, and does not interact with the BPheo. This spectrum also indicates an interaction between the BChl molecules absorbing at 850nm and 830nm.

1.4.4.3. The circular dichroism spectrum of the chemically reduced reaction centre

Photoreduction of bacteriopheophytin in *Rps. viridis* reaction centres, by illumination at low redox potential (Shuvalov & Asadov, 1979), results in a decrease in intensity of the 790 nm CD band, a decrease and shift of the CD band at 830nm to 819nm, and a slight blue shift with no change in intensity of the CD bands at 850 and 980nm. These changes indicated an interaction between the transitions of BPheo and the BChl molecule absorbing at 830nm.

1.4.5.4. Circular dichroism of the carotenoid

The carotenoids in reaction centres of *Rb. sphaeroides* strain 2.4.1 have been studied by Cogdell *et al* (1976). The strong CD in the visible band of the carotenoid, in this case spheroidene, and the ability for energy to be transferred from the carotenoid to bacteriochlorophyll, indicated a close pigment-pigment interaction. The strengths of the carotenoid CD bands decrease in intensity by 30% when the reaction centre is oxidised, perhaps reflecting a change in the environment of the carotenoid, and indicating that the carotenoid is located quite near to the special pair. Refined analysis of the X-ray crystal structure has located the carotenoid on the M subunit, close to the special pair.

1.4.5.5. A model of the pigments and their interactions

From the observed splittings, and altered interactions in photooxised or photoreduced reaction centres, Shuvalov & Asadov (1979) estimated the interaction energies between the pigments of the reaction centre. Together with angles determined from photodichroism measurements, they formulated a model of the relative arrangement of the pigments. This is reproduced in Fig.1.17. It is not clear if the preparation procedure (Pucheu *et al*, 1976) yields a reaction centre containing carotenoid. The authors do not include carotenoid in their model. The model bears remarkable similarity to the model obtained by X-ray crystallography, and predates it by six years.

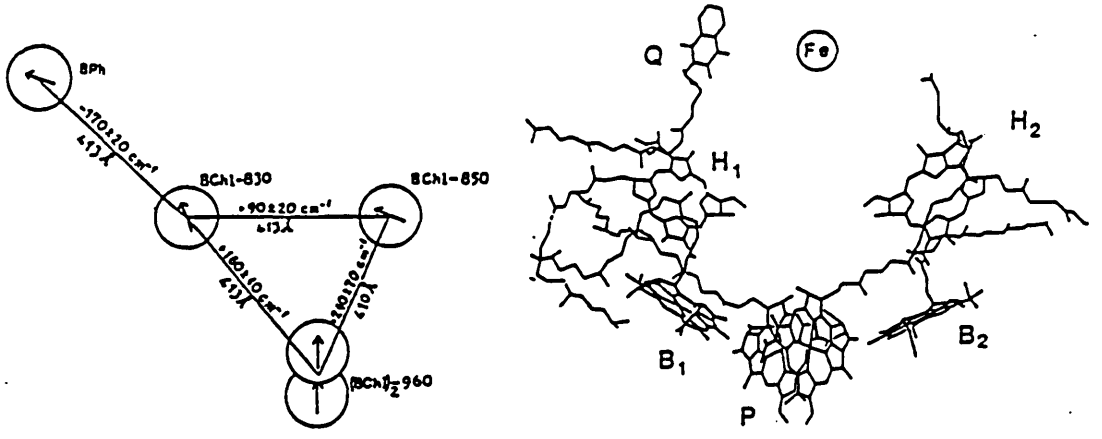


Fig. 1.17.(a) Arrangement of the pigments in *Rps. viridis* reaction centres, determined from circular dichroism and photodichroism. (Shuvalov & Asadov, 1979). (b) The arrangement of BChl and BPheo in bacterial reaction centres, determined from X-ray crystallography (Michel *et al*, 1986).

1.4.4.6. Ultraviolet Circular Dichroism of the Bacterial Reaction Centre

A different application of circular dichroism is the semi-empirical determination of protein secondary structure from the CD spectrum in the far ultraviolet (260-190nm). The methods of analysis, and the problems associated with them for the analysis of hydrophobic membrane-bound proteins, were discussed in the previous section. Despite these deficiencies, Nabedryk *et al* (1982) were able to estimate the relative amounts of different secondary structures in several pigment-protein complexes. Breton & Nabedryk (1987) report the amounts of α, β, and less ordered structures in different complexes from *Rb. sphaeroides*. They note a higher amount of α-helical structure in the L and M subunits (55%) than in the H-subunit (31%).

1.4.5. LINEAR DICHROIC SPECTROSCOPY

The techniques employed in the measurement of the anisotropic arrangement of components in a sample were described above. Below, I summarise the results of such experiments performed on bacterial reaction centres. Larger LD signals are obtained for particles which have a high degree of orientation in the squeezed gel. For this reason, LD of bacterial reaction centres has been measured using aggregated particles. Comparison of the LD of these aggregates with that of chromatophores shows that the reaction centres aggregate in discs, the plane of which is equivalent to the membrane plane (Breton, 1985). That is, the transmembrane axis of the reaction centre is perpendicular to the plane of the aggregate. The orientations of the pigments determined from LD spectra have been confirmed by the X-ray structure, and Breton (1985) gives a detailed discussion of the transitions.

The low temperature linear dichroism spectrum of the reaction centre from *Rps. viridis* is shown in Fig.1.18. Breton (1985) ascribes the 990nm and 850nm transitions to the (+) and (-) exciton states of the Q_y transitions of the special pair. The equivalent Q_X transitions occur at 620nm and at 660nm. The LD/A spectra show that all four transitions of the two monomeric accessory BChls (B_L, B_M) are oriented at approximately 70° from the C_2 symmetry axis. The Q_y transitions of the two bacteriopheophytin molecules are oriented at approximately 40° from the C_2 symmetry axis, while the Q_X transitions are tilted at 70-75° from this axis.

Similar assignments are made for the pigments in the reaction centre of *Rb. sphaeroides*, by comparison with the better resolved spectrum from *Rps. viridis* (Breton & Nabedryk, 1987). The LD spectrum again agrees well with the model derived from X-ray crystallography.

Photoselection experiments have shown the angle between the carotenoid transition and

the long wavelength transition of the special pair is about 75° (Vermeglio *et al*, 1978). Thus, the carotenoid molecule has its transition quite perpendicular to both the C_2 symmetry axis and to the 990nm transition. For the carotenoid to act as an efficient triplet energy acceptor from the reaction centre spin-polarised triplet, it must be located quite close to the special pair for orbital overlap between the two species (Parson & Monger, 1977). Resonance Raman spectroscopy has demonstrated that the carotenoid in purple bacterial reaction centres contains *cis* bonds, leading to a bent structure for the carotenoid. Refinements of the X-ray model have shown that this bent molecule lies between the special pair and the accessory bacteriochlorophyll on the non-photochemical (M) arm of the reaction centre (Yeates et al, 1988).

1.4.6. INFRARED SPECTROSCOPY OF THE AMIDE BOND IN REACTION CENTRES

The first infrared investigation of isolated bacterial reaction centres from *Rb. sphaeroides* was performed by Nabedryk *et al* (1982). Amide infrared bands were observed at 3300 cm^{-1} (Amide A, N-H stretch), 1656 cm^{-1} (Amide I, C=O stretch), and 1543 cm^{-1} (Amide II, N-H bend). The transition at 1738 cm^{-1} is due to a lipid ester carbonyl stretch, and indicates that lipid is bound to the complex. The transition at 1250 cm^{-1} is due to PO_2^- stretching, those at around 2900 cm^{-1} due to the different CH_2 stretching modes, and the shoulder at 1515 cm^{-1} arises from absorption by tyrosine residues. The presence of α-helical structure is evident from the position of the Amide I maximum at 1656 cm^{-1}. The assymetry of the amide I band was tentatively ascribed to the presence of some β-sheet absorbing at about 1630 cm^{-1}.

The dichroism of the amide transitions was measured using reaction centres reconstituted into lipid vesicles and then air-dried onto CaF_2 windows. The various amide IR bands were dichroic when passing linearly polarised light. The Amide A and Amide I bands showed the same dichroism for both native chromatophore membranes and for the reconstituted reaction centres. The 1630 cm^{-1} shoulder on the Amide I absorption band had the opposite dichroism. It is known that the Amide I (C=O stretch) and the Amide A (N-H stretch) are oriented parallel to the axis of an α-helix, and that Amide II (N-H bend) is oriented perpendicular to the helix axis (see above). This experiment qualitatively demonstrates that in both native chromatophores and reconstituted reaction centres the α-helices of the membrane-bound proteins are oriented with their axes rather perpendicular to the membrane plane.

The average tilt angle of the trans-membrane helices was estimated at between 20 and 25°. In the model derived from the X-ray diffraction pattern, the 10 roughly parallel

helices of the L/M complex lie at less than 30° to the C_2 symmetry axis. Combining these two observations, Breton & Nabedryk (1987) conclude that the C_2 symmetry axis is aligned *in vivo* along the normal to the membrane plane, as was previously proposed (Deisenhofer *et al*, 1985).

1.4.7. ESR AND ENDOR SPECTROSCOPY

The many EPR measurements on the bacterial reaction centre have identified features of the primary donor and acceptors.

1.4.7.1. The Primary Donor

Loach & Walsh (1969) observed a photoinduced g=2 signal in purified reaction centres from *Rb. sphaeroides* R-26 which had the same rise and decay kinetics as the 870nm bleach, and the same mid-point redox potential. Further evidence that this EPR signal is due to the oxidised primary donor is provided by their identical action spectra, their production by chemical oxidants, and the absence of the EPR signal in mutants lacking reaction centres. Feher's group compared this signal with that of oxidised bacteriochlorophyll *in vitro* (McElroy *et al*, 1972, 1972; Feher, 1971), and found the proton hyperfine splittings reduced by a factor of 1.4 in the reaction centre. Norris *et al* (1971) proposed that the unpaired electron on the oxidised reaction centre primary donor may be shared equally by two bacteriochlorophyll molecules. The primary electron donor appeared to be a dimer, or "special pair" of strongly interacting bacteriochlorophyll molecules. This proposal was strengthened by results from the related technique of electron nuclear double resonance (ENDOR) (Feher *et al*, 1973, 1975; Norris *et al*, 1973).

Reaction centres from *Rps. viridis* showed reduction in the splittings of 1.16, suggesting less equal sharing of the electron over the "special pair". A slightly different geometry of the special pair is observed in the crystal structures of the two reaction centres, that may explain the difference in the EPR signals.

1.4.7.2. The primary acceptors

Illumination of *Rb. sphaeroides* reaction centres at low temperature results in the formation of the g=2 signal, and a much broader g=1.8 signal (McElroy *et al*, 1970, Feher, 1971; Feher *et al*, 1972). This has a mid-point redox potential equivalent to that of the primary electron acceptor (-50 mV, pH 7.0) and can also be generated by chemical reduction (Dutton & Leigh, 1973). Removal of iron from reaction centres results in loss of the g=1.8 signal. Removal of quinones prevents the light-driven appearance of this signal (Okamura *et al*, 1975). An Fe-Q primary acceptor complex, a "ferroquinone

complex", was proposed (Feher *et al*, 1972; Okamura *et al*, 1975). Removal of iron from the reaction centre results in a 50% reduction in the rate of electron transfer from Q_a^- to Q_b (Debus *et al*, 1986), but a much larger reduction in the rate of electron transfer from $BPheo_L^-$ to Q_a (to 2% of the original rate). However, relacement of the iron atom by zinc does not affect the electron transfer rate. This suggested (Kirmaier et al, 1986), that it is the electric field surrounding the metal atom that is important for efficient transfer from BPheo to quinone.

The oxidation of the reaction centre special pair occurs in less than 10 psec (Netzell *et al*, 1973). The g=1.8 signal is not observed until 150 psec later. Therefore it was concluded that there must be an intermediate electron acceptor. A photoinduced EPR signal is observed under reducing conditions, and is similar to that of singly reduced chlorophyll or pheophytin. Thus the primary electron acceptor is a monomeric tetrapyrrole, in contrast to the dimeric electron donor. Optical data identified this intermediary acceptor as a photoreducible bacteropheophytin (see above).

A different EPR signal is observed under reducing conditions, which has two additional broad lines (Tiede *et al*, 1976). This doublet signal is attributed to a magnetic interaction between the unpaired electron on $Pheo^-$ and the Fe^{2+}-Q^- complex. The magnitude of the exchange coupling predicts a distance of 8Å between Pheo and Q (Hopfield, 1974).

1.4.7.3. The spin-polarised reaction centre triplet

When reaction centres are chemically reduced (e.g. by sodium dithionite), the bacteriochlorophyll cation (doublet) EPR signal can no longer be seen. It is replaced by an EPR triplet signal with unusual properties (Dutton *et al*, 1972; Leigh & Dutton, 1974; Thurnauer *et al*, 1975). In normal triplets formed by intersystem crossing, the two unpaired electrons split into three energy levels in a strong magnetic field. The reaction centre triplet is unusual because only the centre T_o level is populated, i.e. the spin of the unpaired electron is strongly polarised, and the triplet is known as the "spin-polarised triplet". Such polarisation indicates that the triplet is formed from some polarised intermediate, such as a biradical or charge transfer state, and not directly from the unpolarised single state (Dutton *et al*, 1973; Uphaus *et al*, 1975). Thus recombination of charges when forward electron transfer is blocked is a likely mechanism for generating this triplet.

The spin-polarised triplet signal was first observed in reaction centres from carotenoidless mutants, e.g. *Rb. sphaeroides* R-26. It is never detected in carotenoid-containing strains. Instead, optical signals are observed which correspond to the formation of a carotenoid triplet (Cogdell *et al*, 1975). Carotenoids are efficient quenchers of chlorophyll triplets in solution (Raman & Tollin, 1971, and see Halliwell &

Gutteridge, 1985), so it was concluded that the reaction centre triplet was quenched rapidly by the carotenoid, such that it is not observed. The harmful consequences of formation of the spin-polarised triplet and the protective role of carotenoids were discussed above.

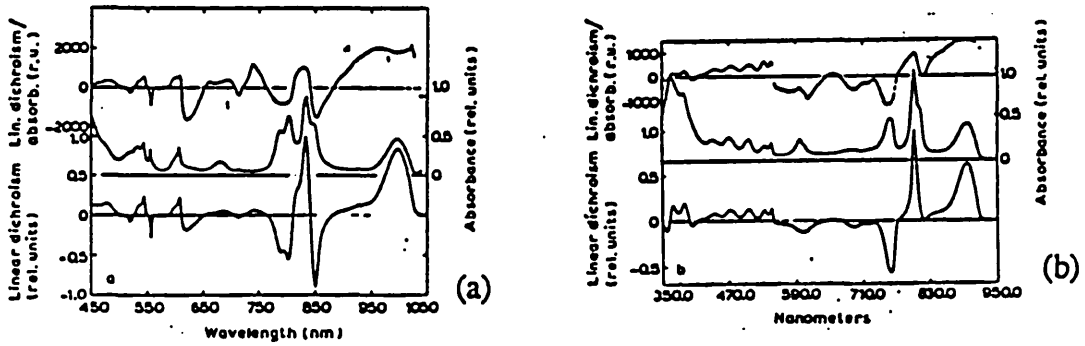


Fig. 1.18. Low temperature (4K) linear dichroism (LD), absorption (A), and LD/A spectra of neutral reaction centres from (a) *Rps. viridis*, and (b) *Rb. spharoides* 2.4.1 (from Breton & Nabedryk, 1987).

1.5. SPECTROSCOPIC PROPERTIES OF PHOTOSYSTEM 2

The light reactions occuring in higher plants are more complex than in bacteria, due to the presence of two photosystems with different redox properties which cooperate to extract electrons from water to reduce NADP. The properties of the two photosystems can be studied individually in intact membrane systems through the use of electron transport inhibitors, artificial electron donors and acceptors, or by excitation with light actinic for one or the other system. An alternative approach is to physically separate the systems by biochemical fractionation of the thylakoid membranes with detergents. Because of the large number of different pigment-protein complexes in the thylakoid membrane, and the close association of antenna pigment-proteins with the reaction centres, it has been possible only recently to obtain reaction centre preparations of comparable purity to those obtained from bacteria. I therefore summarise some results from preparations of different degrees of purity with respect to the reaction centre of Photosystem 2.

1.5.1. STEADY-STATE ABSORPTION PROPERTIES OF DIFFERENT PARTICLES

1.5.1.1. Thylakoid membranes

The absorption spectrum of fully-stacked thylakoid membranes from pea (Fig. 1.19) shows transitions due to Chl*a* (438, 679nm) and Chl*b* (653nm) and carotenoid pigments (450-510nm). The ratio of Chl*a* to Chl*b* varies between 2.7 and 3.2, depending on growth conditions.

1.5.1.2. Photosystem 2-enriched membranes

Photosystem 2-enriched membranes (granal membrane fragments) also show peaks due to Chl*a* (679, 436nm) and Chl*b* (468nm peak, 484nm shoulder) (Fig. 1.19). The ratio of Chl*a* to Chl*b* is 1.8-1.9. This enrichment in Chl*b* with respect to thylakoid membranes is due to the location of the Chl *a/b* light-harvesting complex primarily in the granal stacks. This is seen in the absorption spectrum as a larger ratio of the Chl*b* absorption at 470nm to the Chl*a* absorption at 436nm in PS2-enriched membranes.

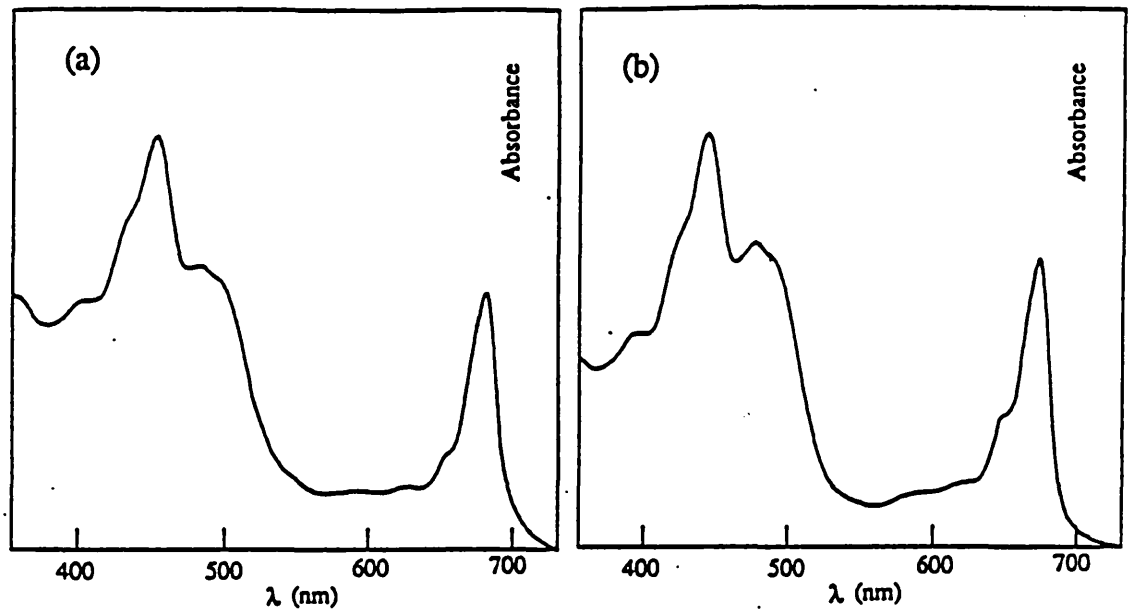


Fig.1.19. Absorption spectra of (a) fully stacked thylakoid membranes from pea, and (b) PS2-enriched membranes (BBY's) from pea, both in 50mM Tris-Cl buffer, pH 7.2.

1.5.1.3. Purer PS2 samples

The absorption properties of more highly purified PS2 complexes (core and reaction centre complexes) are discussed in Chapter 3 of this thesis.

Various chemically- or light-induced absorption changes have revealed the nature of the primary donor and acceptors of Photosystem 2. This work is now reviewed.

1.5.2. ABSORPTION DIFFERENCE SPECTROSCOPY OF THE PRIMARY ELECTRON DONOR

An absorption change attributed to oxidation of the primary donor of Photosystem 2 was measured by Doring *et al* (1969). This consisted of a large bleach at 680nm with a smaller bleach observed at 635nm. These changes were not excited by far-red light, (>720nm), and were inhibited by DCMU. It has large bleaches at 677-680nm, 430nm, and a broad absorption increase at 820nm. This long wavelength band is analogous to the 1025nm absorption band of the BChl*a* cation and the 1245nm band of the BChl*b* cation seen in oxidised reaction centres of purple photosynthetic bacteria, and predicted from molecular orbital calculations (Otten, 1971). The difference spectrum alone is not sufficient to determine whether P680 is a monomeric Chl*a*, or a dimer forming a "special pair", like the primary donor of purple bacterial reaction centres. The mid-point redox potential of this difference spectrum has not been measured directly, since it is very oxidising, but indirect estimates have been made (see below, Section 1.5.3.5).

1.5.3. ABSORPTION DIFFERENCE SPECTROSCOPY OF THE PRIMARY ELECTRON ACCEPTORS

1.5.3.1. Quinone

The first stable primary electron acceptor of PS2, Q_a, was identified as a plastoquinone molecule, from the similarity of the flash-induced absorption difference spectrum of thylakoids at relatively low redox potential (van Gorkom, 1974) to the spectrum of the plastosemiquinone anion *in vitro* (Bensasson & Land, 1973). Features of this spectrum include an absorption band at 320nm, and a shift in the band at 550nm. The first stable acceptor is thus very similar in purple bacteria and PS2. However, redox transitions indicate two pools of Q_a with potentials of 35 mV and -270 mV (Horton & Croze, 1979). This heterogeneity in Q is not fully understood, but it has been suggested (Evans & Ford, 1986) that there are two Q_a species present before the site at which lipid-soluble quinone binds. The question remains unresolved.

The presence of a secondary quinone electron acceptor (Q_b), with a very similar difference spectrum to Q_a, was indicated by flash experiments in the presence or absence of herbicide. Oscillatory behaviour was observed when no herbicide was present, but not when it was (Pulles *et al*, 1976). Thus Q_a was deduced to a one-electron acceptor, and Q_b a two-electron acceptor.

1.5.3.2. Pheophytin

Following the discovery of bacteriopheophytin (*a* or *b*) as an intermediary electron acceptor in bacterial reaction centres (see section 1.4.4.2.), the same experiment was repeated on PS2-enriched thylakoid fragments (Klevanik *et al*, 1977; Klimov *et al*, 1977). A reversible light-induced difference spectrum was obtained in pea sub-chloroplast particles at redox potentials between -50mV and -550mV, when Q_a is reduced. The spectrum was observed at room temperature and at -170°C, and was accompanied by a 2-3 fold decrease in the fluorescence yield. The light-induced absorption changes and the decrease in fluorescence yield showed identical kinetics. The absorption difference spectrum is characterised by bleaching of absorption bands at 545, 670, and 685 nm, and at 408, 422-428 and 518 nm, and by the appearance of bands at 676, 655, 450 and 658 nm. The positions of these absorbance changes are consistent with those of the pheophytin anion in solution (Fujita *et al*, 1978) but red-shifted by about 20nm. The light-induced absorption changes became steadily less reversible when the redox potential of the medium was lowered from -200 mV to -400 mV.

Concurrently, these authors observed a steady decline in the fluorescence yield. The mid-point redox potential for these phenomena was measured as -610mV (Klimov *et al*, 1979). The *in vitro* potential of Pheo/Pheo$^-$ is between -610 and -640 mV (Fujita *et al*, 1978).

1.5.3.3. Reaction centre fluorescence and charge recombination

The decrease in fluorescence under conditions when pheophytin is expected to be reduced (see above) led to the proposal (Breton,1982) that this fluorescence is short-lived luminescence from P680 excitation following charge recombination from the biradical [P680$^+$Pheo$^-$]. The unpaired electron on Pheo$^-$ would reoccupy the LUMO of P, regenerating P*, which could relax to the ground state by emitting a fluorescent photon. Following reduction of P680$^+$ to P680 by an exogenous reductant, charge recombination is no longer possible when the reaction centre is in the state [P680 Pheo$^-$], since there is no available hole on P680$^+$. Reoccupation of the LUMO on P is no longer possible, since it is already occupied.

1.5.3.4. Activation energy of fluorescence from Photosystem 2

If the fluorescence does originate from a biradical, then the charge recombination may have an associated activation energy, corresponding to the energy gap between states P$^+$I$^-$X$^-$ and P*IX$^-$ (postulate Klimov *et al*, 1978). The luminescence yield was indeed observed to be temperature dependent, indicating an activation energy for the process. The fluorescence decreased when the temperature was lowered from -30 to -100°C. These data revealed an energy gap between Pheo$^-$ and P680* of 0.04eV for DT-20 fragments (PS2-enriched membranes), and 0.08eV for the more intact chloroplasts.

1.5.3.5. Estimation of the oxidising potential of P680$^+$

Given values for the mid-point redox potential for the Pheo/Pheo$^-$ couple (Klimov *et al*, 1979), the energy gap between Pheo$^-$ and P680* (Klimov *et al*, 1978), and the energy of the quantum absorbed by P680 (1.8-1.82 eV, the energy of a 680 nm photon), then the mid-point redox potential for the P680/P680$^+$ is estimated to be +1.12 ± 0.05V (Klimov *et al*, 1979). This is more than sufficient for oxidation of water ($E_{m,7}$ H_2O/O_2 = 0.82 V). The energy difference of 0.3eV also allows for the inclusion of intermediary electron transfer components between P680$^+$ and H_2O, allowing for greater flexibilty or stability. This remains the only estimate of the oxidising potential of P680$^+$. Direct redox titrations would result in the chemical oxidation of most of the pigments and protein.

1.5.4. CIRCULAR DICHROISM OF HIGHER PLANT PIGMENT-PROTEIN COMPLEXES

The first CD spectrum from a bacterial system was measured twenty years ago (Sauer *et al*, 1968) and has been the subject of much detailed discussion since. The delay in obtaining complexes of comparable purity from higher plants has meant that our present understanding of the CD signals of higher plant complexes (with the exception of those from the light-harvesting complex) is relatively poor. The CD spectra of a variety of systems have been measured : thylakoid membranes (Canaani & Sauer, 1978), BBY's (van Dorssen *et al*, 1987a), the Chl*a*/*b* light-harvesting complex (Gregory *et al*, 1980) PS2 core and reaction centre complexes (van Dorssen *et al*, 1987b; Newell *et al*, 1988). The CD spectrum of BBY's is dominated by the signal from LHC (Gregory *et al*, 1980). Some features in the CD spectrum of LHC may arise from a trimeric exciton (van Metter, 1977). Interaction between Chl *a* and Chl *b* was deduced by Gulen *et al* (1986). The carotenoid has strong CD. Core complexes show the largest CD in the Q_y chlorophyll absorption band. There is a strong negative band at 679nm, with weaker bands at 659 and 665nm.

The CD spectrum of isolated PS1 has been measured by Nabedryk *et al* (1984b). The Q_y region consists of a negative CD at 686nm, and a positive CD 670nm. As in the spectrum of thylakoids, the lowest energy CD is negative.

I postpone detailed discussion of the PS2 reaction centre CD until Chapter 5.

1.5.5. STEADY-STATE LINEAR DICHROISM OF THYLAKOID MEMBRANES

Just as the analysis of CD spectra of thylakoid-derived pigment-protein complexes has been less sophisticated than that of bacterial complexes, due to the relatively short history of highly-purified plant complexes, so the linear dichroic properties have been interpreted rather qualitatively. The linear dichroism spectrum of thylakoid membranes has a large positive peak at 680nm (Haworth *et al*, 1982a), which is due to chlorophyll molecules oriented with their Q_y transitions parallel to the membrane plane. A highly anisotropic arrangement of pigments was also observed by these authors in isolated PS1 and LHC. Thus the pigments are arranged in a specific manner in pigment-protein complexes of higher plants, and the majority of pigments have the same orientation with their Q_y transitions oriented parallel to the plane of the membrane.

I discuss the steady-state linear dichroic properties of purer preparations in Chapter 4 of this thesis.

1.5.6. LINEAR DICHROISM OF ABSORBANCE CHANGES

1.5.6.1. Orientation of the primary donor

The anisotropy of the 820nm transition of the primary donor radical cations of P680 and P700 were measured in chloroplasts oriented in a magnetic field (Mathis *et al*, 1976). Molecular orbital calculations predicted that the 820nm transition of the chlorophyll cation was polarised along the y-axis of the chlorophyll ring. This was observed experimentally for $P700^+$ (Otten, 1971), and thus assumed to be the same for $P680^+$. The absorption increase at 825 nm induced by an actinic 600nm laser flash decayed in a fast phase (t = 2.8 ms), followed by a slower phase. The rapid decay was assigned to the reduction of $P680^+$ by secondary electron donors, the slow phase to reduction of $P700^+$. The rapidly decaying absorption change was oriented in the plane of the membrane. Therefore, the Q_y transition of P680 is parallel to the plane of the membrane.

1.5.6.2. Orientation of the primary acceptor

The anisotropy of the absorption changes attributed to the $Pheo^-$ anion (see above) were invesigated by Ganago *et al* (1981). PS2-enriched membranes (DT-20 particles) were embedded in polyacrylamide gels, which were then incubated in a buffer solution containing dithionite (E_m = -450 mV). Sharp changes in the dichroism were observed in the range 660-695nm indicating the overlap of at least two components with different polarisation. The shape of these components was found using the method of Shuvalov & Asadov (1979). This separation yielded a difference spectrum for reduced pheophytin with the Q_y transition oriented approximately normal to the membrane plane, and the Q_x transition approximately parallel to the membrane. Therefore, the plane of the pheophytin tetrapyrrole was shown to lie approximately perpendicular to the plane of the membrane.

1.5.7. INFRARED SPECTROSCOPY OF THE AMIDE BOND IN HIGHER PLANT PIGMENT-PROTEIN COMPLEXES

Nabedryk *et al* (1984a) have measured the infrared spectra of thylakoids and reconstituted LHC and of reconstituted PS1 particles. The polarised infrared spectrum of the reconstituted LHC indicates a transmembrane orientation of α-helices, with the helices oriented at less than 30° to the membrane normal. A very similar arrangement was observed for the reconstituted PS1 particles (Nabedryk *et al*, 1984b).

Light-induced FTIR difference spectra have been measured by Tavitian *et al* (1986) to investigate the primary reactions in PS1 and PS2. They conclude from the photooxidised and photoreduced difference spectra that no large changes in the conformation of the protein occur as a result of charge separation in the reaction centres.

1.5.8. EPR SIGNALS FROM PHOTOSYSTEM 2

Many of the EPR signals observed in reaction centres of purple bacteria have also been seen in PS2 preparations (see Rutherford, 1985b). These include the g=2.0027 signal of P^+ (Visser *et al*, 1977), the EPR doublet signal from the primary semiquinone-iron complex, Q_a-Fe (Nugent *et al*, 1981), its altered signal when Pheo is reduced (Klimov *et al*, 1980a), and the spin polarised triplet formed after radical pair charge recombination (Klimov *et al*, 1980b). The signals due to the primary electron acceptors are essentially identical to the equivalent signals observed in purple bacterial reaction centres, indicating that both systems have a very similar arrangement of the primary electron acceptor complex. The EPR signal of the primary donor, however, suggests a monomeric chlorophyll rather than a dimeric "special pair", and the spin-polarised triplet signal is polarised parallel to the plane of the membrane, in contrast to the same signal in bacterial systems which is oriented perpendicular to the membrane plane (see Rutherford, 1985a, 1985b).

Several EPR signals have been observed that are peculiar to Photosystem 2. These are the S_2 multiline signal associated with the OEC, a g=4 component from an oxidised carrier close to S_2, a signal ascribed to cytochrome b_{559} in its oxidised form, and signal II from an electron donor in PS2. All these signals belong to components on the oxidising side of PS2.

1.5.8.1. The S_2 multiline signal

This signal is thought to arise from the oxidation of a manganese complex which catalyses the oxidation of water to molecular oxygen. It is associated with the S_2 state of the water-splitting complex (Dismukes & Siderer, 1980).

1.5.8.2. The g=4 component

This signal is thought to arise from a component acting as a carrier closer to the reaction centre than S_2 (Zimmerman & Rutherford, 1984). It may function as a donor to the component which gives rise to Signal II_{vf}, and further as an acceptor to bring about the oxidation of S_1 to S_2.

1.5.8.3. Signal II

An EPR signal at g = 2.0045 is formed after direct electron donation to the oxidised primary donor, $P680^+$ (Ghanotakis & Babcock, 1983). Its kinetics vary dependent on the state of the water-oxidising system. In intact preparations, it is denoted Signal II_{vf} (very fast), and in Tris-treated samples, in which the water-splitting complex is inactivated, as Signal II_f (fast). The species giving rise to these signals is called Z.

Another EPR signal has been observed which is almost identical to that from Z, except that it is very stable and is present in all untreated plant material in the dark. This signal is denoted Signal II_s (slow), and the molecular species giving rise to it is called D. The physiological role of D is not known, but when reduced it can reduce S2 and S3 (Velthuys & Visser, 1975; Boussac & Etienne, 1982), as well as Z^+ in Tris-washed material. It has been attributed to a plastosemiquinone cation (O'Malley & Babcock, 1984).

Recent site-directed mutagenesis of the D2 polypeptide has revealed that D is identical with tyrosine D2-160 (Debus *et al*, 1988; Vermaas *et al*, 1988). In view of the symmetry of D1 and D2, it was suggested that Z is the tyrosine residue D1-161, and not a radical of plastoquinone as earlier suggested (see Prince, 1988). Substitution of this residue with phenylalanine leads to loss of oygen-evolution,a slower fluorescence induction rise in the presence of DCMU, and an altered fluorescence emission maximum (Debus *et al*, 1989, submitted). Metz *et al* (in preparation) have accomplished the same substitution, and observe loss of Signal II_f in Tris-washed Photosystem 2 particles. This particle also lacks the optical spectrum of Z^+, but retains Signal II_s, due to D^+ (P. Nixon, DuPont, pers. comm.).

1.5.9. SPECTROSCOPIC SIMILARITIES BETWEEN THE REACTION CENTRES OF PURPLE BACTERIA AND PHOTOSYSTEM 2

From the summary above, it is clear that the bacterial and oxygen-evolving systems share some common features in both their pigments and proteins. The reducing side in both systems employs photoreducible primary and secondary quinone, a non-haem iron atom, and (bacterio)pheophytin. The proteins of both systems are rather hydrophobic, are located in lipid membranes, and contain a large proportion of transmembrane α-helices. However, there are significant differences, mostly revealed by the EPR signals associated with the water-splitting complex which are peculiar to Photosystem 2.

CHAPTER 2 : MATERIALS AND METHODS

2.1 PREPARATION OF COMPLEXES FROM HIGHER PLANTS

2.1.1. Thylakoid membranes

Chloroplast thylakoid membranes were isolated according to a published method (Nakatani & Barber, 1977) except for the use of a modified grinding medium of 50mM KH_2PO_4 (pH 7.5, with NaOH), 0.35M KCl, 0.5mM EDTA, followed by centrifugation (5000 x g, 4°C, 10 min) to pellet the chloroplast fraction. The pellet was resuspended in 6mM $MgCl_2$ to rupture intact chloroplasts by osmotic shock. The thylakoid membranes were then resuspended in a buffer containing 0.2M sucrose, 0.1M NaCl, 3mM $MgCl_2$,and 50mM Tricine (pH 8.0) before further centrifugation to separate thylakoid membranes (as a pellet) from the outer envelopes of the chloroplasts.

2.1.2. PS2-enriched membranes (BBY's)

Membranes enriched in PS2 were prepared from the pelleted thylakoids according to the method of Berthold *et al* (1981) by resuspension to a chlorophyll concentration of 3mg chlorophyll/ ml in a solubilisation buffer of 5mM $MgCl_2$, 15mM NaCl, 20mM Mes (pH 6.3) and incubation on ice in the dark for 45 min before adding 10% Triton X-100 (TX-100) (w/v) in the same solubilisation buffer to a final detergent concentration of 3%. The mixture was incubated for a further 30 min on ice in the dark. Centrifugation (40000 x g, 4°C, 30 min) yielded a pellet which was resuspended and washed in solubilisation buffer containing 10% (w/v) glycerol. After the membranes were pelleted again, they were resuspended in the same buffer and stored at -80°C.

2.1.3. Oxygen-evolving PS2 core complex

Oxygen-evolving cores were prepared according to the method of Ikeuchi et al (1985). BBY's were washed with a medium containing 0.4M sucrose, 10mM NaCl and 40mM Mes-NaOH (pH 6.5) (MSN medium), and solubilised with 60mM OGP (1-O-n-octyl-β-D-glucopyranoside), 10mM NaCl and 20mM Mes-NaOH (pH 6.5) at a chlorophyll concentration of 1 mg/ml. Undissolved material was removed by centrifugation (20,500 x g, 10 min). The resulting supernatant was placed on a 10-30% sucrose linear gradient which contained 60mM OGP, 10mM NaCl, 20mM Mes-NaOH (pH 6.5), which was then centrifuged with a Kontron TFT 65.38 fixed-angle rotor (150,000 x g , 4°C, 4 hours). The pellet of oxygen-evolving PS2 core complexes was

resuspended in the MSN medium and stored at -80°C. The sample was subsequently resuspended in 50mM Tris-Cl (pH 7.2), for spectroscopic measurements.

2.1.4. Photosystem 2 reaction centre preparation

Reaction centres were prepared from pea (*Pisum sativum var.* Feltham's First) following the original procedure of Nanba & Satoh (1987) for isolation of a similar complex from spinach (*Spinacia oleracea*) with some modifications introduced by Chapman *et al* (1988). The procedure consists of solubilisation of PS2-enriched membranes (see above) with the detergent Triton X-100 (TX-100), followed by ion-exchange chromatography.

This is the method described by Barber *et al* (1987) and Chapman *et al* (1988). PS2-enriched membranes (200 mg chlorophyll) were washed in 50mM Tris-Cl buffer (pH 9.0, 0.8 mg Chl/ml) and incubated on ice in the dark for 10 min to remove the extrinsic polypeptides of the water-splitting apparatus. The pellets obtained after centrifugation (40000 x g, 4°C, 20 min) were resuspended in 50 mM Tris (pH 7.2, 200ml) and 33ml of 30% (w/v) TX-100 added to give a final chlorophyll concentration of 0.8 mg/ml and a ratio Triton:chlorophyll of 50:1 (w/w). The mixture was incubated in the dark on ice (<4°C) whilst being stirred, then centrifuged (100,000 x g, 1h). The supernatant was placed on a chromatography column (20 x 120 mm) containing Fractogel TSK DEAE-650(S) (Merck-BDH). The column was washed overnight with 30mM NaCl in a buffer containing 0.2% TX-100, 50mM Tris-Cl, until no more free chlorophyll emerged from the column. The PS2 reaction centre complex was released from the column following application of a NaCl salt gradient (30 to 200 mM) at approximately 110mM NaCl. The eluted samples were pooled, and applied to a second, smaller, column (10 x 60 mm) containing the same column material (DEAE-Fractogel). Application of a salt gradient (30 to 200 mM NaCl) followed a less extensive wash at 30mM NaCl. Elution of the complex again occurred at 110mM NaCl.

2.2. PREPARATION OF SAMPLES FROM *RHODOBACTER SPHAEROIDES*

2.2.1. Method of culture of *Rb. sphaeroides*

A carotenoid-containing strain of *Rhodobacter sphaeroides* (strain 8253 - kind gift of Dr. Neil Hunter, Sheffield University) was grown anaerobically in the light in a medium comprising M22+ medium, an enriched version of M22 (Sistrom, 1977), Solution C, Vitamins and 0.1% Casamino acids. The composition of each of these components, (given in g/litre), was as follows:

M22+ medium (pH 7.6, autoclaved) : KH_2PO_4 (3.6), $KH_2PO_4.3H_2O$ (3.0), sodium lactate (70% w/v solution, 2.0 g/l), $(NH_4)_2SO_4$ (0.5), sodium succinate (4.6), sodium glutamate (0.27), aspartic acid (0.04), Solution C (20 ml/l).

Solution C (autoclaved, stored at -20°C): Nitrilotriacetic acid (10), $MgCl_2.6H_2O$ (24), $CaCl_2.6H_2O$ (3.34), Na_2EDTA (0.124), $ZnCl_2$ (0.261), $FeCl_2.4H_2O$ (0.251), $(NH_4)Mo_7O_{24}.4H_2O$ (0.009), $CuCl_2.2H_2O$ (0.008), $Co(NO_3)_2.6H_2O$ (0.012), H_3BO_3 (0.006).

1000x vitamin stock solution (filter sterilised, stored at 4°C) (mg/l): Nicotinic acid (1000), thiamine (500), p-aminobenzoic acid (100), biotin (10).

The cells were grown anaerobically in batches of 20 l at a light intensity of 30 W/m^2 provided by 40W light bulbs at a distance of 30 cm from the surface of the flask. The surrounding air was circulated by an electric fan, such that a constant temperature of 35-37°C was maintained inside the flask. The cells were continuously circulated by a magnetic stirrer bar at the bottom of the flask. Anaerobic conditions were maintained by filling the vessel to the top, which was then tightly stoppered.

After 4-5 days growth, the cells were concentrated by passage through a Millipore Pellicon transmembrane tangential flow cell followed by centrifugation (7000 x g, for 20 min). Between 80 and 100 g (wet weight) of cells were obtained from the 20 l culture, and stored in Tris-EDTA (TE) (10mM, pH 7.5) at -20°C.

2.2.2. Preparation of chromatophores

The thawed cells were washed in TE (10mM, pH 7.5), and pelleted by centrifugation (7000 x g, 20 min). Membranes were separated from the cell walls by sonication using an MSE Soniprep 150 sonicator. 50 ml batches were subjected to 3 x 60 sec bursts of sonication, on ice to prevent excessive heating. The sonicated material (10ml portions) was loaded onto a sucrose density step gradient (12ml of 40% (w/v) sucrose in TE, beneath 12ml of 15% (w/v) sucrose in TE). Following centrifugation (27,000 x g, 3 hours), the membranes were obtained as a sharp band at the junction of the step gradient. Cell walls pelletted at the bottom of the tube. Ribosomes occur at the top of the 15% sucrose layer. The membranes were removed from the gradients using a pasteur pipette, and stored at -20°C.

2.2.3. Preparation of the reaction centres

Reaction centre were prepared according to the method of Jolchine and Reiss-Husson (1974), with some modifications suggested by Prof. Richard Cogdell (Glasgow

University). Chromatophores were incubated with the detergent laurylaminediamineoxide (LDAO) at 26°C for 10 min in 0.1M sodium phosphate buffer, pH 7.5, at a concentration 0.25% LDAO and an absorbance at 850nm of 50. The presence of 100mM NaCl increases the extent of solubilisation of the antenna pigment-protein complexes (R. Cogdell, pers. comm.). Insoluble material was removed by centrifugation at 5°C (16000 x g, 10 min), and the supernatant further centrifuged (150,000 x g, 2h).

The absorption spectrum of the supernatant was measured to assess the relative concentration of crude reaction centres. If this was not high enough, i.e. if the ratio of the optical density at 865nm and 800nm was less than 0.25, the supernatant was discarded, and the pellets resuspended in buffer. The solubilisation process was repeated on this sample. A maximum of two solubilisations was sufficient to obtain a satisfactory supernatant.

This supernatant was treated 5°C with ammonium sulphate (22% w/v) in 100mM sodium phosphate buffer, pH 7.5, containing 0.3% LDAO, pH 7.5. The crude reaction centre was recovered after a 10 min centrifugation at 27,000 x g, and redissolved and dialysed against 0.1M sodium phosphate buffer, pH 7.5, containing 0.3% LDAO. Remaining insoluble material was removed by a 10 min centrifugation at 27,000 x g.

The final purification was accomplished according to the method of Feher (1971), which employs successive ammonium sulphate cuts from 22% (w/v) to 16% (w/v). Pure reaction centres were obtained as a floating pellet.

The purity of the sample was estimated from comparison of the absorption spectrum with published spectra. Only the most satisfactory batches were used for subsequent measurements.

2.3. BIOCHEMICAL CHARACTERISATION OF THE PREPARATIONS

2.3.1. Sodium dodecyl sulphate - polyacrylamide gel electrophoresis (SDS-PAGE)

The polypeptide composition of samples was checked by SDS-PAGE. Samples were solubilised by the detergent sodium dodecyl sulphate (SDS) (10 min, 40°C) using a solubilisation buffer with the following composition: 4% (w/v) SDS, 40% sucrose (w/v), 2% (v/v) mercaptoethanol, in 250mM Tris-Cl, pH 7.8.

Solubilised samples were separated by electrophoresis through polyacylamide following the method of Laemmli (1970). The composition of the stacking gel was: 125mM Tris-Cl, pH 6.8, 2mM EDTA, 0.1% (w/v) SDS, 6% (w/v) acrylamide. A 7-17% linear

gradient acrylamide gel was used to resolve the polypeptides. Its composition was: 400mM Tris-Cl, pH 8.9, 2mM EDTA, 0.1% (w/v) SDS, 7-17% (w/v) acrylamide, 2.5-10% glycerol.

2.3.2. Spectroscopic determination of pigment content

The concentrations of chlorophyll *a* and *b* were estimated using the method of Arnon (1949). This method uses the different extinction coefficients of the pigments in an 80% acetone solution at their absorption maxima (663nm for Chl *a*, 645nm for Chl *b*), first measured by MacKinney (1941). Two simultaneous equations are solved:

$OD_{663} = 82.04 * [Chl a] + 9.27 * [Chl b]$,

$OD_{645} = 16.75 * [Chl a] + 45.6 * [Chl b]$,

to give the concentrations of each pigment as a function of the absorbances at 663nm and 645nm:

$[Chl a] = 0.0127 * OD_{663} - 0.00269 * OD_{645}$,

$[Chl b] = 0.0229 * OD_{645} - 0.00468 * OD_{663}$.

Thus the total chlorophyll concentration (g/l) is:

$[Chl]\ (g/l) = 0.0202 * OD_{645} + 0.00802 * OD_{663}$, or

$[Chl]\ (\mu g/ml) = 20.2 * OD_{645} + 8.02 * OD_{663}$.

The pigments were extracted from the sample by addition of 80% acetone to the sample followed by centrifugation to pellet the protein, leaving the extracted pigments in the supernatant.

An alternative spectroscopic method was used to estimate the relative concentrations of chlorophyll and β-carotene (Wellburn & Lichtenhaler, 1984).

The formulae used are those for pigment extracts in 80% acetone:

$[Chl a] = 12.21 * OD_{663} - 2.81 * OD_{646}$,

$[Chl b] = 20.13 * OD_{646} - 5.03 * OD_{663}$,

$[Car_{tot}] = (1000*OD_{470} - 3.27*[Chl a] - 104*[Chl b]) / 229$,

where Car_{tot} is the total concentration of carotenoid (carotenes and xanthophylls).

2.3.3. Cytochrome b_{559} estimation

The concentration of cytochrome b_{559} in a particular sample was measured using a differential extinction coefficient for the fully reduced and fully oxidised cytochrome of $20mM^{-1}cm^{-1}$ (Miyazaki *et al*, 1989; in press). Two identical samples were placed in the sample and reference positions of the spectrophotometer, and the machine corrected to

give zero absorption difference in the range 600-500nm. The sample was then reduced by the addition of a few crystals of sodium dithionite. The absorption spectrum was then recorded, and the cytochrome concentration calculated from the difference in the magnitude of the peak at 559nm and the absorbance at 559nm of the line joining the troughs at 543nm and 575nm.

2.4. SPECTROSCOPIC APPARATUS AND TECHNIQUES

2.4.1. Absorption Spectrophotometry

Absorption spectra were measured using several spectrophotometers. A Perkin Elmer 554 spectrophotometer was used for rapid spectroscopic analysis of samples at different stages in the purification procedures. Higher resolution spectra and second and fourth derivative spectra were measured on a Perkin Elmer 557 double wavelength, double beam spectrophotometer with a temperature-controlled sample chamber. Low temperature (77K) absorption spectra were recorded in the Department of Biophysics, Free University of Amsterdam, using a Cary 219 spectrophotometer and an Oxford cryostat, and in London using an Aminco DW-2 UV/VIS Spectrophotometer made available by Prof. J. Palmer, Department of Pure and Applied Biology, Imperial College.

2.4.2. Absorption difference spectroscopy

The Perkin Elmer 557 spectrophotometer was used to observe light-induced absorption changes, as described in Chapman *et al* (1988) and Barber *et al* (1987). Side illumination was provided by a quartz-iodide light source with a light guide. Illumination at wavelengths longer than 660nm was provided by placing a Calflex heat filter and a 2mm Schott RG 660 cut-off filter in the light path. A 4mm Schott B38 filter was placed over the detector to prevent actinic light entering it.

2.4.3. Derivative Spectroscopy

Second and fourth derivative spectra were recorded in real time on the Perkin-Elmer Model 557 spectrophotometer, using a 5nm differentiating interval ($\delta\lambda$). A scan speed of 30 nm/min was chosen to give low-noise signals. The resolution of this instrument is quoted as ABS / (4 * $\delta\lambda$), which is 0.05*ABS for a 5nm differentiating interval.

2.4.4. Polarised Absorption Spectrophotometry

CD spectra were measured using a Jasco J-40C spectropolarimeter, in the laboratory of Dr. Alex Drake, SERC National CD Service, Department of Chemistry, Birkbeck College, London, with the assistance of Dr. Peter Udvarhelyi. LD spectra were recorded using a modified Cary 61 spectropolarimeter, in the laboratory of Prof. Dr. Rienk van Grondelle, Department of Biophysics, Free University of Amsterdam, with the assistance of Drs. Herbert van Amerongen. Both machines generate polarised light by the technique of polarisation modulation. This involves the application of a variable mechanical stress to a photoelastic modulator to induce changes in the refractive index of the optical block. Superposition of waves with a relative phase difference results in a polarised light wave. A quarter wave phase difference gives left- or right-circularly polarised light, for the measurement of circular dichroism. A half-wave retardation (positive or negative) yields two orthogonal planes of polarised light, for the measurement of linear dichroism. Intermediate retardations yield light waves with elliptical polarisation.

The instrumentation involved in the generation and detection of polarised light by this technique is described by Drake (1986). The optical theory is discussed in detail by Schellman and Jensen (1987).

2.4.5. The partial alignment of samples

Whilst chirality is an intrinsic property of asymmetric molecules, the anisotropic arrangement of components in a molecular complex are only observable if there is a net macroscopic orientation of the sample. There are several methods for introducing a net asymmetric alignment of particles in order to observe their linear dichroic properties. These include alignment in electric and magnetic fields, orientation in a flow field, stroking or stretching a film containing the sample, transport through gels, and natural orientation e.g. in a crystalline array of the sample. The method employed here is that introduced by Abdourakhmanov *et al* (1979). This technique involves thorough mixing of the sample with an unpolymerised acrylamide solution, which is then polymerised by the addition of the catalyst ammonium persulphate (APS). Squeezing the gel induces a net orientation of the samples contained within it, whose dichroic properties can then be measured using polarised light.

The composition of the gel used in this work was as follows: 14.5% (w/v) acrylamide, 0.5% (w/v) N,N'-methylenebisacrylamide, 0.03% (v/v) N,N,N',N' -tetramethyl paraphenylenediamine (TEMED), in 50mM Tris-Cl (pH 7.5). The composition of the gel could be varied, e.g. in detergent concentration or presence of electron donors or acceptors. The sample was allowed to equilibrate with the unpolymerised gel mixture for 20-30 min at 4°C (on ice), and in the dark, to prevent damage to the samples. The gel

was then polymerised by addition of a small volume of concentrated ammonium persulphate stock solution (10% w/v) to a final concentration of 0.05% (w/v).
After polymerisation, the gel was placed in a press for orientation of the sample by compression. For room temperature spectra, the samples were squeezed in one direction perpendicular to the light path in a press designed and built in the Department of Biophysics, Free University of Amsterdam. This press had quartz windows perpendicular to the light beam, enabling further compression of the gel after a mesurement. For low temperature (77K) spectra, a different press was used. This was designed and constructed in the Department of Biophysics, State Univeristy of Leiden, The Netherlands, and described by Meiburg (1985). This press is designed for squeezing the gel in two dimensions simultaneously. Before compression, the starting dimensions of the gel were 14mm x 14mm x 25mm. Compression results in reduction of the two 14mm dimensions to 10mm. The press was designed such that compression induces stresses in the gel which result in movement of the gel out of the press into a cuvette held next to it. The cuvette retains the compression of the gel, which can then be measured.
All LD spectra were measured in the laboratory of Prof. Dr. Rienk van Grondelle, Department of Biophysics, Free University of Amsterdam, The Netherlands.

2.4.7. Modifications for measurement at 77K

The ordinary absorption and linear dichroic properties of the PS2 particles were investigated at 77K using an Oxford cryostat. Formation of crack-free glasses was acheived by replacing water in the buffers with glycerol to a final glycerol concentration of 70-80% (w/v), and by the use of perspex cuvettes, which are more flexible than glass and reduced strain in the cooled samples. Samples were introduced into the pre-cooled sample chamber. Rapid freezing gave more reliable glasses. The sample chamber was flushed with helium between successive measurements, to prevent the condensation of oxygen and nitrogen in the sample chamber. The temperature was kept constant during a measurement by an Oxford Intelligent Temperature Controller.
Spectra recorded in Amsterdam were analysed using the "odp" analysis program written by Drs. Maxim Kuil, in the C programming language.

2.4.8. Fourier Transform Infrared Spectroscopy (FTIR)

2.4.8.1. Measurement of the interferogram

Infrared spectra were measured in the laboratory of Prof. D. Chapman, School of Medicine, Royal Free Hospital, London, with the assistance of Parvez Haris. The

instrument employed was a Perkin-Elmer 1750 FTIR spectrophotometer equipped with a TGS (triglycine sulphate) detector. The samples were placed between CaF_2 windows separated by a 6μm tin spacer. The sample compartment was flushed with dry air (dew point -40°C) to prevent absorption by water vapour. A temperature controller was used to maintain the samples at 4°C during the measuring period. Between 100 and 400 scans were averaged at a resolution of $2cm^{-1}$ using a medium Norton-Beer function for apodisation. All spectra were measured in the range $1400cm^{-1}$ to $1900cm^{-1}$, in the absorption range of the Amide I (C=O stretch) and Amide II (N-H' bend and C-N stretch) vibrational bands. The interferograms were recorded on a Perkin-Elmer microcomputer, and the spectra calculated using Perkin-Elmer's FFT software.
Photosystem 2 samples were manipulated before measuring the infrared spectra. Tris had to be removed, since it contains an amide bond, and thus absorbs in the region of interest. This was acheived by dialysis against 10mM HEPES buffer, pH 7.2, for 24 hours, at 4°C in the dark. The sample was then concentrated by placing the dialysis tube in solid sucrose, to give a final protein concentration of 20-50 mg/ml.

2.4.8.2. Computation of the spectrum

Fourier transform infrared spectra are measured using an interferometer, designed by Michelson in 1880. The Michelson interferometer is a device that can divide a beam of radiation into two paths and then recombine the two beams after introducing a path difference. When the beams are recombined, an interference pattern is obtained as the path length is varied. This is the information yielded by a Fourier transform spectrophotometer. For a single frequency, this interferogram is a sine wavelength with maxima (minima) when the two beams are exactly in (out of) phase. The period of the sine wave corresponds to the wavelength. For a band with a larger spectral width, the interferogram is the sum of the sine waves for all of the frequencies present. This consists of a strong signal at the point where the path difference is zero, falling away rapidly on either side. The recombined beam then passes through the sample. The detector measures the interferogram. To obtain the more useful spectrum of absorbance or transmission as a function of frequency, the interferogram is operated on by the Fourier transformation, using the Fast Fourier Transform algorithm of Cooley & Tukey (1965). The signal to noise ratio is improved by the process of apodisation, which reduce the high spatial frequencies in the interferogram. Reverse Fourier transformation results in a spectrum which is depleted in higher frequencies (e.g. noise). A medium Norton-Beer apodisation function is used in this work. Data acquisition and analysis were performed using a Perkin-Elmer Model 7300 workstation. Susi & Byler (1986) review the computational techniques used in FTIR spectroscopy.

2.4.8.3. Calculation of Second Derivative Spectra

One of the properties of Fourier transforms is that if a single-sided absorbance interferogram is multiplied by a function of the form $a.x^n$ (a parabolic weighting function), then computation of the forward transform gives the nth derivative of the spectrum. The second derivative spectra were calculated over a 13-point moving window using the OBEY program provided by Perkin-Elmer.

2.4.8.4. Fourier Self-Deconvolution

This method was first applied in the analysis of infrared spectra by Kauppinen *et al* (1981), and facilitates the analysis of spectra in which relevant data are contained in heavily overlapping bands. It uses Fourier transforms and intrinsic lineshapes to computationally resolve overlapping bands that cannot be resolved experimentally due to their intrinsic linewidth. The technique involves deconvolution of the interferogram with an intrinsic lineshape function (usually Lorentzian for infrared absorption bands) and multiplication of the interferogram by an exponentially increasing function and an apodisation function. When the reverse transform is performed, a spectrum is obtained in which the new absorbance band is narrower than the original band. The spectral deconvolution was performed using Perkin-Elmer's ENHANCE function, based on the original method of Kauppinen *et al* (1981).

CHAPTER 3 : ABSORPTION PROPERTIES OF THE CORE AND REACTION CENTRE OF PHOTOSYSTEM 2

3.1. INTRODUCTION

Steady-state absorption spectroscopy provides information concerning the type and amount of different pigments in a sample. Steady-state absorption difference spectroscopy identifies components which are altered following an experimental perturbation, such as chemical reduction or illumination. The changes are detected spectroscopically, and the energies of the maximum absorbance changes can be diagnostic for the altered pigment.

In this chapter, I examine the absorption properties of several Photosystem 2 particles, and assign some of the component bands in the absorption spectra to different pigments. The steady-state absorption properties of the isolated D1/D2 reaction centre complex are shown to be sensitive to the composition of the supporting medium. Possible explanations are examined. The absorption properties of thylakoid membranes, PS2-enriched membranes, and their component pigments were discussed in the introduction (Section 1.5.). Here, I discuss the absorption spectra of the isolated PS2 core and reaction centre complexes, and their component pigments.

3.2. RESULTS

3.2.1. Absorption spectra of constituent pigments

The major component pigments in Photosystem 2 are chlorophyll *a*, pheophytin *a*, and β-carotene. The absorption spectra of these pigments in organic solvent are shown in Fig. 3.1. The concentration of each pigment was 10 μM. Chlorophyll *a* and Pheophytin *a* were measured in acetone, β-carotene in hexane. The spectrum of pheophytin *a* was measured after adding HCl to a final concentration of 0.1mM to the chlorophyll solution, which results in replacement of the central magnesium atom by protons (Lichtenhaler, 1987). The relative magnitudes are therefore comparable between Chl*a* and Pheo*a*.

The absorption spectra of Chl*a* and Pheo*a* in ether both have a major Q transition in the red region and B transitions in the blue region of the spectrum, typical of porphyrin spectra. While the intensities of these two bands are approximately equal in the

chlorophyll spectrum, the B band is relatively more intense in the spectrum of pheophytin (approximately four times the strength of the Q band. The major peak positions and magnitudes of the bands are presented in Table 3.1.

Table 3.1 - Peak positions and magnitudes of the pigments (10 μM) in organic solvent

Chlorophyll *a*		Pheophytin *a*		β-carotene	
Position	magnitude	position	magnitude	position	magnitude
663	0.750	658	0.450	-	-
615	0.225	608	0.083	-	-
580	0.113	560	0.056	-	-
534	0.038	535	0.090	-	-
-	-	-	-	477	1.198
-	-	-	-	451	1.370
430	0.750	-	-	430	1.028
413	0.713	415	1.400	-	-
385	0.049	-	-	-	-
335	0.030	320	0.080	-	-

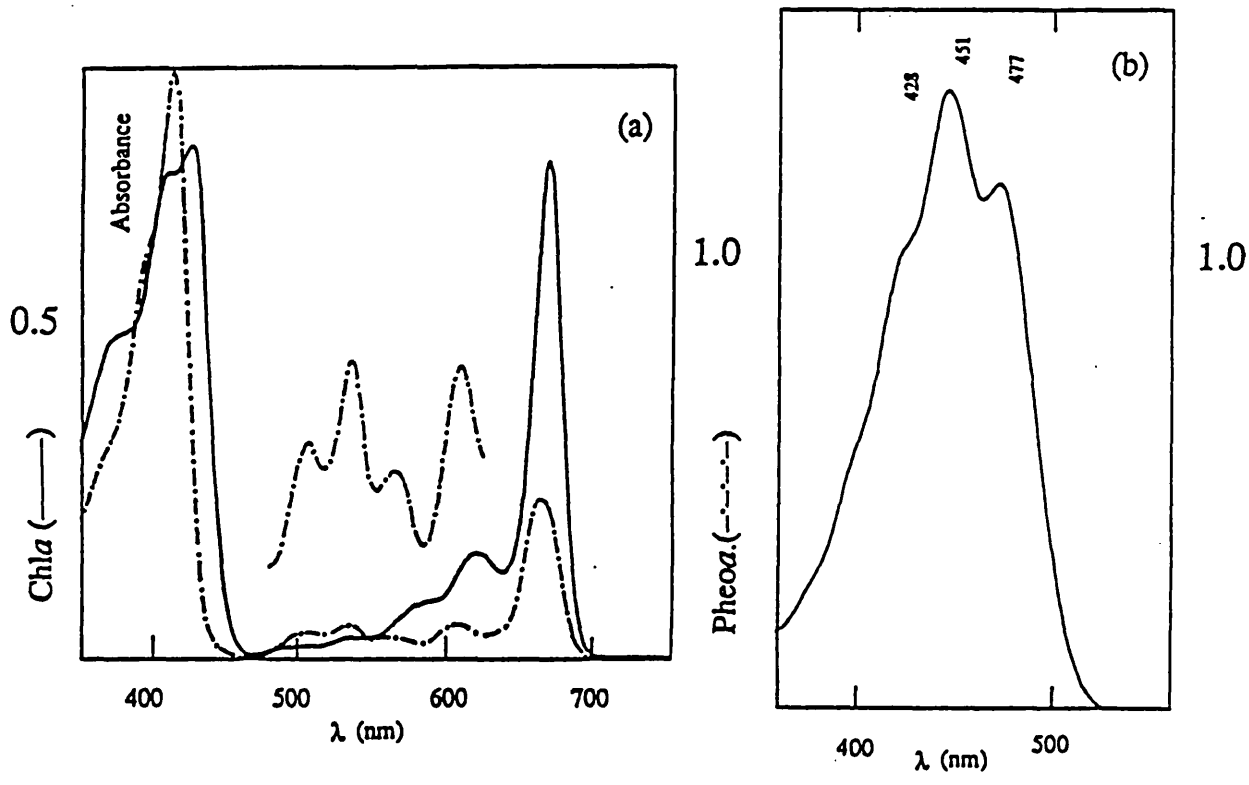


Fig. 3.1. Absorption spectra of (a) Chl*a* (———)and Pheo*a*.(–·–·–·–)(10μM in acetone), and (b) β-carotene (10μM in hexane). The spectrum of Pheo*a* was measured after addition of HCl (final concentration 100μM) to the chlorophyll solution, resulting in the replacement of the central magnesium atom by protons (see Lichtenhaler, 1987).

3.2.2. Absorption properties of the PS2 oxygen-evolving core complex

The isolation of the oxygen-evolving PS2 core complex results in loss of the LHC, and consequent loss of the Chl*b* absorption from LHC. The major Q_y Chl*a* peak is at 676nm, and the major B transition at 437nm. Two shoulders are seen in the carotenoid absorption region, at 464nm and 490nm. A transition due to pheophytin occurs at 542nm.

The low temperature spectrum of the PS2 core complex resolves the carotenoid peaks. They are seen at 463nm and 495nm. The Q_y peak is clearly composite at 77K, with the maximum at 674nm, and shoulders at 670nm, and at approximately 682nm.

The second derivative spectrum of the core complex measured at 4°C locates more precisely the positions of the component bands. It shows two transitions in the $Q_{y(0\text{-}0)}$ band, at 669nm and 679nm. The two carotenoid bands which are resolved in the absorption spectrum are seen in the second derivative spectrum at 468nm and 491nm. In the Soret region, transitions occur at 384nm, 413nm and 435nm. The 413nm transition is due to absorption by Chl*a* and Pheo*a*, and the 435nm transition exclusively to Chl*a* absorption. An inflection at 440nm possibly corresponds to the highest energy transition of β-carotene, which is obscured in the absorption spectrum by overlap with the lowest energy Soret peak of Chl*a*.

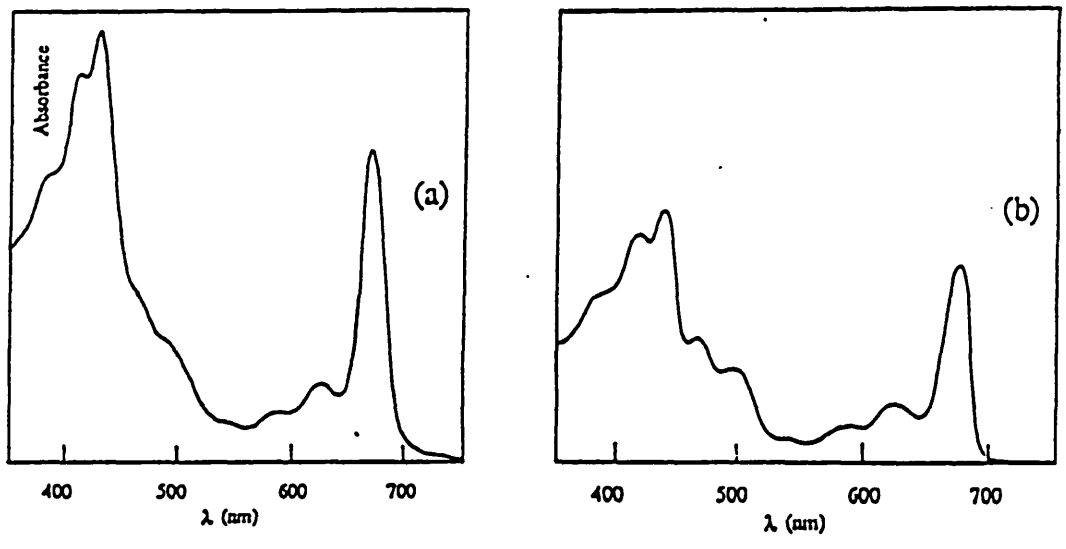


Fig.3.2. Absorption spectra of the PS2 oxygen-evolving core complex at (a) 4°C, and (b) 77K.

3.2.3. PS2 reaction centre complex

The room temperature absorption spectrum of the PS2 reaction centre complex diluted in Tris-Cl buffer (50mM, pH 7.2) is shown in Fig.3.3. I discuss the visible spectral region below, but note here the absorption of the aromatic amino acids at 270 (tyrosine absorption) and 280nm (trytophan absorption). The absorption by aromatic amino acids was shown in the original paper by Nanba & Satoh (1987). However, the magnitude of this peak with respect to the peaks in the visible region is different in their report.

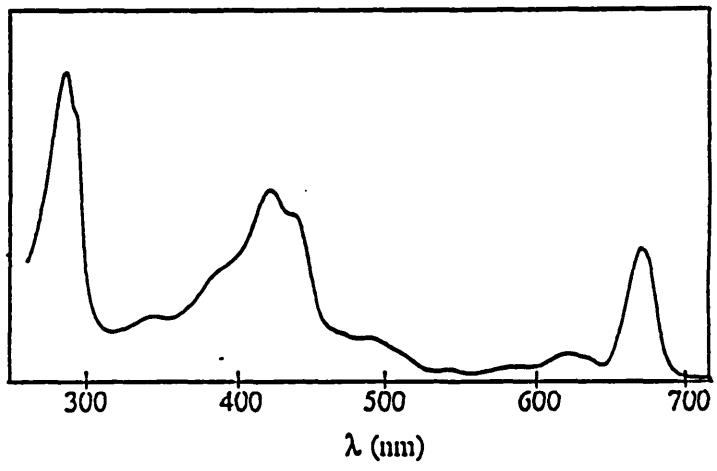


Fig.3.3. Absorption spectrum of the PS2 reaction centre (720-250nm).

Below, I present results which demonstrate that the absorption properties of the isolated D1/D2 reaction centre complex depend on both temperature and the concentration of detergent in the buffer. Absorption spectra have been measured in high detergent concentrations (0.2% Triton X-100) and in low detergent (0.02% Triton X-100), both at room temperature (4°C) and at 77K.

In all the PS2 reaction centre spectra, the relative magnitudes of the two major B transitions is reversed with respect to the core absorption spectrum. This has been ascribed to enrichment in the reaction centre of pheophytin (Barber *et al*, 1987; van Dorssen *et al*, 1987b) and $Cytb_{559}$ (van Dorssen *et al*, 1987b).

The absorption spectrum depends on the composition of the supporting medium. Two extreme and reproducible spectra are identified which are obtained in a buffer containing a high concentration (0.2%) of the detergent TX-100 (Spectrum 1) and a low concentration (0.02%) of TX-100.

The peak positions and relative magnitudes of the transitions are summarised in Table 3.2. (postn. = position of transition (nm); mag. = magnitude of the transition, normalised to the 416nm peak magnitude).

Table 3.2(a) Band positions of the absorption spectrum of the PS2 reaction centre in 0.2% TX-100.

277K			77K		
postn.	**mag.**	**assignment**	**postn.**	**mag.**	**assignment**
672	0.68	Chl/Pheo $Q_{y(0,0)}$	672	0.69	Chl/Pheo $Q_{y(0,0)}$
616	0.13	" " $Q_{y(0,1)}$	616	0.09	" " $Q_{y(0,1)}$
536	0.11	Pheo Q_x	537	0.06	Pheo Q_x
490	0.29	β-carotene	500	0.38	β-carotene
460	0.34	" "	467	0.42	" "
436	0.95	Chl*a* B	436	0.84	Chl*a* B
416	1.00	Pheo/Chl B	416	1.00	Pheo/Chl B
380	0.70	" "	380	0.58	" "

Table 3.2(b) Band positions of the absorption spectrum of the PS2 reaction centre in 0.02% TX-100.

277K			77K		
postn.	**mag.**	**assignment**	**postn.**	**mag.**	**assignment**
-	-	-	(677)	0.62	Chl/Pheo $Q_{y(0,0)}$
676	0.64	Chl/Pheo $Q_{y(0,0)}$	674	0.66	" "
620	0.12	" " $Q_{y(0,1)}$	620	0.16	" " $Q_{y(0,1)}$
542	0.10	Pheo Q_x	542	0.11	Pheo Q_x
506	0.22	β-carotene	506	0.23	β-carotene
487	0.30	" "	488	0.34	" "
460	0.33	" "	460	0.36	" "
431	0.89	Chl B_{xy}	431	0.87	Chl B_{xy}
416	1.00	Pheo / Chl B_{xy}	416	1.00	Pheo / Chl B_{xy}
380	0.57	" "	380	0.65	" "

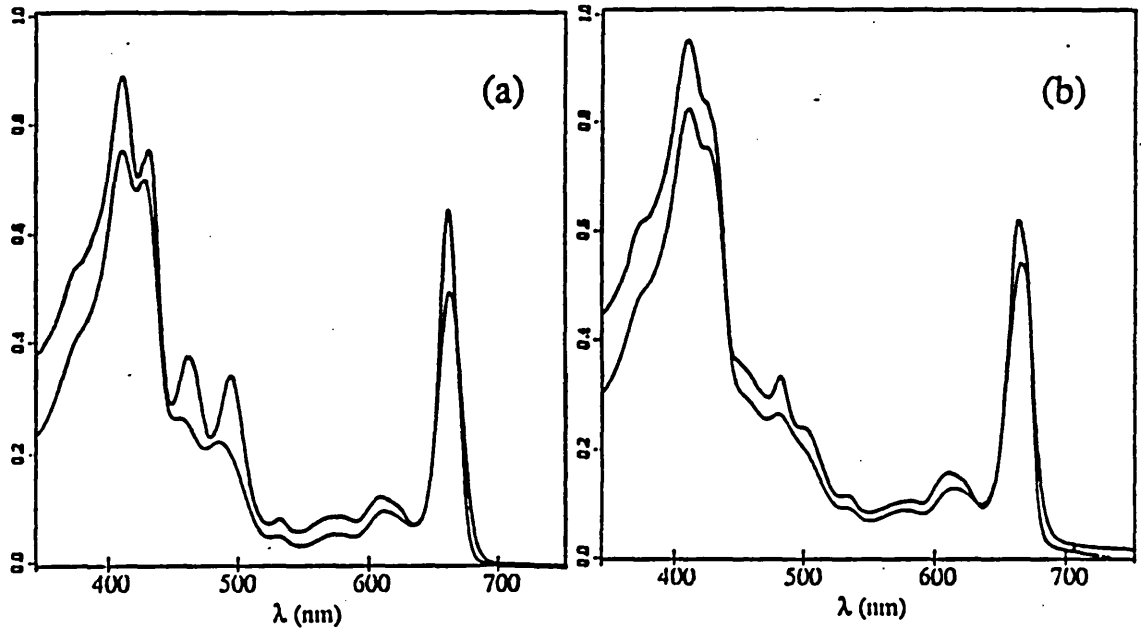


Fig.3.4. Absortion spectra of the PS2 reaction centre complex in Tris-Cl buffer, pH7.2, containing (a) 0.20% TX-100, and (b) 0.02% TX-100, at 4°C (lower traces) and 77K (upper traces).

3.2.3.1. High detergent spectrum - 4°C

The absorption spectrum of the PS2 reaction centre measured at 4°C in the presence of 10% glycerol, 0.2% TX-100, in 50 mM Tris-Cl buffer, pH 7.2, is shown in Fig.3.4.(a). The Q_y maximum occurs at 672-3nm. Two peaks due to β-carotene are seen at 458-460nm and 487-490nm (experimental variation). The Soret absorption band is dominated by two peaks at 436nm and 416nm, with a trough between them. The 416nm is the more intense.

3.2.3.2. High detergent spectrum - 77K

On cooling this sample, several changes are observed on the absorption spectrum. Most pronounced is the red-shift in the absorption of the carotenoid; the two peaks at 460 and 490nm shift to 467 and 500nm at 77K. They also increase in magnitude, and become narrower at low temperature. Thus the integrated peak area remains relatively constant.

3.2.3.3. Low detergent spectrum (0.02% TX-100) - 4°C

The absorption spectrum of the reaction centre at lower concentrations af the detergent TX-100 shows differences from the spectrum described above in the chlorophyll Q_y absorption, and in the carotenoid transitions. The Q_y absorption maximum is seen at 674nm at 277K, and at 676nm at 77K. The carotenoid absorption now appears to be composed of three transitions. A major peak is seen at 488nm, with shoulders at 506nm and 458nm. The Soret band is also different. The major peak remains at 416nm, with the less intense absorption at 431nm. There is no trough between the two peaks.

3.2.3.4. Low detergent spectrum (0.02% TX-100) - 77K

The spectra of this sample at 277K and at 77K are very similar, apart from an increase in the relative magnitude of the 488nm carotenoid peak, and resolution of a minimum of two peaks in the $Q_{y(0-0)}$ band.

3.2.3.5. The $Q_{y(0-0)}$ absorption band at 77K - 0.02%, 0.10% & 0.20% TX-100

The lowest energy Q_y peak of the isolated reaction centre exhibits altered properties depending on the concentration of detergent in the buffer. Two peaks are clearly resolved in low detergent concentrations, the lower energy transition giving rise to a peak at 677nm. This transition becomes weaker at higher detergent concentrations. The difference spectrum between the 0.02% and 0.10% spectra exhibits two peaks between 670nm and 680nm.

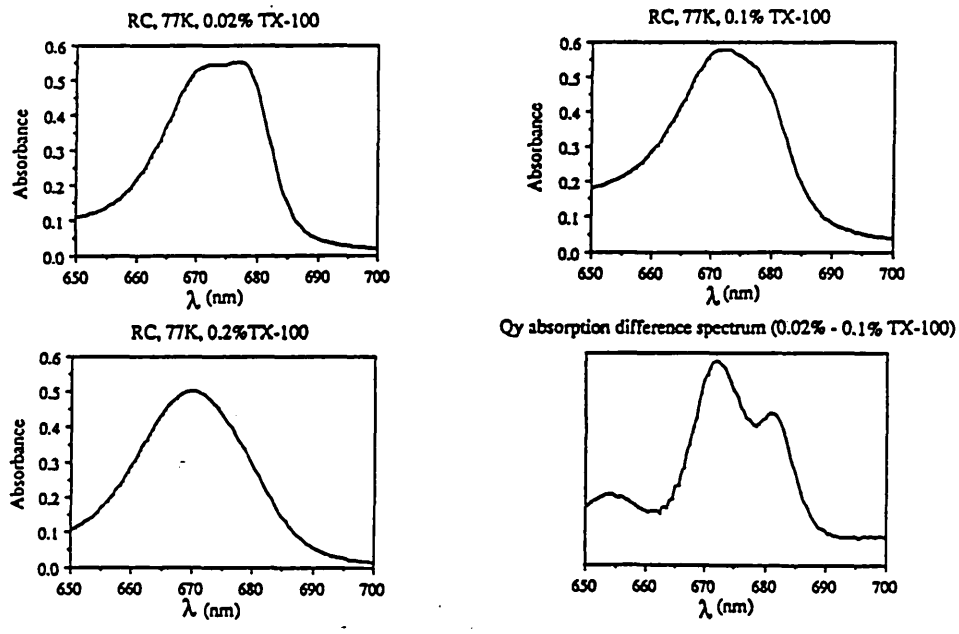


Fig.3.5. The Q_y absorption peak of the PS2 reaction centre at 77K in (a) 0.02% TX-100, (b) 0.10% TX-100, and (c) 0.20% TX-100. (d) - absorption difference spectrum (a) - (b).

3.2.3.6. Derivative spectroscopy of the aggregated complex

The second and fourth derivatives of the absorption spectrum can distinguish overlapping bands in a composite absorption peak, and have been used to identify the number of components in the complex at low detergent concentrations.

The second derivative of the aggregated complex has extrema at 670nm and 678nm in the $Q_{y(0-0)}$ absorption band. The fourth derivative spectrum has maxima at 668nm, 677nm, and 679nm. However, the fourth derivative spectrum is noisy, and is subject to artifactual side-lobes. Van Dorssen *et al* (1987b) observe peaks in the fourth derivative of the fluorescence excitation spectrum at 664nm, 670nm, and 681nm. Scherz *et al* (1989) fit the Q_y peak with three Gaussians centred at 669nm, 672nm, and 679nm.

The second derivative spectrum in the region 400-450nm identifies three main transitions: at 410nm, 415nm, and 433nm. The 410nm is probably due to Chl*a*, the 415nm to Chl*a* and Pheophytin*a*, and the 433nm band exclusively to Chl*a*. A slight inflection is seen at around 438nm, and may correspond to the highest energy transition of β-carotene. This inflection occurs at a similar position in the second derivative spectrum of the core complex (440nm).

Three transitions are observed in the region 450-530nm in the second derivative spectrum. These occur at 463nm, 485nm, and 508nm.

3.2.3.7. Chemically reduced - oxidised difference spectrum

The spectrum of the PS2 reaction centre complex after correcting for the absorption of the sample, and chemically reducing one of the samples is shown in Fig.3.6.

This spectrum is characterised by a positive peaks at 559nm, 530nm and 428nm, and a negative peak at 410nm. These correspond to the peaks observed by Garewal & Wasserman (1974) in the difference spectrum (reduced vs. oxidised) of purified cytochrome b_{559}, confirming the presence of this component in the D1/D2 complex.

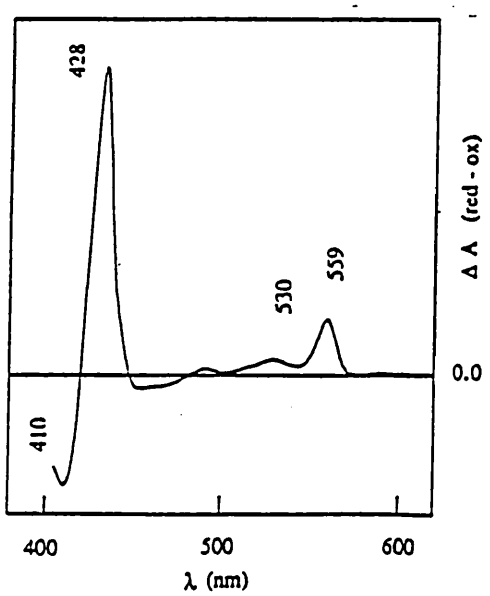


Fig.3.6. Chemically reduced (dithionite) - oxidised absorption difference spectrum of the PS2 reaction centre complex.

3.3. DISCUSSION

3.3.1. Detergent dependence of the reaction centre absorption properties

The reaction centre complex exhibits different spectral properties when suspended in buffers containing different concentrations of the detergent Triton X-100. The differences are most apparent in the carotenoid bands, and in the chlorophyll Q_y and B bands. The changes are most easily interpreted as arising as a result of different degrees of aggregation of the monomeric complexes to form dimers or larger aggregates. If pigments lie at the periphery of a monomeric complex, then aggregation could occur such that pigments are brought into close contact in the aggregate. Depending on the mutual orientation of the pigments and the distance between them, dipolar interactions can occur, which can alter the spectroscopic properties of the coupled system with respect to the monomer. This is the exciton model which was discussed in Chapter 1.

3.3.2. Monomeric and aggregated reaction centres - carotenoid excitons

The LD data presented in Chapter 4 of this thesis provide strong evidence that carotenoid excitons are formed in the PS2 reaction centre complex at lower detergent concentrations. The absorption spectra are harder to interpret, since they are less discriminating than LD spectra, and only the position and magnitude of individual transitions is observed. However, differences are apparent in the carotenoid absorption in media containing high and low concentrations of detergent. At low detergent concentrations, additional carotenoid transitions are observed.

For clarity of argument, I consider the simplest aggregate - a dimer. Exciton theory predicts that for every monomeric transition, there are two transitions in the coupled dimer, which occur at a lower and higher energy than the monomeric transition. The relative strengths of these two transitions is orientation-dependent. Thus the exciton interaction can be observed as a maximal blue- or red-shift with respect to the monomer transition, or as two bands whose relative magnitude varies between these two extremes. The carotenoid has two distinguishable transitions at 460nm and 490nm at 4°C in the proposed monomeric reaction centre complex at 0.2% TX-100, which shift to 467nm and 500nm at 77K. The third, higher energy, transition overlaps with the chlorophyll B transitions, and cannot be resolved. The absorption spectrum of the carotenoid at lower detergent concentrations is more complex, comprising a major peak at 489nm, and shoulders at 460nm and 507nm. Distinguishable carotenoid transitions are observed in the LD spectra at 459nm (-), 474nm (+), 494nm (-), and 507nm (+). I propose that these are two pairs of exciton-split transitions, centred at 466nm, and 500nm, respectively. These transitions should be observable in the absorption spectra. The absorption

shoulder at 507nm corresponds with LD507; the shoulder at 460nm with LD459. Thus the 507nm transition may be the lower energy exciton transition of a pair centred at 500nm. The higher energy transition should then be at 493-494nm. Similarly, if the 460nm shoulder is the higher energy transition of a dimer centred at 467nm, the lower energy transition will occur at 473nm. The observed peak at 489nm is then a composite peak, and the envelope of the two transitions at 474nm and 494nm. The correspondence is not very good, if the two transitions have equal dipole strength. However, the dipole strength of excitonic transitions has a complex orientation dependence, and the observed transition at 489nm could well be composite, with the 494nm having larger dipole strength than the 473nm transition. This would result in the position of the composite peak further to the red.

A further problem with this interpretation is the absence of the proposed transitions at 474 and 494nm in the second derivative spectrum. Their absence may be due to an unsuitable choice of the differentiating interval, and/or to the different relative magnitudes and widths of the two peaks. This requires a more detailed analysis than has been possible in this work. It is to be noted that van Dorssen *et al* (1987) obtained a satisfactory fit of the absorption spectrum in this region to Gaussians centred at 456nm, 474nm, 489nm, and 506nm.

3.3.3. Q_y blue shift in "disaggregated" spectrum

The position of the Q_y peak of the reaction centre is blue-shifted when the complex is suspended in buffer containing high concentrations of TX-100 with respect to the Q_y transition of the same sample in lower detergent concentrations. This might be due to detergent-induced release of chlorophyll from the protein matrix, or to preferential bleaching of long-wavelength components when the sample is disaggregated, or to another process. The first alternative seems unlikely, since even at 1.0% TX-100, the magnitude of the circular dichroism spectrum decreases by only 10% (Chapter 5). It could be discounted by lifetime measurements of the complex at different detergent concentrations. This deserves further investigation.

3.3.4. Conditions for aggregation and disaggregation

I consider the two extreme spectra 1 and 2 as arising from the particle in its monomeric and aggregated forms. The transition between the two forms is dependent on the composition of the supporting buffer. Spectrum 2 is obtained simply by diluting concentrated stock of sample in buffer containing no Triton X-100. The dilution is usually between 20 and 50, thus the final concentration of TX-100 is 0.004-0.01%. The sample is aggregated at these concentrations of detergent. Subsequent disaggregation of

the sample (which I assume can be estimated from a change in the absorption spectrum from 2 to 1) cannot be achieved simply by the addition of concentrated Triton X-100 to a concentration of 0.2% or higher. The absorption spectrum remains unaltered. Only at 1.0% Triton do the monomeric carotenoid peaks become visible. However, the sample can become disaggregated at lower detergent concentrations if either glycerol or acrylamide, or both, are present in the buffer. Both contain dipolar groups: three hydroxyl groups in glycerol, and one carbonyl group in acrylamide. Thus it appears that disaggregation of the complex is effected through the synergistic action of these polar groups with the detergent.

3.3.5. Change in the conformation of β-carotene at 77K and on aggregation

The observed cryogenic red-shift of the carotenoid in the monomeric complex must arise from a conformational change in the carotenoid on cooling. This could be a change in the protein conformation near the carotenoid. However, since the CD data suggest that the carotenoid is located at the periphery of the complex (see Chapter 5), it is more likely due to a change in the conformation of the carotenoid itself. This might be a cis-trans isomerisation induced by lowering the temperature.

The band centre energies of the two carotenoid exciton pairs observed in LD at both 277K and at 77K are centred at the monomeric transition energies observed at 77K. This implies that, if the interpretation of the LD spectra in terms of exciton formation is correct, then a similar change in the conformation of the carotenoid as occurs on lowering the temperature, also occurs as a result of aggregation of the monomeric complex. The nature of this conformational change has not yet been investigated, but may be revealed using other spectroscopic techniques such as resonance Raman spectroscopy.

3.3.6. Comparison with other published spectra

The first absorption spectrum of the D1/D2 reaction centre to be published was that of Nanba & Satoh (1987). It has a Q_y absorption maximum at 673nm, a Soret peak at 415nm and a shoulder at 430nm. Carotenoid absorption is observed as shoulders in the range 460-490nm. A subsequent publication (van Dorssen *et al*, 1987b) reported the 4K absorption spectrum of the complex. The Q_y absorption maximum occurs at 670nm, and there is a trough between the two major Soret peaks. These are at 417nm and 436nm. The higher energy transition is still the more intense. In the region of carotenoid absorption the spectrum is complex, with some fine structure superimposed on the quoted peak positions of 467nm, 489nm, and 503nm. Breton & Duranton (1988) publish three absorption spectra measured at 4K, which appear to differ from each other,

especially in the carotenoid bands. Fig. 4(a) may show only two major distinguishable carotenoid transitions, while Fig. 4(b) has the major 489nm transition, with shoulders to higher and lower energy. These authors attribute the variability of the spectral features to the application of the same isolation procedure in different laboratories. Considering the results presented in this chapter, it is possible that the sample used in each case was the same, and the variability in the spectral properties a consequence of the possibly different buffers used in each measurement.

CHAPTER 4 : LINEAR DICHROISM OF PHOTOSYSTEM 2 PARTICLES

4.1 INTRODUCTION

The anisotropic arrangement of pigments in a variety of PS2 particles has been investigated using polarised light and the gel-squeezing technique to orient samples with respect to the measuring beam. These techniques, and the modifications for measurement at 77K, have been described in Chapter 2 and are not discussed further. I note here only general features of the interpretation of the LD spectra. LD is defined as the difference between the absorption of vertically and horizontally polarised light, $(A_v - A_h)$. Thus positive LD represents more absorption of vertically polarised light than of horizontally polarised light. In all the following discussions, a positive (negative) LD signal is attributed to a transition dipole that is oriented at less (more) than 55° to the longest axis of the particle. This arises from the net orientation of the particles with their longest axis lying towards the vertical, since the gel is squeezed in a horizontal direction, perpendicular to the light path. Since the longest axis of the particle lies in a more vertical direction as a result of squeezing, then positive LD arises from transitions oriented along the long axis of the particle. The actual magnitude of the LD is given by:

$LD / 3A = < 3 \cos^2 \alpha - 1 > . \Phi (n)$,

where $LD = A_v - A_h$,

A = absorption,

α is the angle between the transition dipole and the orientation axis of the particle,

and Φ (n) is the orientation function for the press (different for each press).

The linear dichroic properties of thylakoid membranes were discussed in Chapter 1. They indicate that the majority of chlorophyll molecules are oriented in the plane of the thylakoid membrane. This arrangement may increase the efficiency of excitation energy transfer from the antenna to the reaction centre.

4.2. RESULTS

4.2.1. LD spectrum of PS2-enriched membranes (BBY's)

The LD spectrum of PS2-enriched membranes is shown in Fig. 4.1. The Q_y transitions of the chlorophyll molecules in BBY's show positive LD at 682 nm, as they do in thylakoid membranes. If we assume that the BBY's orient in a similar fashion to thylakoid membranes, i.e. with their planes in a vertical direction, then the chlorophyll Q_y transitions lie parallel to the membrane plane. There are major positive peaks in the blue region of the spectrum at 443nm and 476nm, with a shoulder at 497nm. The 476nm peak and 497nm shoulder is due to absorption by carotenoids oriented in the plane of the membrane. These carotenoids are contained in the LHC2 complex (6-9 molecules of xanthophyll per LHC2 trimer) and in the PS2 core complex (7-8 molecules of β-carotene per oxidisable primary donor). This is a similar spectrum to that obtained by van Dorssen *et al* (1987).

4.2.2. LD spectrum of the PS2 core complex

The room temperature and low temperature (77K) LD spectra of the PS2 core complex are shown in Figs. 4.2.(a) and (b), respectively, and are very similar in shape. The largest LD peaks are in the Q_y region of the chlorophyll at 682nm (positive LD), and in the B bands of the chlorophyll at 410-430nm (negative LD). The positive Q_y LD at 682nm indicates that the chlorophyll Q_y transition dipoles are oriented rather parallel to the long axis of the particle. The lowest-energy transitions in the blue region of the spectrum appear to be oriented perpendicular to this axis. The sign changes in the carotenoid absorption region have been attributed by two independent groups (van Dorssen *et al*, 1987; Newell *et al* ,1988) to two spectrally distinct populations of carotenoid with different orientation, one parallel, the other perpendicular, to the orientation axis.

Since the majority of the chlorophylls in the core complex are oriented with their Q_y transitions along the long axis of the particle, as shown by the positive LD of the Q_y LD transition, and the majority of the chlorophyll Q_y transitions in thylakoid membranes and BBY's lie in the plane of the membrane, then it is reasonable to conclude that the longest axis of the core complex lies in the plane of the membranes. I propose likely dimensions in Chapter 7.

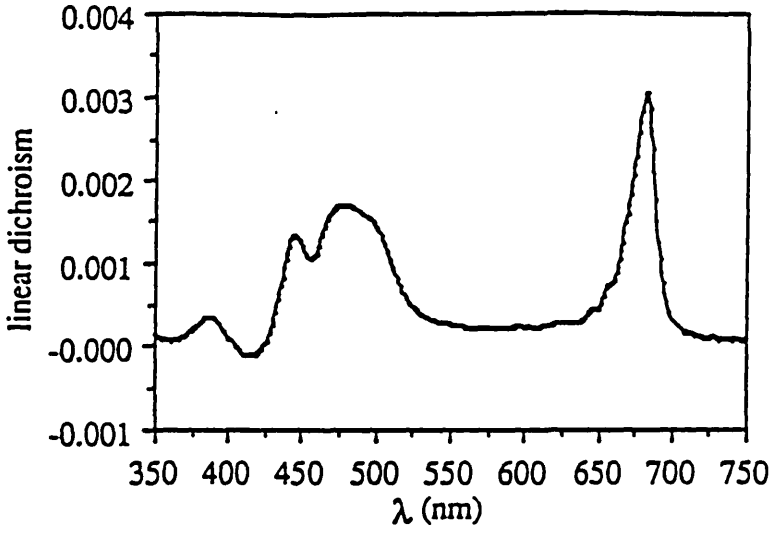


Fig.4.1. Linear dichroism spectrum of PS2-enriched membranes (BBY's). [Chl] = 2.5 μg/ml.

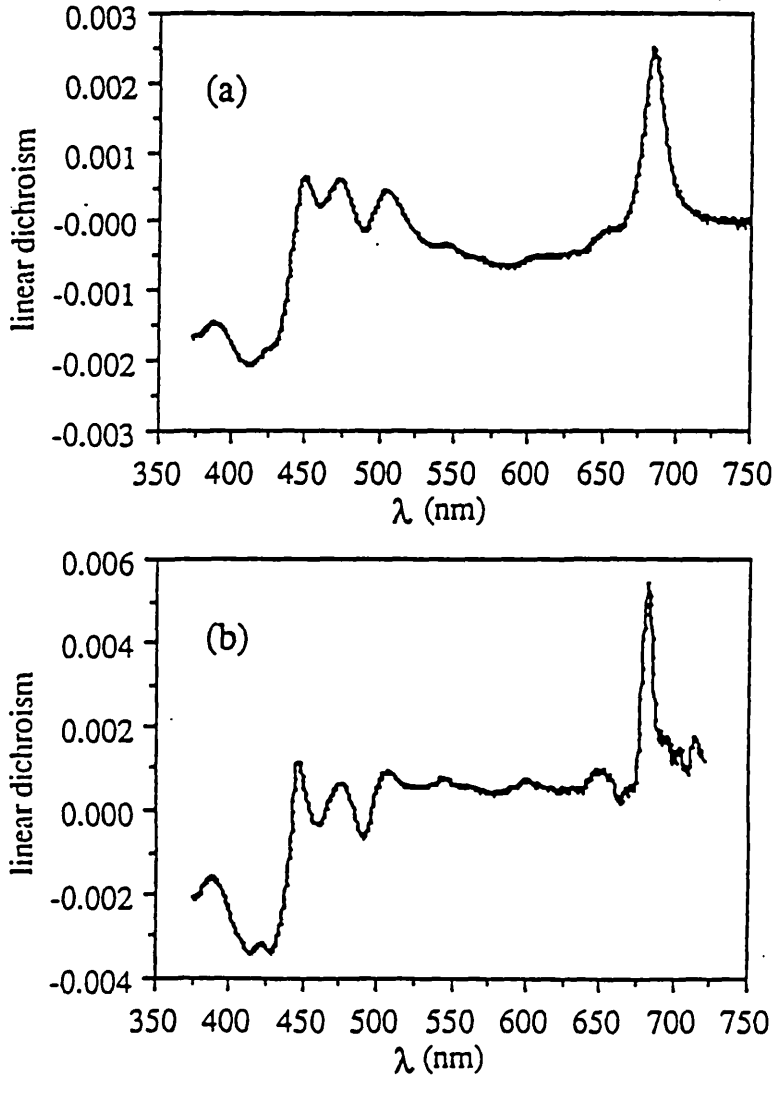


Fig.4.2. Linear dichroism spectra of the PS2 oxygen-evolving core complex at (a) 277K, and (b) 77K. [Chl] = 5 μg/ml.

4.2.3. LD spectrum of PS2 reaction centre complex

The observed anisotropy of the pigments in the isolated D1/D2 reaction centre complex is sensitive to the composition of the supporting medium, specifically to the concentration of the detergent Triton X-100 (TX-100). Two extreme spectra are observed at 4°C, when the sample is incubated in the unpolymerised gel containing high (0.2%) or low (0.02%) detergent concentration, before polymerisation with APS. I refer to these two extreme spectra as Spectrum 1 and Spectrum 2, respectively, for comparison with the equivalent absorption spectra presented in the preceding chapter. The two spectra correspond to the spectra published previously by two independent groups; the high detergent spectrum to that of Newell *et al* (1988), and the low detergent spectrum to that of van Dorssen *et al* (1987).

Table 4.1.(a) Positions, relative magnitudes, and signs of the LD absorption extrema of the PS2 reaction centre in 0.2% TX-100 (Spectrum 1) (magnitudes are normalised to the major blue peak at 436-438 nm)

	277K			77K	
Position	**Magnitude**	**sign**	**Position**	**magnitude**	**sign**
673	0.10	-	673	0.10	-
490	0.80	+	498	1.15	+
462	0.85	+	466	1.30	+
436	1.00	+	438	1.00	+

Table 4.1.(b) Positions, relative magnitudes, and signs of the LD absorption extrema of the PS2 reaction centre in 0.02% TX-100. (magnitudes are normalised to the peak at 685nm)

	277K			77K	
Position	**magnitude**	**sign**	**Position**	**magnitude**	**sign**
685	1.00	+	685	1.00	+
670	1.41	-	673	1.38	-
617	0.20	-	622	0.22	-
542	0.43	+	541	0.45	+
506	0.97	+	506	1.01	+
489	0.80	-	488	0.75	-
474	0.53	+	474	0.55	+
457	0.53	-	456	0.55	-
442	1.77	+	442	1.75	+
427	1.08	-	427	1.12	-

4.2.3.1. LD spectrum of the PS2 reaction centre in high detergent (0.2% TX-100) (Spectrum 1) - 4°C - Figure 4.3.(a).

The major features of the LD spectrum of the sample in 0.2% TX-100 are the negative Q_y LD at 672nm, and three positive LD peaks at 490, 462, and 436nm. Smaller positive

shoulders are seen at 575, 538, 419, and 332nm. This particle thus has a net Q_y transition which is oriented perpendicular to the long axis. The other Q_y transitions which are indicated by other spectroscopic measurements may be present, but not observed in the LD spectrum because they lie close to the magic angle, and thus have small LD. The negative Q_y LD arises from the transitions of all the porphyrin pigments, which will have different magnitudes depending on the angle they make with the orientation axis. The two positive peaks at 490 and 462nm are definitely assigned to β-carotene whose long axis lies at less than 55° to the orientation axis of the particle. The large magnitude of the LD suggests that it lies nearly parallel to the particle's longest axis. The 541 nm Q_x transition of Pheophytin a is not observed, suggesting that it lies close to the magic angle.

4.2.3.2. LD spectrum of the PS2 reaction centre in high detergent (0.2% TX-100) (Spectrum 1) - 77K - Figure 4.3.(b).

The same sample, measured at 77K, has an LD spectrum that is similar to the 4°C spectrum in form, i.e. a negative Q_y LD and three positive LD maxima in the blue region. This similarity indicates that no macromolecular conformational changes are induced in the complex by lowering the temperature. The most apparent difference is the red-shift of the two bands which at 4°C are located at 462nm and 490nm, to 466nm and 498nm, respectively. The peak heights of these bands increase with respect to the band at 436nm, and become narrower. Thus the integrated absorption of each band may be the same at 277K and 77K. This red-shift, increase in peak height, and band narrowing are to be expected, since the same changes were seen under the same conditions in the absorption spectrum. Possible explanations invoking conformational or environmental changes in the carotenoid were discussed in Chapter 3, and have the same applicability to these results. The slight shift in the position of the 436nm band to 438nm at low temperature may arise from the shift of the neighbouring band from 462nm to 466nm, the actual position of this transition remaining unaltered.

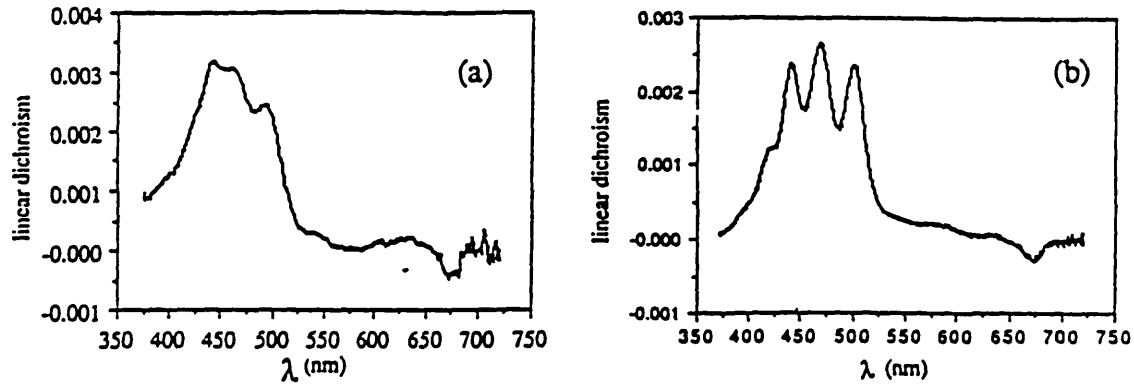


Fig.4.3. Linear dichroism spectra of the PS2 reaction centre complex in buffer containing 0.2% TX-100 at (a) 277K, and (b) 77K. [Chl] = 2.5 μg/ml.

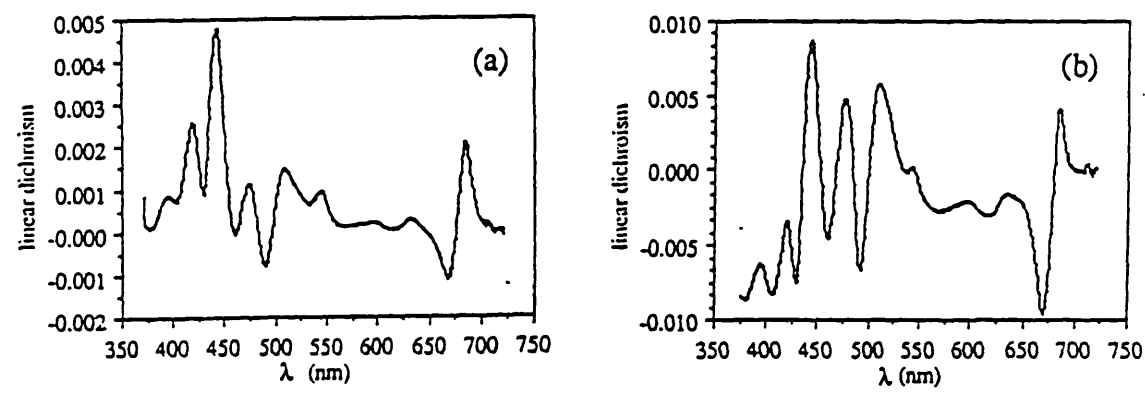


Fig.4.4. Linear dichroism spectra of the PS2 reaction centre complex in buffer containing 0.02% TX-100 at (a) 277K, and (b) 77K. [Chl] = 2.5 μg/ml.

4.2.3.3. LD spectrum of the PS2 reaction centre in low detergent (0.02% TX-100) (Spectrum 2) - 4°C - Figure 4.4.(a).

The LD spectrum of the sample embedded in a gel containing 0.02% TX-100 is different from the two spectra described above. The Q_y now comprises two peaks: a positive LD extremum at 684-5nm, and a negative LD extremum at 670nm. This LD spectrum thus clearly indicates the presence of two transitions in the Q_y absorption band, which do not have the same orientation in the complex. The pheophytin absorption at 542nm has positive LD. An equivalent LD peak is not obvious in the sample in higher detergent concentrations. The carotenoid absorption now exhibits several LD peaks of opposite sign in the region 508nm to 457nm. This suggests the presence of two transitions with mutually perpendicular orientation, associated with each of the single transitions observed in Spectrum 1. One of these transitions lies parallel to the orientation axis, the other perpendicular. The pheophytin Q_x transition shows positive LD, and thus lies rather parallel to the long axis of the particle.

4.2.3.4. LD spectrum of the PS2 reaction centre in low detergent (0.02% TX-100) (Spectrum 2) - 77K - Figure 4.4.(b).

Cooling this sample to 77K does not dramatically alter the LD spectrum, and the positive and negative Q_y peaks and the sign changes in the carotenoid region are again seen at the same positions. This is consistent with the invariance of the absorption spectrum with temperature in the same conditions. The conformation of the pigments appears unaltered on cooling the sample.

4.2.3.5. Intermediate spectra

At intermediate detergent concentrations, intermediate spectral features are observed. These include variability in the relative magnitudes of the 685nm and 670nm LD extrema, and in the magnitude of the 506nm positive LD.

4.3. DISCUSSION

4.3.1. General effects of detergent on linear dichroic properties

The only difference in the composition of the samples giving rise to the extreme Spectra 1 and 2 is the detergent concentration of the supporting medium: higher for spectrum 1 (0.2% TX-100) than for spectrum 2 (0.02% TX-100). In general, lowering the concentration of detergent will reduce the surface area of detergent hydrophilic groups for interaction with the aqueous environment. Entropy considerations predict the formation of more hydrophobic interactions between the hydrophobic amino acids of neighbouring reaction centre complexes. Such aggregation occurs amongst isolated bacterial reaction centres (Breton, 1985), giving rise to large planar discs. I conclude that most of the different spectral features observed under different detergent conditions arise as a result of aggregation or disaggregation of PS2 reaction centres.

Comparison of the LD spectra of aggregates with those of the monomeric units is complicated, since aggregation may alter the LD in three (and possibly more) ways:

4.3.1.1. The shape of the aggregate

Aggregates may have a different shape to that of the monomer unit and might therefore orient differently (with respect to the particle dimensions, and the degree of orientation) when the gel is squeezed. Juszczak *et al* (1988) observe very different LD spectral features in different-sized aggregates of phycobilisomes and their subunits, which are interpreted in terms of the different geometries of the aggregates. Generally, the degree of aggregation (formation of dimers, trimers, and higher aggregates) might depend in a sensitive way on the composition of the medium. Further, it is not possible to predict *a priori* whether aggregation will occur in a specific (i.e. non-random) and reproducible way.

4.3.1.2. Exciton formation

Depending on the hydrophobic interactions involved, dimerisation may occur such that pigments on the periphery of a two monomeric units may come close enough together in a dimer to experience dipolar (excitonic) interactions. Such interactions (see Introduction, Chapter 1) can give rise to band splittings, blue or red shifts, depending on the mutual orientation of the monomeric transitions and the distance between them.

4.3.1.3. Conformational changes in the monomer

Energetically favourable conformations of aggregates may necessitate small conformational changes in parts of the monomer units before aggregates can form.

4.3.2. The effect of the detergent on the linear dichroic properties of Photosystem 2

I now discuss in more detail each of these effects in the PS2 reaction centre. I consider the simplest (least extensive) aggregate, i.e. a dimer, to clarify the discussion. Several other independent results suggest that dimers of PS2 occur *in vitro* and *in vivo*. These are reviewed in Chapter 7.

4.3.2.1. Different shapes and orientation axes of the monomer and aggregates

The assumption that the monomer and aggregated forms have different shapes, and therefore orient differently in the gel provides the simplest explanation for the observation of the positive Q_y LD at 684nm in aggregated samples, and its absence in the LD spectrum of the monomer. The second derivative of the absorption spectrum reveals two major transitions in the $Q_{y(0-0)}$ band, at 678nm and 670nm. The higher energy transition (670nm) is oriented more perpendicular to the orientation axis in the monomeric unit; the 678nm transition is not resolved as a distinct transition, and must therefore lie close to the "magic angle", the angle at which the linear dichroism of a transition is zero (55° to the orientation axis). In the aggregate, the 670nm transition is still perpendicular to the long axis of the aggregate (LD670 is negative). The shape of the aggregate is however different from that of the monomer such that the 678nm transition now lies along its long axis. LD spectra are a linear combination of bands with different signs; if the higher energy Q_y transition is strong, it may shift the observed LD maximum of the 678nm transition to longer wavelength, even though the actual band centre energy of this transition remains unaltered. This is a possible explanation for the red-shifted LD maximum with respect to the absorption maximum revealed from the second derivative spectrum. The simplest aggregate of a monomeric unit is a dimer. The simplest model for orientation of the 670nm and 678nm transitions in the monomer and dimer is presented below.

4.3.2.2. Excitonic interactions between monomeric pigments in the aggregate

The presence of two pairs of positive and negative LD extrema due to β-carotene in the range 510-450nm in the aggregate, where in higher concentrations of TX-100 only two single positive transitions are observed, has two possible explanations. First, the proposed dimerisation induces a red absorption shift in the carotenoid of one of the monomers and a blue shift in the carotenoid of the other. Second, dimerisation may

occur such that the two carotenoid molecules are located at the junction of the two monomeric reaction centre units, and are close enough to be excitonically coupled. The second alternative seems more likely, since it requires fewer assumptions, and is therefore examined in more detail here.

The two pairs of LD extrema at 508nm (positive), 485nm (negative), and 474nm (positive), 457nm (negative) might arise from excitonic coupling between two monomeric transitions of neighbouring chromophores which interact in a dimeric aggregate. The Davydov splitting is 765 cm^{-1} for the first pair, and 785 cm^{-1} for the second. The two proposed monomer bands would therefore occur at 498nm and 465nm, respectively, and the magnitude of the dipolar perturbation is almost the same for each monomer band. The band-centre energies of the two exciton pairs correspond rather well to the LD maxima (at 466 and 498nm) of the carotenoid in its red-shifted form which exists at 77K.

As discussed in Chapter 1.3. the excitonic transitions of a coupled dimer correspond to the in-phase and out-of-phase combination of the locally excited states of each monomer, and therefore have the direction and magnitude of the vector sum and difference of the two monomer transitions. The magnitudes depend on the mutual orientation of the dipoles; the directions are always orthogonal. The LD spectrum reveals that one of these transitions is oriented parallel (or at less than 55°) to the orientation axis of the aggregate, and the other oriented perpendicular (or at more than 55°) to the orientation axis. If the simplest aggregate (a dimer) has a 180° rotational axis of symmetry (C_2 symmetry), then one of the carotenoid exciton bands must lie along this axis, and the other perpendicular to it (van Amerongen, pers. comm.). They may therefore exhibit LD of opposite sign, depending on the geometry of the aggregate.

The exciton model is very sensitive to the distance between the monomer pigments, and their relative orientations. If the proposed aggregation was not specific, resulting in formation of a variety of different aggregated structures, then we would observe many more different spectra. I have repeatedly observed just one LD spectrum at low detergent concentrations, suggesting a reproducible and specific aggregation between monomeric complexes.

4.3.2.3. Conformational change of carotenoid on aggregation

It was noted above that the band centre energies of the two proposed carotenoid exciton peak pairs correspond well with two of the monomeric transitions of the carotenoid at low temperature (77K). The peak positions of aggregated sample do not change on lowering the temperature. This is in contrast to the bathochromic shift of the carotenoid in the disaggregated state, which most probably reflects a change in the conformation of the carotenoid molecule on cooling. Thus it appears that the same conformational change

of the carotenoid on cooling to 77K also occurs on aggregation, and it is the monomeric transitions of the carotenoid in this conformation that give rise to the proposed exciton splittings in the aggregated state at 77K and at 277K. This conformational change may be a cis/trans isomerisation which occurs as a result of cooling the complex in its monomeric form to 77K, and as a result of dimerisation between two complexes at 4°C. The precise conformation of the carotenoid in the different states is not revealed by visible absorption spectroscopy. Resonance Raman techniques provide information concerning the proposed differences in conformation.

4.3.2.4. Comparison of the aggregated PS2 reaction centre LD with the PS2 core complex LD

The sign changes in the PS2 RC carotenoid LD were first observed by van Dorssen *et al* (1987), and attributed to two populations of carotenoid with different absorption maxima and different relative orientations. Similar sign changes in the carotenoid LD of PS2 core complexes have been observed (van Dorssen *et al*, 1987, Newell *et al*, 1988), and the same conclusion drawn for these larger complexes. This interpretation invokes a different spectral shift, imposed by the environment or a conformational change, for each of the two carotenoids, since only one type of carotenoid (β-carotene) is present in PS2 core complexes (Ohno *et al*, 1986; Gounaris & Barber, 1987). However, if the interpretation of the PS2 RC carotenoid LD sign changes in terms of excitonic interactions is correct, then it might also be a correct interpretation of the carotenoid LD in the PS2 core. That is, the carotenoid LD sign changes arise from excitonic interactions between β-carotene molecules associated with D1/D2 with are present in an aggregated form in the measured PS2 core. The positions of the LD extrema do correspond rather well between aggregated PS2 reaction centres and core complex; reaction centre (core); 457 (458), 474 (471), 489 (487), and 508 (506)nm. The presence of only two major peaks due to carotenoid in the absorption spectrum of the core complex would suggest that the core contains additional carotenoid which have the same absorption maxima, but are oriented randomly, or close to the magic angle, and are therefore not observed in the LD spectrum. Ohno *et al* (1986) detect eight moles of β-carotene per mole of Q_a in purified oxygen-evolving PS2 cores from *Synechococcus*.

The close correspondence between the core and aggregated reaction centre LD peak positions might suggest that the same "aggregation site" causes dimerisation of isolated PS2 reaction centres, and dimerisation of PS2 RC in core complexes. Part of this aggregation site in the core complexes would then reside on a region of the D1/D2/$Cytb_{559}$ complex. The sign changes in the carotenoid LD are also seen in the LD spectrum of thylakoid membranes from the Chl*b*-less *Chlorina* mutant of wheat (Haworth *et al*, 1982b).

4.4. IMPLICATIONS AND POSSIBLE MODEL STRUCTURES

From this comparison of the LD in the carotenoid region for aggregated PS2 reaction centres and core complexes, it is possible that isolated PS2 core complexes *in vitro* consist of a dimer of D1/D2 reaction centre units, together with their associated 43 and 47 kD antenna pigment-proteins and other polypeptide components. Discussion of other independent evidence consistent with this proposal is presented in Chapter 8. Here, I consider possible models that are consistent with the LD spectroscopic data.

4.4.1. The monomeric reaction centre

This model contains the β-carotene close to the long axis of the particle, the 670nm transition oriented more perpendicular to the long axis, and the 678nm transition oriented close to 55° to the carotenoid transition dipole. This orientation will give small, or zero, LD for the 678nm transition, and a weak negative LD for the 670nm transition. The protein subunits of the reaction centre, comprising the predicted transmembrane helices of D1, D2, and the α and β subunits of Cytb559 (see Chapter 7), are represented as a cylinder. The longest axis of the *in vitro* particle lies close to the β-carotene transition. This axis probably lies close to the axis of the transmembrane α-helices, but is not necessarily exactly coincident with it.

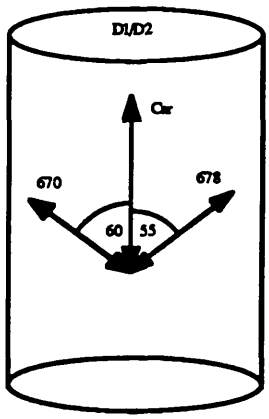


Fig.4.5. Model of the transitions in the monomeric PS2 reaction centre complex

4.4.2. The dimeric reaction centre

Dimerisation occurs along faces of the two monomers which are parallel to the long axis of the monomer (discussed in Chapter 7). The long axis now lies along a line running through the two monomers (parallel to the x-axis in the figure), and perpendicular to the plane between them (z-axis in the figure). The 670nm transition is perpendicular to this new long axis (y-axis); the 678nm transition is now parallel to it, due to the rotation through 90° of the long axis of the dimer with respect to that of the monomer. The carotenoids lie close to each other at the junction of the monomers. Components of the monomeric carotenoid transitions lie along the x, y, and z axes, such that one of the exciton transitions lies parallel to the long axis of the dimer (x-axis), and the other perpendicular to it (and parallel to the long axis of the monomer - z-axis). It is reasonable to assume that the carotenoid belonging to the reaction centre is specifically associated with one of the reaction centre polypeptides. This is likely to be D1 or D2, since the two subunits of $Cytb_{559}$ are small, and are involved in haem binding. Then the proposed specific aggregation between reaction centre monomers will occur either between two D1 subunits, or between two D2 subunits. The cylinder representing the protein component of the reaction centre has been omitted in the diagram to increase clarity. The α-helices are proposed to be oriented nearly parallel to the z-axis of the aggregate.

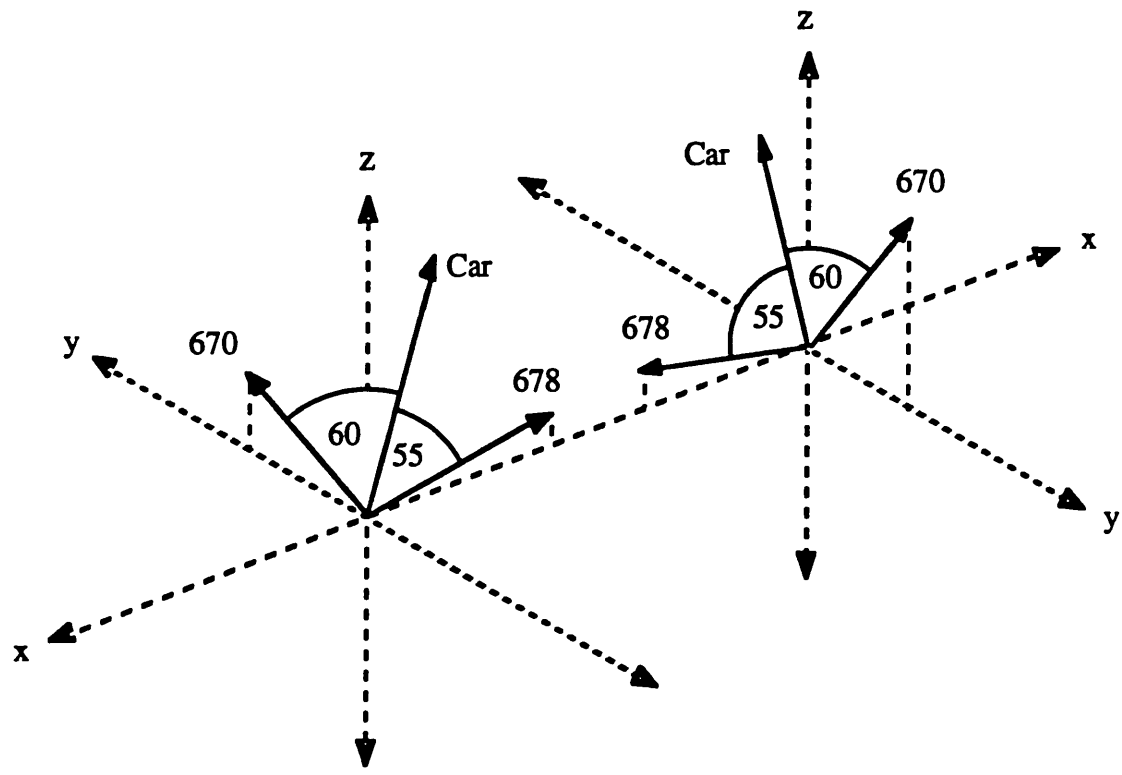


Fig.4.6. Model of the transitions in the dimeric PS2 reaction centre complex.

4.4.3. The PS2 core complex

A stoichiometric study of PS2 core protein components (Gounaris *et al*, 1987) showed that the proteins of the core occurred in the ratio 47:43:D1:D2:$Cytb_{559}$ = 1:1:1:1:1. Therefore, the *in vitro* core must also contain two copies of each of the 47 and 43 kD polypeptides. If it is assumed that part of the aggregation site belongs to the D1/D2/$Cytb_{559}$ complex (see Chapter 7 for discussion of other indirect evidence for this), the 43 and 47 kD polypeptides must be arranged in the core monomeric unit such that part of the reaction centre remains exposed. Furthermore, the longest and shortest axes must have the same orientation with respect to the orientation of the carotenoids in both the core and the aggregated reaction centre, so that the signs of the LD extrema due to β-carotene are the same in both systems, as is experimentally observed. The predicted six helices (see Chapter 7) of the 47 and 43 kD polypeptides are represented as sheets, as are the five predicted helices of D1 and D2, and placed at convenient positions relative to the reaction centre components to fulfil the conditions set out above.

The approximate C_2 rotational symmetry axis in the model of the monomeric D1/D2/CP47/CP43 core complex might be correlated with the minor furrow observed in electron micrographs of PS2 by Morschel & Schatz (1987), which is discussed in Chapter 7.

With no spectroscopic data yet available to make the choice between D1 and D2 as the carotenoid binding polypeptide, we must look at other evidence. I suggested above that accessibility of the reaction centre within the core complex is necessary for aggregation. After aggregation, the "aggregation site" is no longer exposed to the lipid environment. Thus either the D1 or the D2 subunits of the reaction centre are concealed from the environment at the junction of the two monomer units, and either the two D2 or two D1 subunits of the dimer are exposed at opposite ends of the complex. The observation of the rapid turnover of the D1 polypeptide (Ellis & Baraclough, 1978; Edelman & Reisfield, 1980) might imply that D1 is exposed at the ends of the dimer, allowing access to this protein by the processing apparatus without the need for complete disassembly of the core complex. The two D2 subunits would then lie in the centre of the complex, binding the two carotenoid molecules such that they are excitonically coupled. In the bacterial reaction centre, the carotenoid is associated with the M subunit, which is thought to be analogous to D2 in the PS2 reaction centre. However, placing the two D1 subunits at opposite ends of the core complex *in vivo* assumes that complexes aggregate in a similar way in the membrane *in vivo*, as occurs between isolated complexes *in vitro*. This is discussed further in Chapter 7, as is the possible position of $Cytb_{559}$ in this model.

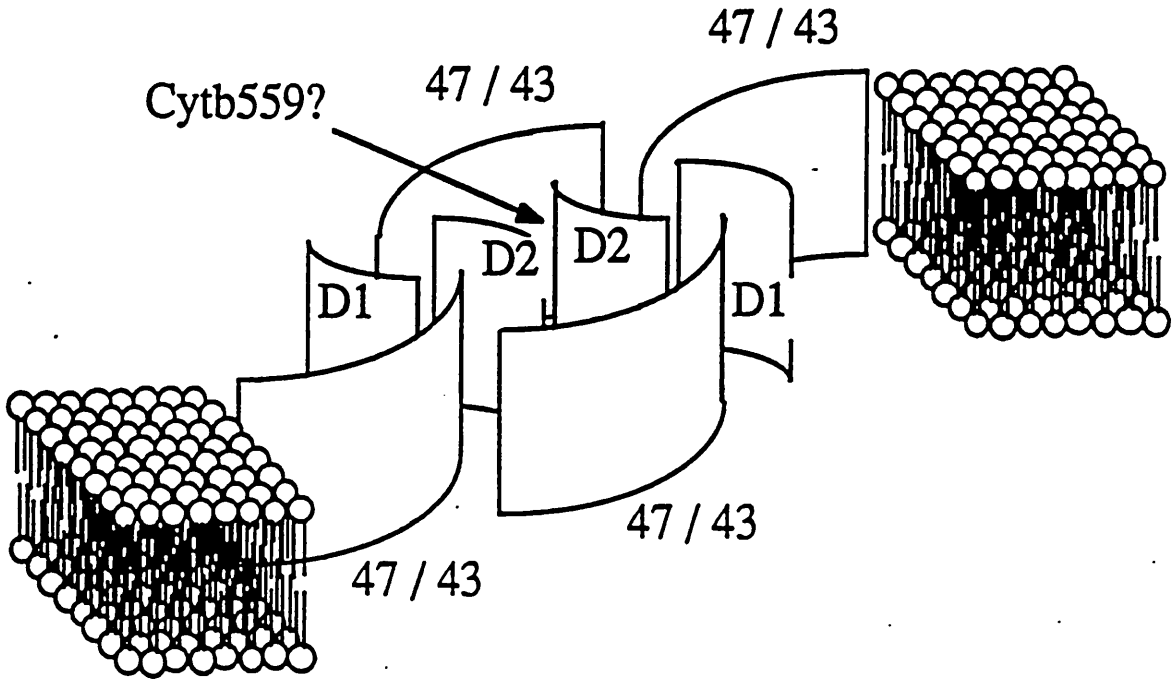


Fig. 4.7. Arrangement of the polypeptides in the dimeric PS2 core complex in the thylakoid membrane.

CHAPTER 5 : CIRCULAR DICHROISM OF PHOTOSYSTEM 2 PARTICLES

5.1. INTRODUCTION

Although monomeric pigments may be optically active, and show intrinsic differential absorption of left- and right-circularly polarised light (circular dichroism, CD), much larger CD signals are observed from pigment aggregates such as occur in photosynthetic pigment-protein complexes. These arise from dipolar (excitonic) interactions between neighbouring pigments (see Introduction, Chapter 1). I repeat here that the CD of the two exciton components of a coupled pigment pair is given by:

$CD_{+/-} = \pm V_{12} \cdot R_{12} \cdot (\mu_1 \times \mu_2)$

where V_{12} is the dipolar interaction energy, R_{12} is the distance between the two dipoles, and μ_1, μ_2 are the transition moments of the two monomeric pigments 1 and 2.

This equation indicates the following significant and characteristic properties of exciton split CD signals:

(1) The CD maxima of the two excitonic transitions have identical magnitudes of opposite sign. The two maxima are conservative, and satisfy the sum rule:

$\Sigma_{a=1,2} CD_a = 0,$

(2) The rotational strength is proportional to the triple product of the interchromophoric distance and electric transition moments of the two monomers1 and 2.

In this chapter, I present CD spectra of the PS2 core and reaction centre complexes, and of monomeric and dimeric Chl*a* in the visible region of the spectrum (750-350nm).

The peptide bond also exhibits circular dichroism in the ultraviolet (260-190nm), which is dependent on the conformation of the protein being examined. Changes in the conformation of the PS2 reaction centre polypeptides following exposure to light have been revealed through UVCD spectroscopy.

5.2. RESULTS

The major peak positions, magnitudes and signs of the CD spectra of the different systems are tabulated in Table 5.1. [Chl] = 10 μg/ml for all spectra.

Table 5.1. Peak positions (nm), magnitudes (x 10^{-3}), and signs of the CD spectra of the different systems (tr - trough).

chlorophyll *a* monomer			chlorophyll *a* dimer		
position	magnitude	sign	position	magnitude	sign
			680	0.26	+
661	0.045	-	664	0.20	-
			445	0.18	-
428	0.042	+	426	0.23	+
417	0.016	+(tr)	412	0.08	+(tr)
402	0.022	+	402	0.11	+
370	0.002		366	0.16	-

PS2 core complex			PS2 reaction centre		
position	magnitude	sign	position	magnitude	sign
678	0.36	-	682	1.03	+
667	0.18	+	670	0.33	-
444	0.13	-	449	0.59	-
434	0.10	-	439	1.28	+
			426	0.62	+(tr)
410	0.09	+	419	0.69	+
386	0.06	+	396	0.12	+
			364	0.33	-

5.2.1. CD spectrum of the PS2 oxygen-evolving core

The CD spectrum of the PS2 cores prepared by the method of Ikeuchi *et al* (1985) is shown in Fig 5.1. This spectrum is similar to that of a similar core preparation (van Dorssen *et al*, 1987a). The spectrum is characterised by a pair of peaks of opposite sign in the Q_y region of chlorophyll absorption, at 678nm (positive) and 667nm (negative). Negative extrema are observed in the B bands at 444nm and 434nm, and positive extrema at 410nm and 386nm.

5.2.2. CD of the PS2 reaction centre complex

The CD spectrum of the isolated PS2 reaction centre complex is shown in Fig 5.2. The Q_y region of the CD spectrum has a positive extremum at 682nm, and a smaller (about 30%) negative extremum at 670nm. Thus the PS2 reaction centre exhibits the opposite chirality in this region with respect to the PS2 core. Another Q_y negative CD (weak) is seen at 638nm, and a negative Q_x transition at 591nm. The CD integrated over the Q_y and Q_x regions is non-conservative, and is net positive.

The largest CD is observed as a positive and negative pair of peaks at 439nm (positive) and 449nm (negative). To the lower energy side of the negative 449nm extremum is a region of positive CD extending from 520nm to the positive maximum at 466nm, and further until the CD becomes zero at 459nm. Another peak occurs at 419nm, with a trough at 426nm.

5.2.3. CD of the PS2 reaction following exposure to light

The CD spectra of the isolated reaction centre after increasing time of exposure to light at 4°C (0, 2, 10, 60 min) are shown in Fig.5.3. The spectra are similar in shape, but differ in magnitude. There is a reduction in the strength of all the bands to approximately the same extent. The CD maximum in the Q_y region of porphyrin absorption is positive in all samples. This is in contrast to the CD of the Q_y transition of monomeric Chl*a* which has a negative extremum at 661nm. Therefore, it is possible that light damage to the isolated reaction centre does not result simply in release of chlorophyll from the protein matrix, but induces a more complex rearrangement of the pigment and protein components.

5.2.4. The effect of aggregation on the reaction centre CD

The major features of the CD spectrum remain largely unaltered over the range of detergent concentrations (0.01% - 1.0% TX-100) which induce major changes in the LD spectra (Fig.5.5). There is a slight (about 20%) decrease in the magnitude of the entire CD spectrum at higher detergent concentrations. In view of the dramatic changes on the LD spectrum of the PS2 RC at different states of aggregation in 0.2% and 0.02% Triton X-100, I note the relatively small changes in the CD spectrum under the same conditions.

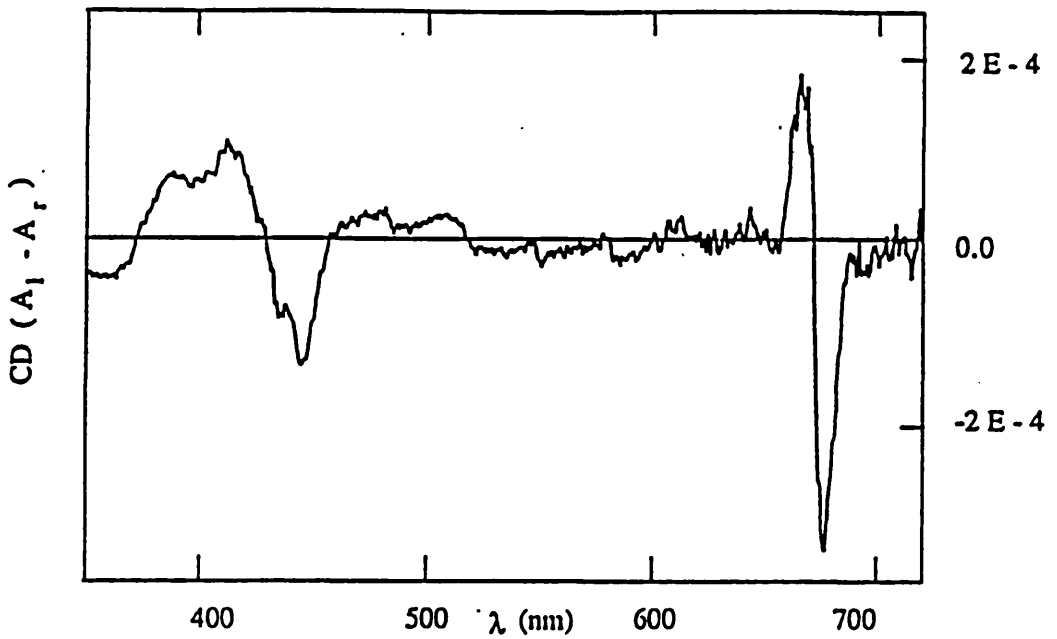


Fig.5.1. Circular dichroism spectrum of the oxygen-evolving Photosystem 2 core complex. [Chl] = 10 μg/ml, in Tris-Cl buffer (50mM, pH 7.2).

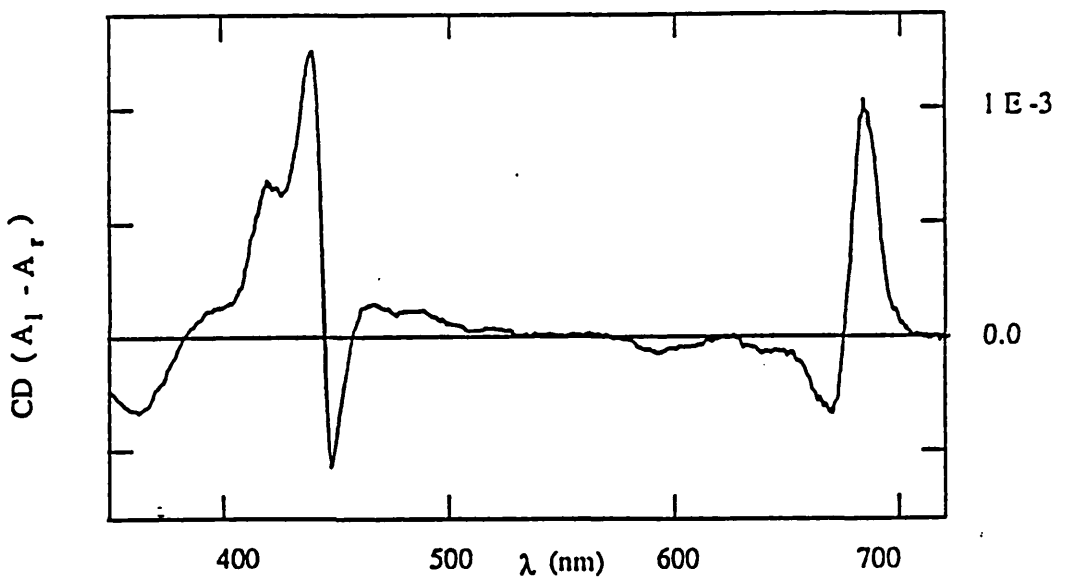


Fig.5.2. Circular dichroism spectrum of the Photosystem 2 D1/D2/Cytb$_{559}$ reaction centre complex. [Chl] = 10 μg/ml, in Tris-Cl buffer (50mM, pH 7.2), 0.01% TX-100.

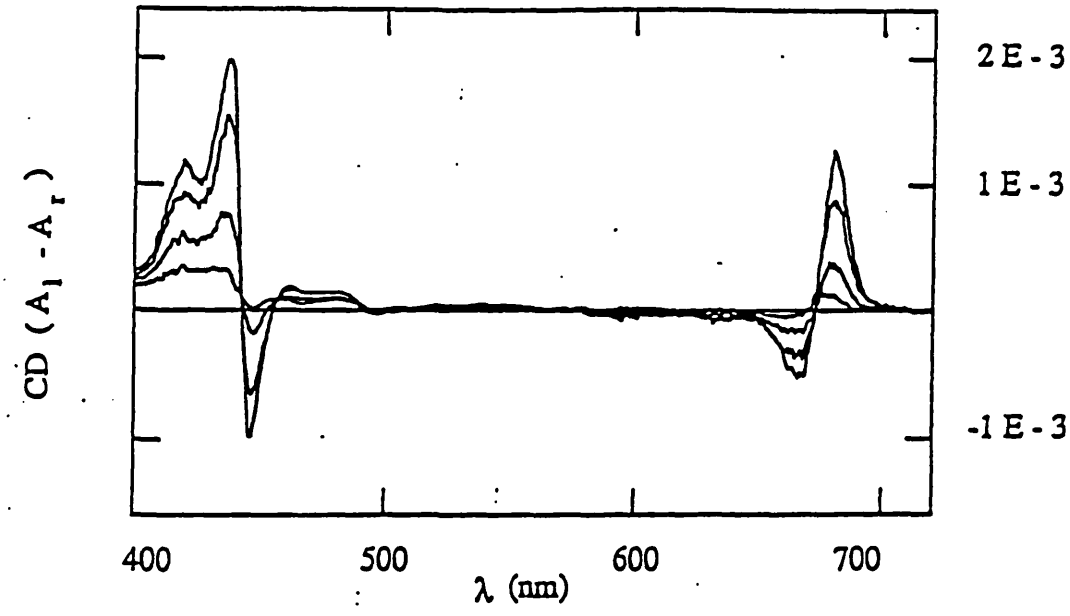


Fig.5.3. Circular dichroism spectrum of the PS2 reaction centre following exposure to light (50 μE m^{-2} s^{-1}) for different periods (0, 2, 10, 60 min). The CD signal steadily decreases following exposure to light for longer periods.

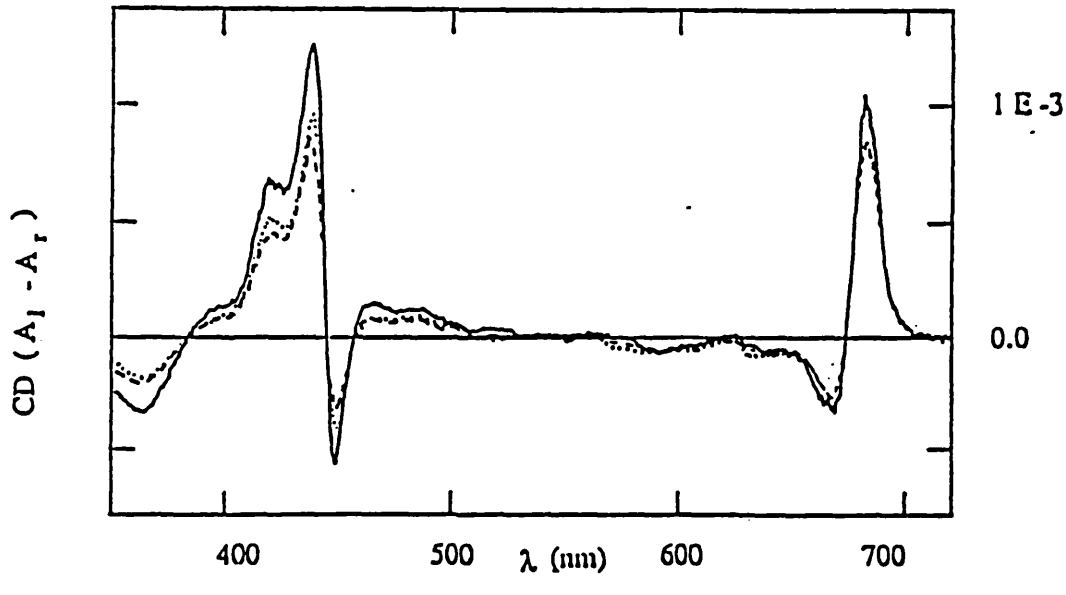


Fig.5.4. Circular dichroism spectrum of the PS2 reaction centre in different concentrations of the detergent TX-100: —— 0.01% TX-100; ····· 0.1% TX-100; - - - - - 1.0% TX-100.

5.2.5. CD spectra of monomeric and dimeric Chl*a*

The agggregation properties of Chl*a* in different solvents have been studied extensively. From these studies, it has been established that Chl*a* exists as monomers in ether containing a small amount of pyridine, and as dimers in CCl_4 (see Sauer,1975).

The CD spectrum of monomeric Chl*a* in ether is relatively simple (Fig 5.4(a)), and consists of one negative extremum at around 662 nm in the Q band, and positive extrema in the B band at 428 nm and 402 nm, with a trough at 417 nm between them. Optical activity from monomeric pigments arises from interaction of the electromagnetic wave with asymmetric centres in the molecule. CD is one manifestation of optical activity, and the CD observed from monomeric Chl*a* is presumed to arise from interaction of the circularly polarised wave with the asymmetric carbon atoms of the Chl*a* molecule. The five asymmetric carbon atoms are indicated in the figure of Chl*a*. (Section 1.3.).

Dimeric Chl*a* has more CD features than monomeric Chl*a* (Fig 5.4(b)), which can be attributed to dipolar (exciton) interactions in the dimer. As described in the introduction, a pair of interacting chromophores is predicted to have a CD spectrum composed of a positive and negative pair of peaks, with zero CD at the energy of the monomeric transition. The integrated CD over each excitonically coupled transition should sum to zero, i.e. is "conservative". The CD spectrum of dimeric Chl*a* in CCl_4 shows clear differences from that of monomeric Chl*a* in ether. The Q_y region has a positive extremum at 680nm, in addition to the negative extremum at 664nm. The total CD is non-conservative, i.e. does not sum to zero, but is nett positive. The B band of the Chl also has different CD in the dimeric form. The major difference is the presence of an additional negative CD band at 445nm. The positions of the positive bands at 426nm and 402nm, and the trough between them at 412nm seem equivalent to bands at similar positions in the monomeric CD spectrum.

The appearance of an extra CD band in both the Q and B transitions clearly indicates the presence of exciton interactions between the two monomers in the dimer.

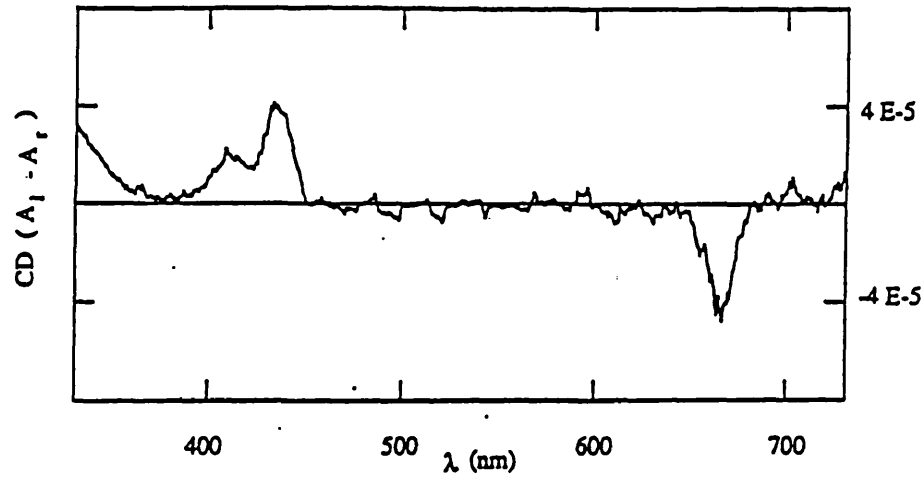


Fig.5.5.(a) Circular dichroism spectrum of monomeric Chl*a* (10μg/ml, in ether).

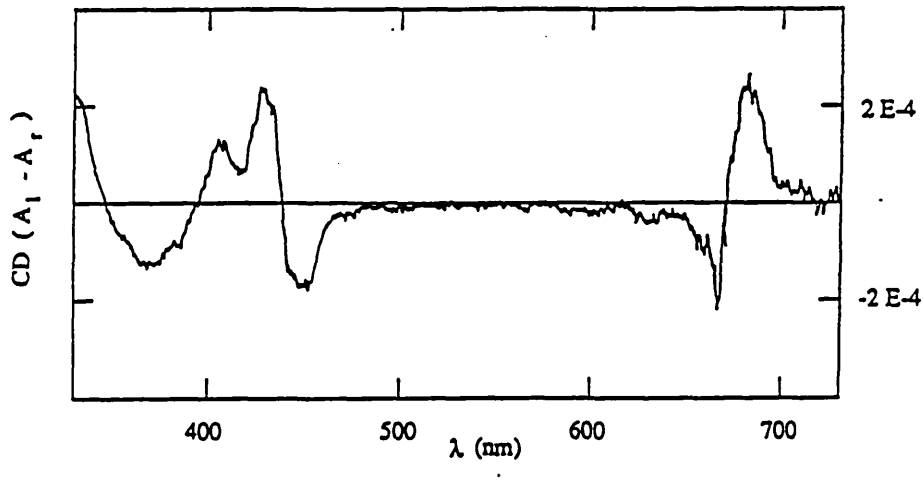


Fig.5.5.(b) Circular dichroism spectrum of dimeric Chl*a* (10μg/ml, in CCl_4).

5.2.6. UVCD of the Photosystem 2 reaction centre

For the reasons outlined in the introduction concerning the serious problems that can be encountered in the analysis of protein secondary structure by ultraviolet circular dichroism (UVCD), the analysis presented here of the PS2 reaction centre is qualitative. With more sophisticated analytical procedures, it is to be hoped that a more quantitative analysis will be performed in the future.

The UVCD spectrum of the isolated PS2 reaction centre is shown in Fig. 5.6. By comparison with the standard spectra of the homopolypeptides and those of Wetlaufer (see Figs.1.14, 1.15), it is clear that the reaction centre contains a large proportion of α-helix, from the double minimum at 206nm and 222nm. A third minimum at 215nm is due to β-sheet structure.

When the sample is exposed to light for prolonged periods, the secondary structure of the protein undergoes changes as revealed by the UVCD spectra in Fig.5.7. As shown in the following chapter of this thesis, infrared spectroscopy has shown the change to be from α-helix to β-sheet. The decrease in the magnitude of the UVCD spectrum should then be interpreted as due to a superposition of the α-helix standard CD spectrum and the β-sheet standard CD spectrum. The observed shift of the 222nm minimum to shorter wavelength (218nm) is consistent with this interpretation. This change in secondary structure is discussed more extensively in Chapter 6.

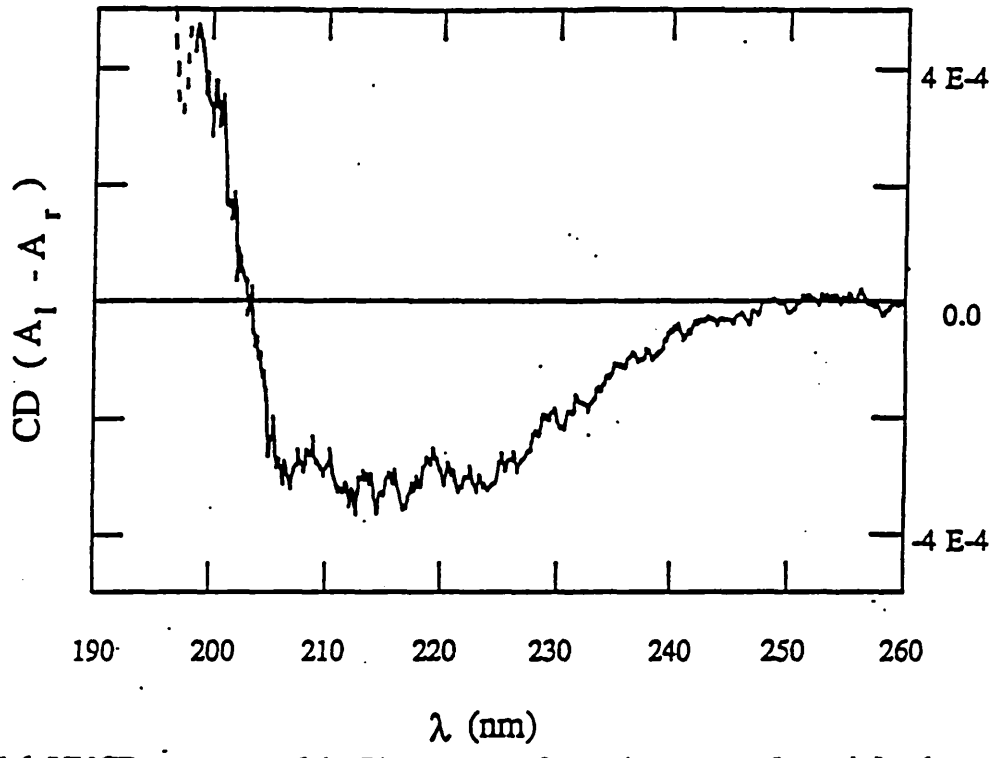
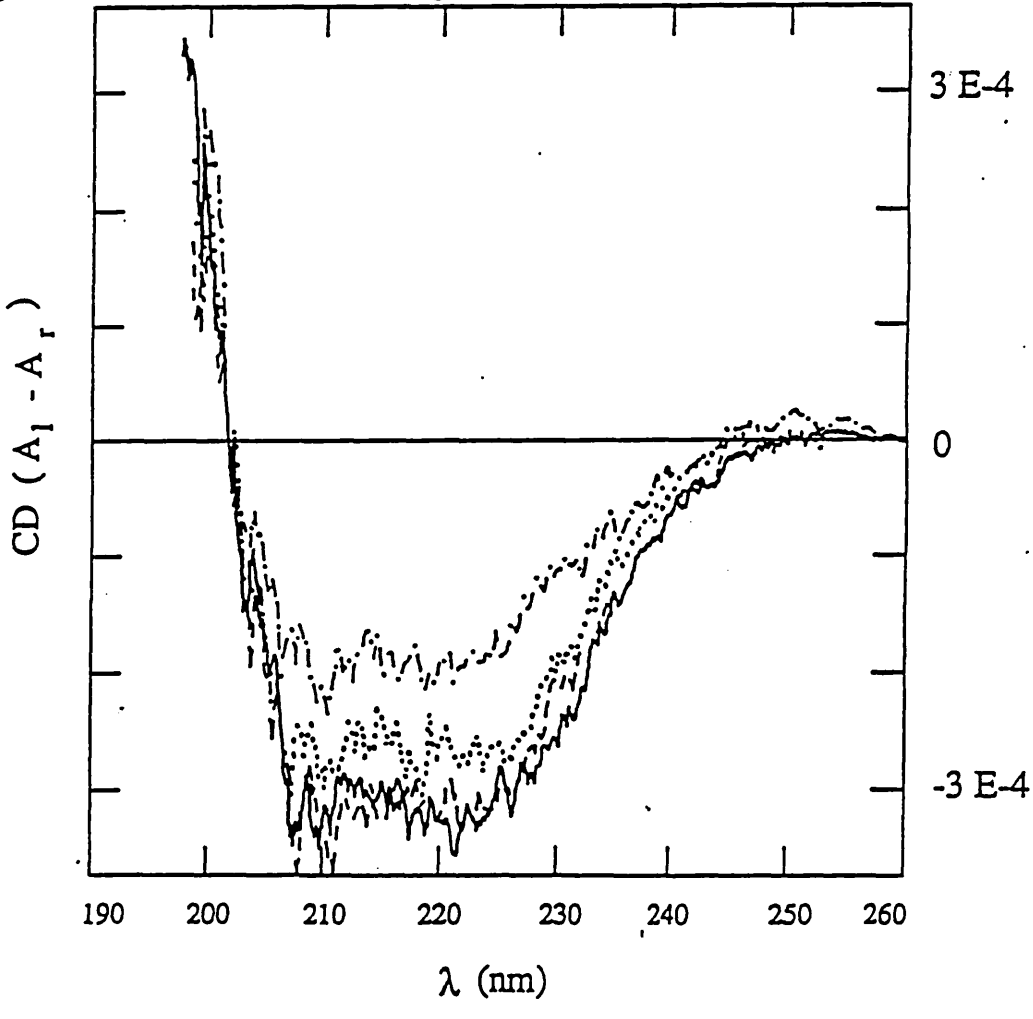


Fig.5.6. UVCD spectrum of the Photosystem 2 reaction centre. [protein] = 1 mg/ml.

Fig.5.7. UVCD spectra of the Photosystem 2 reaction centre after exposure to light (50 μE m^{-2} s^{-1}) and heat (25°C). ——— no pre-treatment; - - - - 10 min light, 4°C; ····· 10 min light, 25°C; –·–·–·–·–·– 60 min light, 25°C.



5.3. DISCUSSION

5.3.1. PS2 reaction centre CD spectrum

The positive contribution to the spectrum at 682nm may be due to the special pair, and is possibly analogous to the P870 part of the CD spectrum of BChl*a*-containing purple photosynthetic bacteria. Similarly, the CD at 670 nm may arise from pheophytin. The main difference from the CD spectrum of the purple bacterial reaction centre is then the absence of the contribution from the 'voyeur' chlorophylls of the reaction centre. Previously, we noted the absence of CD signals equivalent to those of the accessory BChls in BChl*a* containing reaction centres from purple bacteria. The absence of these bands in the PS2 RC CD spectrum could be attributed to their weak interaction and nearly degenerate transitions (Newell *et al*, 1988). However, this does not explain the non-conservative nature of this region of the spectrum. Similar non-conservative CD spectra have been noted in other pigment-protein complexes, e.g. bacterial reaction centres (Philipson & Sauer, 1973), and antenna bacteriochlorophyll complexes (Morita *et al*, 1977; Hayashi *et al*, 1981; Clayton & Clayton, 1981). Schertz & Parson (1984a) noticed similar spectral features in oligomers of BChl and BPheo which form in some organic solvents, and attributed the phenomenon in all these systems to electrostatic coupling between non-degenerate transitions (Scherz & Parson, 1984b). The same phenomenon gives rise to hyper- and hypochromism and seems the most likely explanation of the non-conservative integrated CD in the Q bands of the PS2 reaction centre CD spectrum.

5.3.2. The effect of aggregation on the reaction centre CD

The conformation of the pigments giving rise to the CD spectrum remains largely unaltered after aggregation or disaggregation of monomeric reaction centre units, as judged by the almost unchanged CD spectrum at the two extreme concentrations TX-100. The rotational strength of a model dimer is proportional to the product of the dipole transition moments of the two monomers. If the dipole strength of one of the monomers decreases, then the rotational strength will also decrease. I attribute the 20% decrease in the CD of the Q_y bands to a slight reduction in dipole strength of the 677-680nm transition. This is consistent with the observed blue shift in the absorption maximum of the reaction centre at high detergent concentrations (see Chapter 3). I attributed this to preferential bleaching of the longest wavelength composite peak in the $Q_{y\,(0\text{-}0)}$ band, due to photooxidation of the primary donor. Possible explanations for the observation of this proposed photooxidation in the disaggregated form of the reaction centre, but not in its aggregated form were discussed in Chapter 3, and are applicable here. The magnitude of the CD of a coupled dimer is proportional to the triple product of

the two dipole moments and the distance between them. Therefore, a reduction of 20% in the strength of one of the dipoles will result in a 20% decrease in the strength of the associated CD bands.

There are small differences in the carotenoid region which shows slight oscillations about the net positive CD in the range 530 to 440nm in the low detergent spectrum. These oscillations, although very small, seem to be completely absent in the high detergent spectrum. The positions of the maxima and minima correspond closely to those observed in the LD spectrum of aggregated reaction centres, and may therefore confirm the interpretation of the excitonic origin of the carotenoid LD in aggregated samples. The oscillations in the carotenoid CD are not large, implying that the two excitonically coupled carotenoid molecules are nearly coplanar.

5.3.3. Similarity of the Chl*a* dimer CD with the PS2 reaction centre CD

The CD spectrum of Chl*a* dimers in CCl_4 is qualitatively similar to the CD of the intact PS2 reaction centre. In both spectra, the Q_y CD is composed of a lower energy positive CD extremum, and a higher energy negative CD extremum. The lowest energy CD maximum at about 680nm is relatively stronger in the reaction centre. The pattern of the sign changes in the B band is the same in the two systems, but there are differences in the positions and widths of the bands. The dimeric Chl*a* CD are broader, and some are shifted to shorter wavelengths with respect to the reaction centre CD bands. Excitonic splitting between CD bands depends on the dipolar coupling between the monomers, so we can say that Chl*a* molecules in CCl_4 interact more strongly than in the PS2 reaction centre. The broad positive CD to the lower energy side of the double CD in the B band of the reaction centre CD is absent in the dimeric Chl*a* spectrum. A possible explanation for this is that it results from interactions between a larger number of pigments in the reaction centre. Given the lack of detailed information on the conformation of the dimer in CCl_4, and the strong possibilty that the reaction centre CD arises from interactions between more than two pigments, the remarkable similarity between the two spectra can only be noted. Similar comparisons have been made by Scherz & Parson (1984a) between the circular dichroic properties of bacteriochlorophyll and bacteriopheophytin in organic solvent and in bacterial pigment-protein complexes.

5.3.4. Comparison of PS2 reaction centre CD spectrum with that of the PS2 core

The most notable difference between the two spectra is the opposite chirality of the two bands in the Q_y region occurring at 682nm (+) in the reaction centre and 678nm (-) in the core, and at 670nm (-) in the RC and 667nm (+) in the core. This indicates strong coupling between pigments in the core complex which is different to that in the reaction centre, and which dominates the core CD spectrum. Different coupling is also shown by the different CD pattern in the Soret bands of chlorophyll absorption. The 444nm transition (core) and 449nm transition (RC) are both negative and might be equivalent, but towards higher energy, the reaction centre exhibits a positive peak at 439nm, where the core has a negative extremum at 434nm. The core CD is weaker than the reaction centre CD. The magnitude of the peaks in the core spectrum are between 10% and 30% of the equivalent peaks in the reaction centre.

5.3.5. Comparison of the reaction centre CD spectrum with other published spectra

The main features of all these spectra of the PS2 reaction centre are different to those of another published spectrum (van Dorssen *et al*, 1987), notably in the Q_y region of the chlorophyll absorption region. All of our spectra show a lower energy positive extremum at 680-682nm, and a negative extremum at 666nm. The spectrum of van Dorssen *et al* shows the opposite chirality of these two bands. Plijter (1988) concludes that their CD spectrum reflects a conformation of the D1/D2 complex which is closer to the native structure *in vivo* than that of the complexes measured in this work. The reproducibilty of our spectrum from sample to sample, and at different concentrations of TX-100, and in samples in which TX-100 has been exchanged for maltoside which have an identical spectrum, puts this conclusion in doubt. Scherz *et al*(1989) report a similar CD spectrum to the one presented in this thesis with the same general features in the Q and B bands. Their spectrum lacks the region of positive CD in the range 530-460 nm.

CHAPTER 6: FOURIER TRANSFORM INFRARED (FTIR) SPECTROSCOPY OF THE REACTION CENTRES FROM *RHODOPSEUDOMONAS SPHAEROIDES* AND PHOTOSYSTEM 2

6.1. INTRODUCTION

Infrared absorption spectra of the reaction centres from the purple photosynthetic bacterium *Rhodobacter sphaeroides* and Photosystem 2 have been measured in the range 1500cm^{-1} to 1900cm^{-1}. The two most prominent peptide infrared transitions occur in this region: the Amide I (C=O stretch; 1600-1690 cm^{-1}) and the Amide II (N-H' bend and C-N stretch; 1480-1575 cm^{-1}) vibrational bands. The position of the Amide I band is sensitive to the conformation of the peptide bond (see Table 6.1), as discussed in the introduction. FTIR spectroscopy has been used here to carry out a comparative study of the protein secondary structure of the PS2 reaction centre complex and the reaction centre from the purple photosynthetic bacterium *Rb. sphaeroides*. Below, I present a summary table of the absorption frequencies relevant to this study. The assignments to different protein structures are from Cantor and Timasheff (1982).

Table 6.1 - Standard infrared absorption frequencies

frequency (cm^{-1})	assignment
1736	Phospholipidester carbonyl stretch
1695	Amide I - anti-parallel β-sheet
1695	Amide I - β-turn (strong)
1656	Amide I - unordered conformation
1652	Amide I - α-helical form
1643	Amide I - random coil form
1635	Amide I - β-turn (weak)
1632	Amide I - anti-parallel β-sheet
1563	COO^- groups (glutamate and aspartate)
1523-1555	Amide II - anti-parallel β-sheet
1536-1562	Amide II - calculated turn frequency
1515	Tyrosine (aromatic ring stretch)
1546	Amide II - N-H bend and C-N stretch

6.2. RESULTS

6.2.1. Absorption spectra

The infrared absorption spectra of the reaction centres from *Rb. sphaeroides* and from Photosystem 2 isolated from pea are shown in Fig. 6.1. The most intense band in the spectra of both reaction centres is located near 1654 cm^{-1}, and corresponds to the Amide I absorption when the peptide bond is located in α-helical regions. The major secondary structure thus appears to be α-helix in both complexes. The main Amide I band of the PS2 reaction centre is narrower than that of the bacterial reaction centre, due to the lower absorption at 1630 cm^{-1}. The Amide II band occurs at 1550 cm^{-1} in both complexes. A notable difference between the FTIR spectra of the two complexes is the occurrence of a distinguishable peak at 1517 cm^{-1} in the spectrum of the PS2 reaction centre, which is present only as a shoulder on the Amide II band of the bacterial reaction centre. This band is due to tyrosine absorption.

6.2.2. Second derivative spectra

Considerable improvement in the resolution of overlapping absorption bands is achieved by differentiation. Derivative spectra were obtained by a simple operation on the interferogram, followed by reverse transformation, as described in Chapter 2. The component peaks in the absorption spectrum appear as negative peaks in the second derivative spectrum.

The positions and assignments of the component vibrations of the reaction centres from *Rb. sphaeroides* PS2 as revealed in their second derivative spectra (Fig. 6.2), are presented in Tables 6.2 and 6.3, respectively.

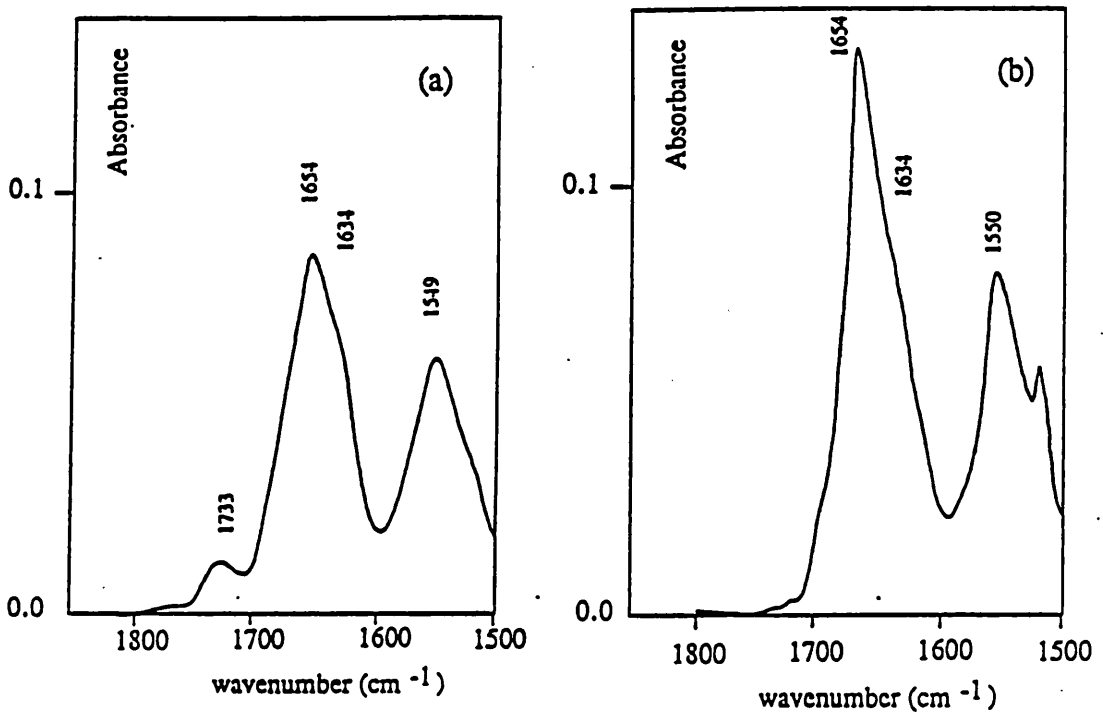


Fig.6.1. FTIR spectra of the reaction centres from (a) *Rb. sphaeroides*, and (b) Photosystem 2. [protein] = 10-30 mg/ml.

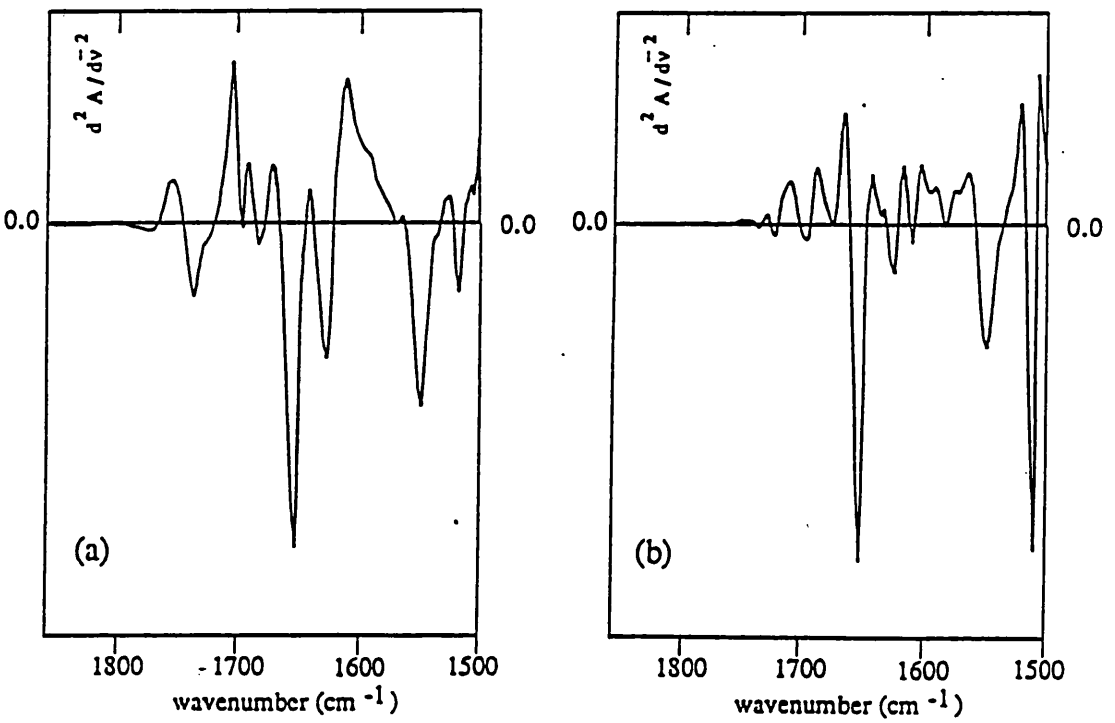


Fig.6.2. Second derivative FTIR spectra of the reaction centres from (a) *Rb. sphaeroides*, and (b) Photosystem 2.

Table 6.2 Band Positions of the Infrared absorption spectrum of *Rb. sphaeroides* reaction centres

Band Position (cm^{-1})	Assignment
1737	C=O stretch in lipid (LDAO or Chl)
1698	chlorophyll or glutamic acid
1684	β-sheet Amide I
1656	α-helical Amide I
1628-34	β-sheet Amide I
1550	Amide II uncertain conformation
1520	Tyrosine
1498	Phenylalanine

Table 6.3 Band positions and assignments of the infrared absorption spectrum of the PS2 reaction centre

Band Position (cm^{-1})	Assignment
1727	C=O stretch (1736?) of lipid
1659	α-helical Amide I (1652?)
1627	β-sheet Amide I (1632?)
1584	ionised COO^- (aspartate, glutamate)
1552	Amide II (1546?) (α-helix?)
1513	Tyrosine (1515?)
1494	Phenylalanine (1495)

6.2.3. Deconvolved spectra

The infrared spectra of the bacterial and higher plant reaction centres have been processed by the deconvolution program ENHANCE (Perkin-Elmer commercial software). This employs the computational technique of Fourier self-deconvolution, described by Kaupinnen *et al* (1981), and discussed in Chapter 2 of this thesis. The deconvolved spectra are shown in Fig. 6.3. The parameters used for satisfactory self-deconvolution, free from artifactual side-lobes, were $\sigma = 7.5$ cm^{-1} (half-width at half peak height) and $K = 2.6$ (resolution enhancement factor).

The major differences between the two complexes is in the Amide I band in the region 1660-1620 cm^{-1}. The bacterial reaction centre has two major peaks at 1655 and 1634 cm^{-1}. These correspond to Amide I absorption in α-helical and β structure, respectively. Three peaks are observed in the same region of the deconvolved spectrum of the PS2 reaction centre. These occur at 1657, 1640, and 1629 cm^{-1}, and correspond to α-helix / unordered, random coil, and anti-parallel β-sheet conformations, respectively.

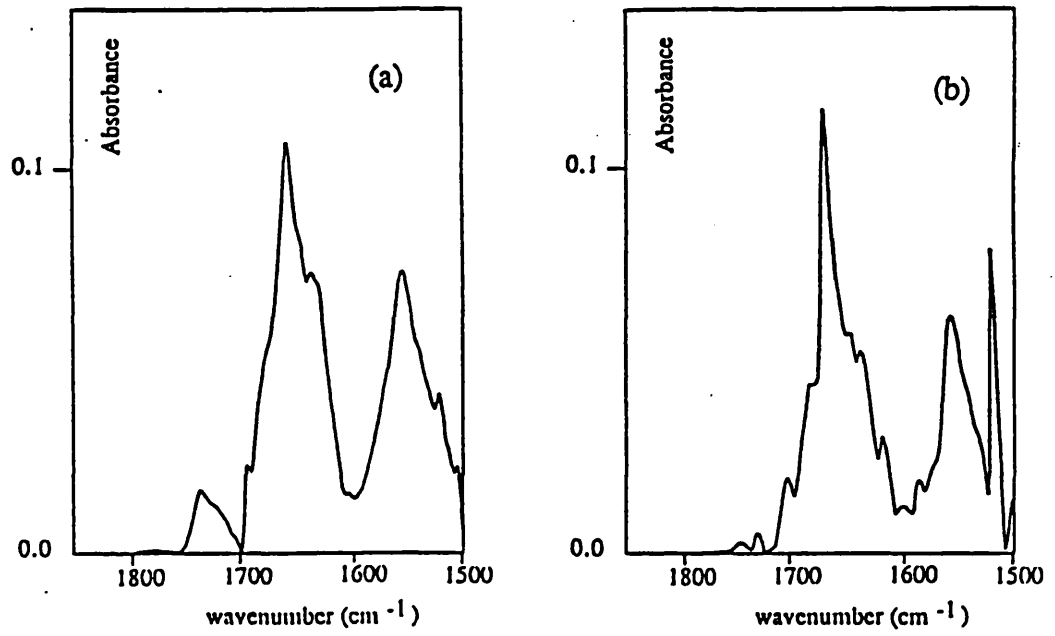


Fig.6.3. Deconvolved FTIR spectra of the reaction centres from (a) *Rb. sphaeroides*, and (b) Photosystem 2, after being processed by the program ENHANCE.

6.2.4. Changes in protein secondary structure of the PS2 RC following exposure to light

Exposure of the isolated photosystem 2 reaction centre to light results in changes in the secondary structure of the constituent polypeptides. After illumination of the sample (30 min of 500 μE m^{-2} s^{-1}, sample on ice) the magnitude of the band at 1633 cm^{-1} increases with a concurrent decrease in the magnitude of the band at 1655 cm^{-1}, relative to the magnitude of the 1550 cm^{-1} band, which remains relatively constant (Fig. 6.4). Leaving the sample at room temperature in the light (8 hours) induces a further increase in the magnitude of the 1633 cm^{-1} band, and decrease in the 1655 cm^{-1} band (Fig. 6.5). From the deconvolved spectra, it is clear that no major new bands appear after photodamage except for a small negative peak in the second derivative spectrum of the damaged sample at about 1530 cm^{-1}. There is a slight shift in the position of the 1700 cm^{-1} band to lower energy. It has been demonstrated that the electron transport activity of the isolated reaction centre complex from PS2 is impaired following exposure to light (Chapman *et al*, 1988).

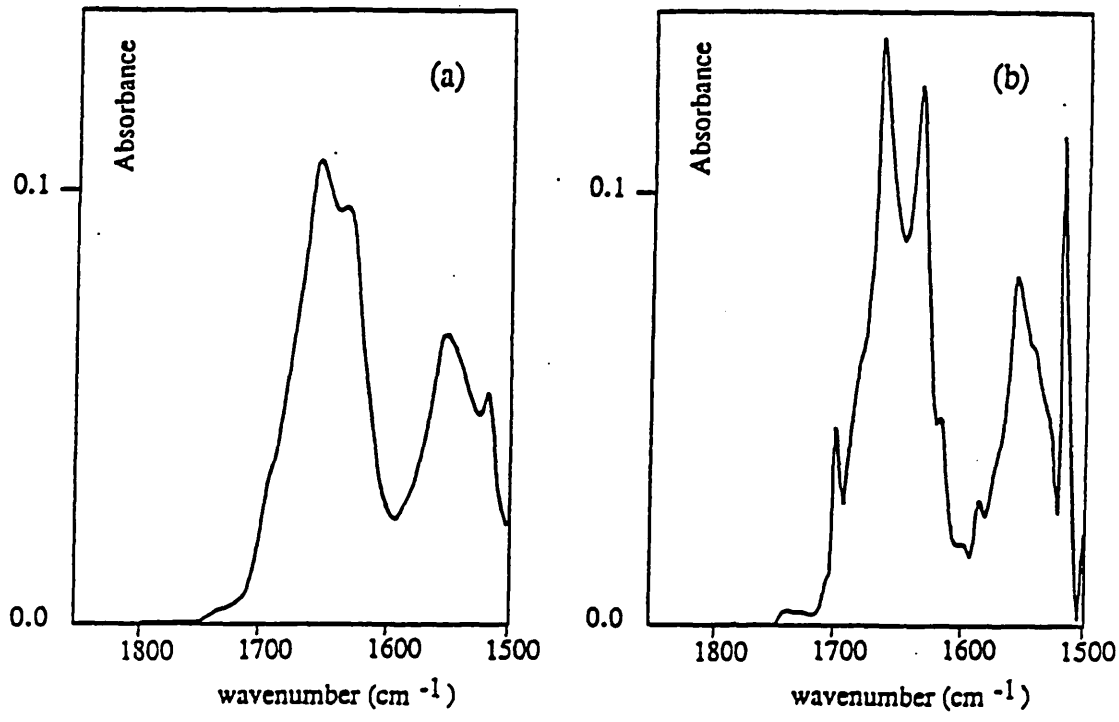


Fig.6.4.(a) FTIR spectrum of the Photosystem 2 reaction centre after exposure to 30 min. of light (50 μE m^{-2} s^{-1}) at 4°C. (b) Deconvolved spectrum of 6.4.(a).

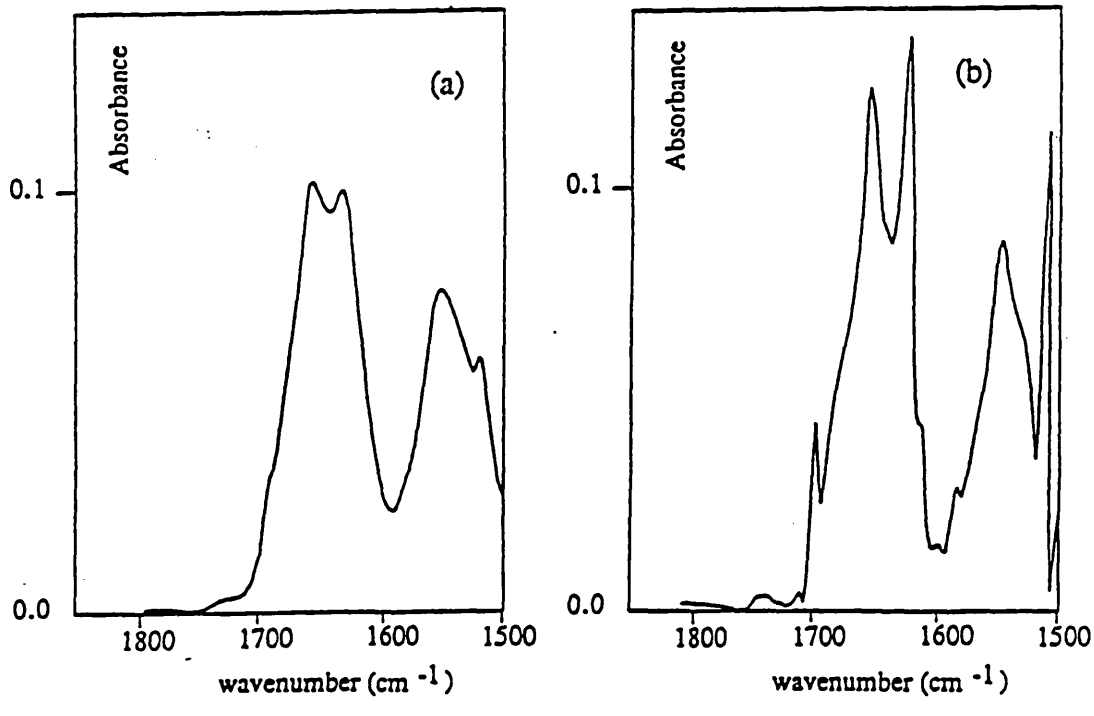


Fig.6.5.(a) FTIR spectrum of the Photosystem 2 reaction centre after exposure to 12 h of light (50 μE m^{-2} s^{-1}) at room temperature. (b) Deconvolved spectrum of 6.5.(a).

6.3. DISCUSSION

6.3.1. Comparison of the FTIR spectrum of the bacterial reaction centre with previously published spectra

The infared spectrum of the reaction centre from *Rb. sphaeroides* was first reported by Nabedryk *et al* (1982). They observed a peak in the Amide I band at 1656 cm^{-1}, which indicated the presence of α-helical structure. They observed that this band is asymmetric, and tentatively ascribe this to some absorption at 1630 cm^{-1} due to β-sheet structure. The second derivative spectrum presented in this study shows a transition at 1628 cm^{-1}, confirming the earlier suggestion that the complex contains some β-sheet structure. The deconvolved spectrum presented here has a main Amide I peak at 1655 cm^{-1} due to α-helical structure. There is a shoulder on the lower energy side of this main transition, which might correspond to the amide transition when in random-coil conformation (1643 cm^{-1}). A second Amide I peak is resolved after deconvolution, centred at 1634 cm^{-1}. This peak is also not symmetric, with a shoulder on the lower energy side. This confirms the presence of β structure, both sheet (giving rise to the shoulder at 1632 cm^{-1}), and turn (1635 cm^{-1}). Nabedryk *et al* (1982) observe a shoulder on the Amide II band at 1515 cm^{-1}, and attribute this to a stretching mode of the aromatic ring of tyrosine. This transition is seen at 1517 cm^{-1} in the second derivative spectrum, and at 1518 cm^{-1} in the deconvolved spectrum.

6.3.2. Comparison of FTIR data with X-ray crystallographic data for the reaction centre from *Rb. sphaeroides*

The three-dimensional structure of the reaction centre from *Rb. sphaeroides* determined by X-ray diffraction (Allen *et al*, 1987) has revealed the secondary structure of the constituent protein subunits L, M, and H. The total number of residues, and the number and percentages of residues in α-helical and β-sheet conformations are summarised in Table 6.4.

Table 6.4 - Number of amino acids and their conformations in the polypeptide subunits of the *Rb. sphaeroides* reaction centre (adapted from Allen et al, 1987b).

subunit	no. aa	helix	(%)	sheet	(%)
L	281	186	(66.2)	36	(12.8)
M	307	198	(64.5)	44	(14.3)
H	207	44	(21.3)	68	(32.8)
LMH	795	428	(53.8)	148	(18.6)

The infrared spectrum of the *Rb. sphaeroides* reaction centre clearly shows α-helix and β-sheet absorption in both the Amide I and Amide II bands.

6.3.3. The quantitative determination of protein structure from FTIR spectra

The assignment of bands to different protein secondary structures from resolution-enhanced spectra should allow an estimation of the amounts of different structures in the protein being investigated. This has been attempted by several groups (see Surewicz & Mantsch, 1988). The methods generally use the peak positions determined from the deconvolved or second derivative spectra as the starting positions for a least-sqaures fit of model Lorentzian bands to the original spectrum. The positions and widths are incremented until a minimum deviation from the measured spectrum is obtained. A serious misuse of this technique (unfortunately the one advised by Susi & Byler, 1986) is to fit Lorentzian curves to the deconvolved spectrum, rather than to the original spectrum. Deconvolution alters the shapes of the measured bands to facilitate visual interpretation of the spectra. Therefore, fitting model curves to these altered spectra to determine component peak areas (i.e. amount of secondary structure absorbing at that frequency) does not bear relation to the actual amounts of different structures in the sample. This problem is discussed, with examples, by Surewicz & Mantsch (1988) who conclude that the information provided by resolution-enhanced spectra is "strictly of a qualitative nature". A satsfactory fit of Lorentzian bands to the original spectrum can be used to determine approximate relative amounts of the different secondary structures, but this method assumes that the extinction coefficients of the different conformations are the same. This has not yet been demonstrated.

Another method, analogous to that used in the analysis of UVCD spectra, would be the use of a database comprising infrared spectra of proteins whose X-ray structure is known, to determine the secondary structure of proteins for which only the infrared spectrum is available. This is an active field of enquiry, but is not yet available as a routine analytical procedure. The recent crystallisation of the reaction centres from *Rps. viridis* and *Rb. sphaeroides* will certainly be of great value in determining the structure of other membrane-bound proteins, whose X-ray structure is not known, from their FTIR spectra.

6.3.4. Comparison of the FTIR spectra of the reaction centres of *Rb. sphaeroides* and Photosystem 2

The spectra after being processed by the deconvolution program ENHANCE are shown in Fig. 6.3. The major differences between the two complexes is in the Amide I band in the region 1660-1620 cm^{-1}. The bacterial reaction centre has two major peaks at 1655 and 1634 cm^{-1}. These correspond to Amide I absorption in α-helical and β-sheet form, respectively. There is more α-helix than β-sheet absorption. Three peaks are observed in

the same region of the deconvolved spectrum of the PS2 reaction centre. These occur at 1657, 1640, and 1629 cm^{-1}, and correspond to α-helix/unordered, random coil, and anti-parallel β-sheet conformations, respectively. The peak at 1657 cm^{-1} corresponding to α-helix / unordered Amide I absorption is relatively more intense in the spectrum of PS2 RC than in that of the bacterial reaction centre, with respect to the β-sheet Amide I transition. In the absence of reliable extinction coefficients, there are three possible interpretations : (1) there is more β-sheet in the bacterial reaction centre, or (2) there are additional helical and/or unordered polypeptide stretches in PS2, or (3) both (1) and (2) contribute to the differences in the spectra. Additional helices are proposed to be present in the PS2 RC in the α- and β-subunits of $Cytb_{559}$ (one helix each). The product of the gene psbI in the isolated PS2 RC (Ikeuchi & Inoue, 1988; Webber *et al*, 1989) may also contain transmembrane helical segments.

The amino acid composition of the two preparations are shown in Table 6.5. The composition of the bacterial system is from Feher and Okamura (1978). The composition of the PS2 reaction centre was determined by Dr. Dave Featherbe (Biochemistry Department, Imperial College, London) using acid hydrolysis and a Beckman 121MB automatic amino acid analyser.

There is clearly a higher proportion of hydrophilic residues in the PS2 reaction centre, some of which might be in α-helical conformation in agreement with the FTIR data. These helices would not be transmembrane, but amphiphilic, associated with the surface of the membrane and not buried within it. Predictions of protein secondary structure based on the average hydrophobicity of short protein segments (see Section 7.4.) place these helices possibly between the transmembrane helices 1 and 2 (residues 77-97 in D1, and 74-94 in D2) and between the transmembrane helices 3 and 4 (residues 166-186 in D1 and D2). This is discussed further in the following chapter.

Table 6.5 Amino Acid Composition of the Reaction Centres of *Rb. sphaeroides* and Photosystem 2

Amino acid	*Rb. sphaeroides*	PS2
Polar residues	**32.3**	**40.7**
Acidic residues	13.61	19.6
Asp	6.91	9.8
Glu	6.70	9.8
Basic residues	8.90	8.3
Lys	2.69	0.9
His	2.38	2.0
Arg	3.83	5.4
Hydroxyl residues	9.77	12.8
Thr	4.83	6.2
Ser	4.94	6.6
Nonpolar residues	**67.7**	**59.5**
Aliphatic rseidues	53.57	49.1
Gly	10.95	10.6
Ala	10.43	9.8
Val	6.49	5.6
Ile	5.49	5.1
Leu	10.84	9.1
Pro	6.04	7.4
Met	2.64	1.5
1/2 Cys (bact)	0.71	---
Aromatic residues	14.13	10.4
Tyr	3.11	2.4
Phe	6.70	8.0
Trp	4.32	---

6.3.5. Photodamage of PS2

The changes observed in the FTIR spectra of PS2 RC after photodamage can be correlated with changes in the migration pattern of the reaction centre polypeptides in SDS-PAGE. It has been observed that the apparent molecular masses of the D1 and D2 polypeptides of photodamaged samples are slightly greater than those from undamaged samples (Chapman *et al*, 1989). These workers also observe that the bands on gels following SDS-PAGE of damaged PS2 reaction centre appear to bind less Coomassie blue stain. The different mobilities cannot be interpreted as due to cleavage of the proteins following damaging light treatment, since then the apparent molecular weights would decrease. They must therefore be interpreted as arising from different conformations adopted by the polypeptides before and after the damaging treatment.

From the FTIR data, we might deduce that the proteins of the reaction centre when in α-helical conformation migrate faster than the same proteins after their light-induced conformational change to β-sheet. This requires that some degree of the original secondary structure is retained during gel electrophoresis even after denaturation by SDS.

The observed changes in protein secondary structure occur on a much longer time-scale (hours) than the light-induced impairment of the electron transport properties of this complex (minutes - Chapman *et al*, 1988,1989). This indicates that only very minor changes in the conformation of the protein (if any at all) are associated with the reduction of the photoactivity of this particle.

6.4. CONCLUSIONS

The results presented in this chapter reveal that the reaction centres from the purple photosynthetic bacterium *Rb. sphaeroides* and higher plant photosystem 2 have similar protein secondary structures. The major conformation adopted by the proteins is α-helical in both complexes. However, there are differences, and the spectra indicate that the higher plant system contains a higher proportion of α-helices. The additional helices may occur as amphiphilic helices connecting the five transmembrane helices that have been proposed for D1 and D2 (Michel & Deisenhofer, 1988; Barber, 1987c), and as transmembrane helices in $Cytb_{559}$ and in the product of gene psbI.

The irreversible light-induced change in the conformation of the photosystem 2 reaction centre proteins from α-helix to β-sheet. This may be related to the general phenomenon of the helix-coil transition, described in detail by Cantor & Schimmel (1980), pp.1041-1108. However, the transitions from α-helix to β-sheet described by these authors are generally induced by a significant temperature increase (to 70°C), or by a large pH change. It appears from this study that light can also induce similar conformational changes, independently of temperature, in the isolated photosystem 2 reaction centre complex. The β-sheet conformation appears to be the more stable for the reaction centre when isolated from the membrane and suspended in buffer, since the light-induced change is irreversible at 4°C in the dark.

While accurate values of the extinction coefficients for the Amide I and II transitions in different conformations are not yet available, protein secondary structure determinations from infrared spectra remain qualitative. However, polarised FTIR spectroscopy is a powerful technique, enabling measurement of the orientation of helices and sheets with

respect to a macroscopic orientation axis. This has been used to identify transmembrane α-helices in the *Rb. sphaeroides* reaction centre (Nabredryk *et al*, 1982), and in the higher plant light-harvesting complex (Nabedryk *et al*, 1984a), and photosystem 1 (Nabedryk *et al*, 1984b). Photosystem 2 has not yet been investigated in this way as an isolated complex.

Light-induced Fourier transform infrared difference spectroscopy has been used to investigate the changes occuring during the primary reactions of photosynthesis in several photoactive complexes (Mantele *et al*, 1985; Tavitian *et al*, 1986; Nabedryk *et al*, 1986; Gerwert *et al*, 1988). In all of these studies, the reaction centre is photooxidised or photoreduced, and the infrared difference absorption spectrum measured. In no case was any large change seen in the protein conformation. All changes could be attributed to redox changes in the pigment molecules. The ability to photoaccumulate $P680^+$ (Barber *et al*, 1987) and $Pheophytin^-$ (Nanba & Satoh, 1987) in the isolated D1/D2 complex has not yet been exploited in FTIR difference spectroscopy.

CHAPTER 7 : CONCLUSIONS AND GENERAL DISCUSSION

In this chapter, I briefly review the most important results of the preceding chapters, and compare these with the results of other independent investigations. It is possible to formulate a speculative model of Photosystem 2 that is consistent with different observations *in vitro* and in the membrane. I conclude with a discussion of some problems which are still unresolved, and propose some future areas of enquiry.

7.1. SUMMARY OF RESULTS

The results of the various spectroscopic measurements presented above have led to the following conclusions:

(1) Many of the absorption and linear dichroism properties of the isolated PS2 reaction centre complex in different supporting media can be explained if the complex occurs in an aggregated form at low concentrations of detergent. The aggregation seems to be specific and reproducible, as judged from the absorption and LD spectra. The complex appears to be monomeric at 0.2% TX-100, and dimeric or more extensively aggregated at 0.02% TX-100.

(2) PS2 reaction centres appear to be aggregated in a similar way in larger oxygen-evolving core complexes. The orientation properties, and therefore the relative dimensions, of the core complex are comparable to those of the proposed dimeric reaction centre complex.

(3) The linear dichroism spectrum of the monomeric reaction centre is consistent with a mutually perpendicular orientation of the primary donor Q_y transition and the dipole moment of the carotenoid, as in bacterial reaction centres. However, the orientations of the two transitions in the bacterial and oxygen-evolving systems differ with respect to the membrane plane, suggesting a difference in the organisation of the donor side in relation to the rest of the reaction centre.

(4) Circular dichroic spectroscopy has revealed the presence of strong excitonic interactions between the pigments of the isolated reaction centre. The strength of this dipolar coupling is only slightly reduced at detergent concentrations judged to be sufficient for complete disaggregation of the particles. Illumination of the sample decreases the strength of the coupling, and all bands decrease at approximately the same rate.

(5) Fourier transform infrared (FTIR) spectroscopy reveals similarities between the

protein secondary structure of reaction centres from the purple bacterium *Rhodobacter sphaeroides* and from Photosystem 2. The Photosystem 2 reaction centre contains relatively more α-helical structure. Illumination of the PS2 reaction centre causes a rearrangement of the proteins from α-helical conformation to β-sheet. Changes are also observed in the ultra-violet circular dichroism (UVCD) spectra of the PS2 reaction centre after the same treatment, indicating a gradual loss of α-helical structure.

I now examine independent evidence which also suggests the existence of aggregated forms of Photosystem 2 *in vivo* and *in vitro*.

7.2. OTHER EVIDENCE FOR AGGREGATION OF PHOTOSYSTEM 2

7.2.1. Cross-linking and binding experiments

The spatial relationships of photosystem 2 polypeptides has been investigated using the reversible cross-linking agent dithiobis (succinimidyl propionate) (DSP) (Millner *et al*, 1987). Their analysis of the off-diagonal spot-pattern on two dimensional gels after cleavage of the cross-linker led to the conclusion that the extrinsic 16kD polypeptide of the water-splitting complex may exist as a homodimer in the PS2 complex in PS2-enriched membranes. They further conclude that because the 16, 23, and 33 kD polypeptides are thought to occur in equimolar amounts (Murata *et al*, 1983; Andersson *et al*, 1984), then PS2 particles contain two copies of each of 23 and 33 kD components in close proximity. That is, an active oxygen-evolving PS2 complex comprises a dimer of two monomeric units. The authors suggest that there may be more than one copy of each of the three polypeptides per PS2 complex.

Recent experiments (Gounaris *et al*, 1988a) have shown that the D1/D2/Cytb$_{559}$ complex binds to the 33kD protein immobilised on Sepharose 4B. These workers also showed that when core complexes (method of Ghanotakis and Yokum, 1986) were solubilised with 1% Triton X-100 and loaded onto the column, the D1/D2/Cytb$_{559}$ complex is retained, and the 47 and 43 kD pass through the column. Thus there appears to be a specific association of the 33kD protein with (a) component(s) of the D1/D2/Cytb$_{559}$ reaction centre complex, but not with either of the two antenna polypeptides. The stoichiometry of binding has not yet been determined.

If the stoichiometry of binding on the column is 1:1, then the results of Millner *et al* (1987) and Gounaris *et al* (1988) together provide indirect evidence that PS2 reaction centres aggregate to form dimers in PS2-enriched membranes, and perhaps also *in vivo* in the granal thylakoid membranes. It also provides some support for the proposal

(Chapter 4) that the recognition site for PS2 association is on the D1/D2/Cytb$_{559}$ complex.

7.2.2. Electron micrographic investigations

Two groups have independently studied the dimensions of PS2 using electron microscopy. Morschell and coworkers (1987, 1988) have examined the thylakoid membrane of cyanobacteria, and isolated PS2 core complexes before and after incorporation into lipid bilyers. Rogner *et al* (1987) investigated PS2 complexes isolated following the same procedure, and purer complexes obtained after further detergent solubilisation. Comparable results were obtained by the two groups.

7.2.2.1. Morschel *et al*

These authors compare the molecular structure of freeze-fracture particles of thylakoid membranes from the thermophilic cyanbacterium *Synechococcus* sp. with that of PS2 complexes reconsituted into soybean phosphatidylcholine liposomes, and with the structure of the TX-100-isolated complexes from the liposomes. The thylakoid membranes contain particles which are either scatterred in the membrane or organised into rows of variable length. The unit particle of the rows measures 10nm x 20nm, and different numbers of these are aligned to give rows of different lengths. The 10nm x 20nm particle appears to be separated perpendicular to the long axis into two parts, and is proposed to represent a dimer of monomeric 10nm x 10nm particles.

Oxygen-evolving PS2 complexes isolated from *Synechococcus* according to the method of Schatz & Witt (1984) were incorporated into lipid vesicles by freeze-thaw and sonication procedures, and examined by negative contrast and freeze-fracture electron microscopy. The structure of these vesicles is similiar to that of the thylakoid membrane fragments. Monomeric 10nm x 10nm particles are seen, as well as 10nm x 20nm particles which have a furrow perpendicular to their long axis. The relative amounts of these two forms depended on the lipid composition of the vesicles. The presence of cholesterol increased the proportion of the dimeric particles, and was correlated with a higher rate of oxygen evolution. The authors propose that the monomeric unit consists of the reaction centre, core antenna complex, and the phycobilisome-binding polypeptides.

The complexes when isolated from the liposomes by TX-100 fall into two classes: spherical ellipsoid and binary. The binary particles measure 20-25nm x 10-14nm and are divided perpendicular to their long axis into two spherical-ellipsoidal parts measuring 10-12nm x 14-16nm.

The similarity in the size of the particles observed *in vitro* and in the PS2 proteoliposomes and thylakoids leads the authors to conclude that the 10nm x 10nm and 10nm x 20nm particles in thylakoids represent monomeric and dimeric PS2 complexes,

respectively. They observe that a dimeric arrangement of PS2 in the membrane is consistent with the size of the phycobilisome antenna, since the two basal phycobilisome core cylinders which are present in each phycobilisome together match the size of the two PS2 monomers.

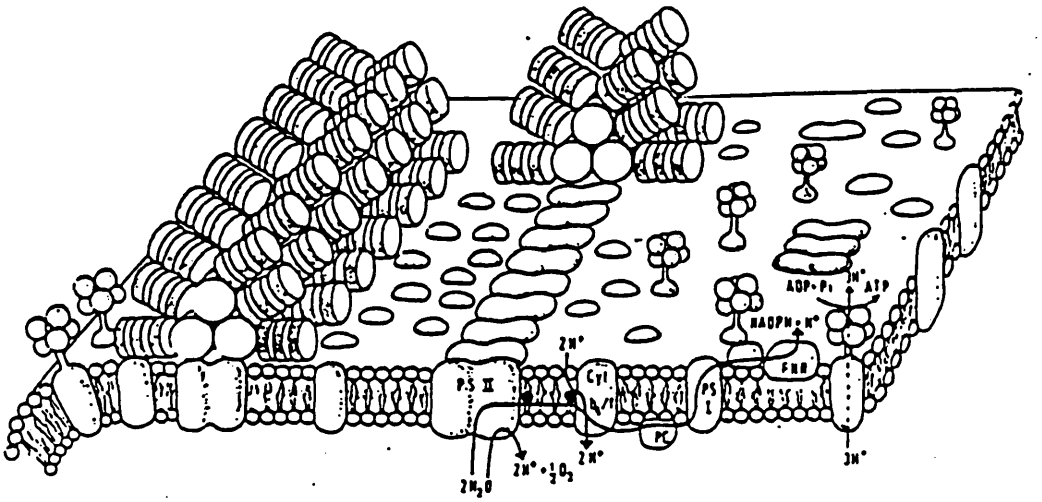


Fig.7.1. Schematic view of the arrangement of phycobilisomes and Photosystem 2 in the thylakoid membrane of cyanobacteria. Drawing by E. Morschel (from Zuber *et al*, 1987).

7.2.2.2. Rogner *et al* (1987)

Comparable results have been obtained by Witt's group in Berlin. These workers present electron micrographs of PS2 complexes isolated from *Synechococcus*, by the method of Schatz & Witt (1984), with some further purification. These particles were fractionated from phycocyanin (PC) and allophycocyanin (APC) by sucrose density gradient ultracentrifugation, and subjected to a further round of solubilisation by the detergent β-octylmaltoside. A second gradient (20 - 40% sucrose) separates two bands with molecular weights (as determined from gel filtration) of 300 kD and 500 kD. The same polypeptides were observed in both the smaller SG-2a complex and the larger SG-2b complex (49, 43, 33, 30, 27 kD and the 9 and 4 kD apoproteins of $Cytb_{559}$), apart from the presence of the 19 and 17 kD APC polypeptides in the larger one.

The 300 kD particle measures 15.8 ± 0.8 nm x 10.5 ± 0.8 x 6.4 ± 0.7 nm, and the 500 kD particle has dimensions 15.1 ± 1.5 nm x 18.5 ±1.0 nm x 6.6 ± 0.6 nm. The particles, especially the larger 500 kD ones, are seen to aggregate such that the side view is seen as a repeating unit.

The authors conclude, on the basis of the molecular mass of the components of the PS2 complex, that the smaller particle represents a monomeric form of the PS2 complex, and

the 500 kD particle is a dimeric form. They suggest that the smallest dimension of the elliptical discs (6.5 nm) spans the membrane with a hydrophilic surface at the top and bottom of the disc.
The aggregation may be an artifact of the isolation procedure, but the authors prefer to consider that the normal, functional PS2 in cyanobacteria is a dimer.

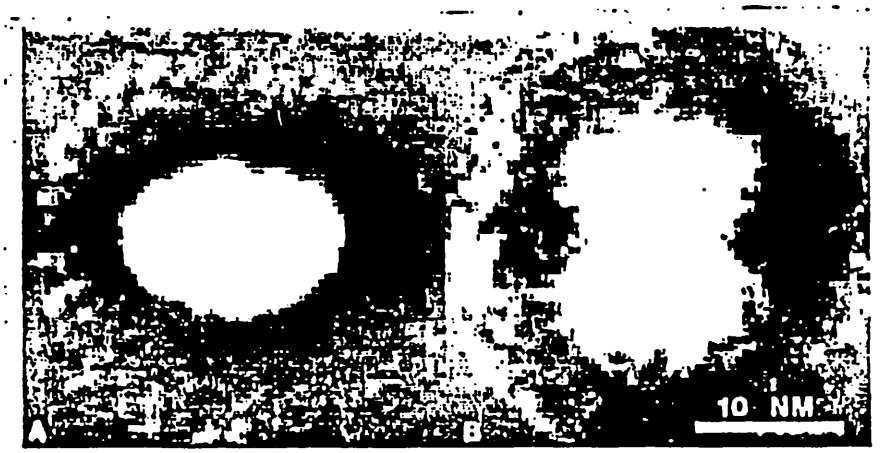


Fig.7.2. Averaged images of (a) 106 top view projections of the monomeric SG-2a complex, and of (b) 16 top views of the dimeric SG-2b complex. (from Rogner *et al*, 1987).

7.2.2.3. Consensus on dimensions from these two studies

There is an approximate correspondence between two of the three dimensions of the monomer and dimer proposed and observed independently by the two groups. The 10nm x 10nm and 10nm x 20nm particles observed in the membrane by Morschel and Schatz appear to correspond to the 15.8nm x 10.5 nm and 15.1nm x 18.5nm particles seen by Rogner *et al.* These dimensions are both parallel to the plane of the membrane as observed by Morschel and Schatz. Thus aggregation of two monomers to form a dimer occurs between parts of the two monomers that are within the lipid bilayer. The third dimension corresponds to the length of the particle perpendicular to the membrane plane. Rogner *et al* measure this as 6.5nm. Morschel and Schatz observe dimeric particles in the liposomes fractured perpendicular to the membrane with a height of 13-16 nm, approximately twice that of Rogner *et al.* Assuming that this dimension belongs to the minimal unit, this imples that in the membrane, two PS2 complexes are stacked on top of each other in the membrane. Since the PS2 complex is vectorial, with the oxidising side in the lumen, and the reducing side towards the stroma, this seems an unlikely arrangement of PS2 in the membrane. A more likely explanation is that this dimension was overestimated by Morschel & Schatz by a factor of two. This may be due to

"membrane collapse", an artifact encountered occasionally in electron microscopy, resulting in overestimation of transmembrane dimensions by a factor of two.

7.3. PREDICTIONS OF THE SECONDARY STRUCTURE OF PHOTOSYSTEM 2

Various computer algorithms have been developed to predict protein secondary structure from the primary amino acid sequence. I have used three of these methods to analyse the sequences of the constituent polypeptides of the reaction centres from *Rb. sphaeroides* and Photosystem 2. The method of Klein *et al* (1985) is an empirical method to discriminate between integral membrane-bound and peripheral proteins using a table of individual amino acid hydrophobicity. If the protein is defined as integral, the algorithm determines the position and length of membrane-spanning segments. Eisenberg *et al* (1984) also employ individual residue hydrophobicity to identify α-helical segments associated with a membrane. These are further characterised by a quantity known as the "hydrophobic moment" (Eisenberg *et al*, 1982). Those helices with a large hydrophobic moment are asymmetric in hydrophobicity, one side of the helix being more hydrophobic than the other. Such helices are predicted to lie along the surface of a membrane, and not lie within it. An empirical discrimination between membrane-bound helices (T), surface-seeking helices (S), and helices found within globular proteins (G) is possible using a plot of the hydrophobic moment against hydrophobicity. Rao & Argos (1986) use additional residue properties to define a "membrane-buried helix parameter" for delineating transmembrane α-helical segments in a protein. These properties are hydration potential, free energy of transfer of an amino acid from a helix in aqueous medium to a helix in a non-polar medium, polarity, bulk, and preference for the location of the amino acid in turns. The weighting factors for each of these parameters were determined to give the best fit between predicted helices and those observed for bacteriorhodopsin. At the time this method was developed, this was the only membrane-bound protein whose structure was known to resonably high resolution (6Å). As a test of the three predictive methods, the sequences of the L, M, and H subunits from *Rb. sphaeroides* were analysed. The sources of the sequences were: Williams *et al*, 1983 (M subunit), 1984 (L subunit), and 1986 (H subunit), Zurawski *et al*, 1982 (D1), Rochaix *et al* , 1984 (D2), Alt *et al*, 1984 (47 and 43 kD), Hermann *et al*, 1984 ($Cytb_{559}$, 9kD and 4kD subunits). All the proteins analysed were classified as integral according to the method of Klein *et al*, and all contained α-helical structure in agreement with the FTIR and UVCD data presented earlier. The positions of the predicted helices are presented in Table 7.1.

Table 7.1. Positions of the transmembrane helices predicted from several different methods

Polypeptide	X-ray	Klein *et al*	Eisenberg *et al*	Rao/Argos
L	32-55	28-59	29-49 (T)	13-55
	83-111	-	78-98 (T)	83-102
	116-138	115-141	113-133 (T)	111-152
	-	-	137-157 (G)	-
	171-198	179-196	175-195 (T)	172-198
	225-250	231-257	232-252 (S)	219-256
	-	-	259-279 (S)	-
M	-	-	32-52 (T)	-
	54-78	54-74	55-75 (T)	50-75
	-	-	89-109 (G)	-
	109-139	111-130	111-131 (T)	112-131
	147-168	146-164	148-168 (S)	146-169
	200-226	-	206-226 (T)	201-227
	262-286	268-291	268-288 (T)	268-291
H	227-244	229-249	230-250 (T)	231-258
D1	-	32-58	33-53 (T)	30-55
	-	-	77-97 (T)	-
	-	112-128	105-125 (T)	-
	-	142-161	143-163 (T)	142-164
	-	-	166-186 (G)	-
	-	-	192-212 (T)	192-221
	-	273-291	271-291 (T)	271-297
D2	-	-	36-56 (T)	-
	-	-	74-94 (G)	-
	-	111-128	108-128 (T)	108-128
	-	142-165	144-164 (T)	144-162
	-	168-186	166-186 (S)	171-189
	-	196-219	199-219 (T)	197-219
	-	270-292	270-290 (T)	267-294
$Cytb_{559}/\alpha$	-	21-38	19-39	20-44
$Cytb_{559}/\beta$	-	15-31	-	9-34
47	-	-	19-39 (T)	22-45
	-	-	60-80 (G)	-
	-	96-112	96-116 (T)	95-116
	-	138-154	138-158 (S)	138-163
	-	203-219	197-217 (T)	201-217
	-	237-253	237-257 (T)	236-263
	-	-	450-470 (T)	449-468
43	-	-	45-65 (T)	45-67
	-	85-102	85-105 (T)	85-102
	-	110-130	113-133 (S)	110-138
	-	158-185	159-179 (S)	159-185
	-	-	206-226 (G)	-
	-	236-254	232-252 (S)	236-254
	-	270-294	272-292 (T)	270-292
	-	-	425-445 (T)	428-443

Considering the functional and structural similarities between Photosystem 2 and the purple bacterial reaction centre, it has been proposed that the polypeptides D1 and D2 each have five transmembrane helices (Deisenhofer *et al*, 1985; Trebst, 1986). The three methods used in this study give contradictory results, although there is some agreement for individual helices. It is apparent from the results presented above that no one method predicts protein structure unequivocally. These methods must be combined with other data for realistic predictions (see McCrea et al, 1988, for a descrition of contradictory models of the acetylcholine receptor, and Argos and Rao, 1986 for a general discussion of protein secondary structure predictions). Deisenhofer *et al* (1985) consider the regions of strong sequence homology between the L, M, D1 and D2 polypeptides, and relate these to the positions of the transmembrane helices of L and M in the structure of the bacterial reaction centre. Trebst (1986) considers in detail the herbicide-binding properties of various bacterial and higher plant mutants which show altered herbicide-binding affinities at the Q_b-binding site. He formulates a model that accomodates the regions of sequence homology which explains the altered properties of the herbicide-resistant mutants. Sayre *et al* (1986) have verified, in part, the five-helix model for D1 using site-specific antibodies to the regions of the protein that are predicted to be exposed at the membrane surface.

The cytochrome subunits are each predicted to have one transmembrane helix, although the Eisenberg method fails to detect a helix in the 4kD subunit.

There is good agreement in the prediction of the majority of the helices in both the 43kD and 47kD subunits, although the exact number of helices in each protein cannot be deduced from these results alone. The choice of six transmembrane helices for each of the 43kD and 47kD complexes in the model of the PS2 core complex presented below is therefore somewhat arbitrary, although Vermaas *et al* (1987) and Chisholm & Williams (1988) both propose a six-helix model for CP43 and CP47 based on sequence data for the psbC and psbB genes in *Synechocystis* 6803. A striking feature shared by both proteins is the presence of a long hydrophilic region between the two helices nearest the C-terminus (133 residues in the 43kD; 186 in the 47kD). It is known that the N-terminus of each of these polypeptides is exposed on the stromal surface of the thylakoid membrane (Michel *et al*, 1988). However, this information cannot be used to determine the location of the long hydrophilic regions until the number of helices has been unequivocally determined by the use of site-specific antibodies. It is possible that they form a large hydrophilic domain, together with residues 34-85 of the α–subunit of $Cytb_{559}$ and the hydrophilic inter-helix segments in D1 and D2, on the luminal surface of the thylakoid membrane. This domain could form a binding-site for the 33kD extrinsic protein. The results of Sayre *et al* (1986) suggest a close association of D1 with the

33kD protein. Tae *et al* (1988) observe that removal of the extrinsic polypeptides of the oxygen-evolving complex from thylakoid membranes results in an increase of the accessibility of the α-subunit of $Cytb_{559}$ to trypsin. The association of the isolated PS2 reaction centre with immobilised 33kD protein (Gounaris *et al*, 1988) was mentioned above (Section 7.2.1).

7.4. THE DIMENSIONS OF THE MODELS OF THE REACTION CENTRE AND CORE COMPLEXES OF PHOTOSYSTEM 2

The number of residues in the transmembrane helices predicted by the computer algorithms varies between 20 and 31 residues, corresponding to a length of 30-47 Å, assuming a translation distance along the helix of 1.5Å per residue. These algorithms have inherent constraints on the minimum length of transmembrane helices, and therefore do not provide new evidence concerning this dimension. Transmembrane helices must be of equal or greater length than the thickness of the lipid bilayer. This has been estimated from electron diffraction studies to be between 3 and 5nm. The transmembrane dimension of the PS2 particles observed by Rogner *et al* is 6.5nm. Thus, there are some regions of the proteins of PS2 that protrude out of the membrane plane.
The two dimensions that are coplanar with the membrane are related to the distances between the α-helices in the plane of the membrane. The diameter of a single helix is 6Å, neglecting side chains. With protruding side chains, the diameter is probably about 10-15Å. The cross-section of the bacterial reaction centre is 70Å x 30Å. The relative positions of the transmembrane helices of the L and M subunits perpendicular to the membrane plane, as revealed by the X-ray crystallographic data, form two arcs related by a rotational axis of symmetry.Below, I draw a diagram for the D1/D2 pair of PS2 for similarity to the bacterial reaction centre, using five transmembrane helices for each as discussed above, with similar dimensions to the bacterial reaction centre.

Fig.7.3. Proposed arrangement of the helices of D1 and D2, viewed perpendicular to the membrane plane.

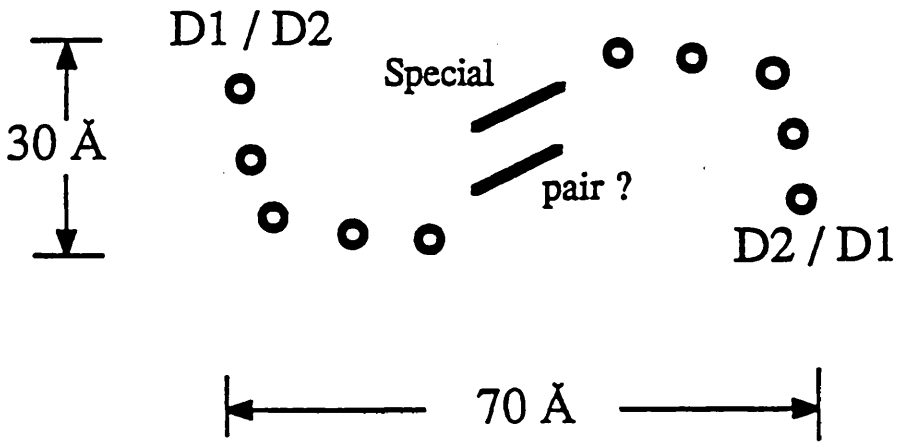
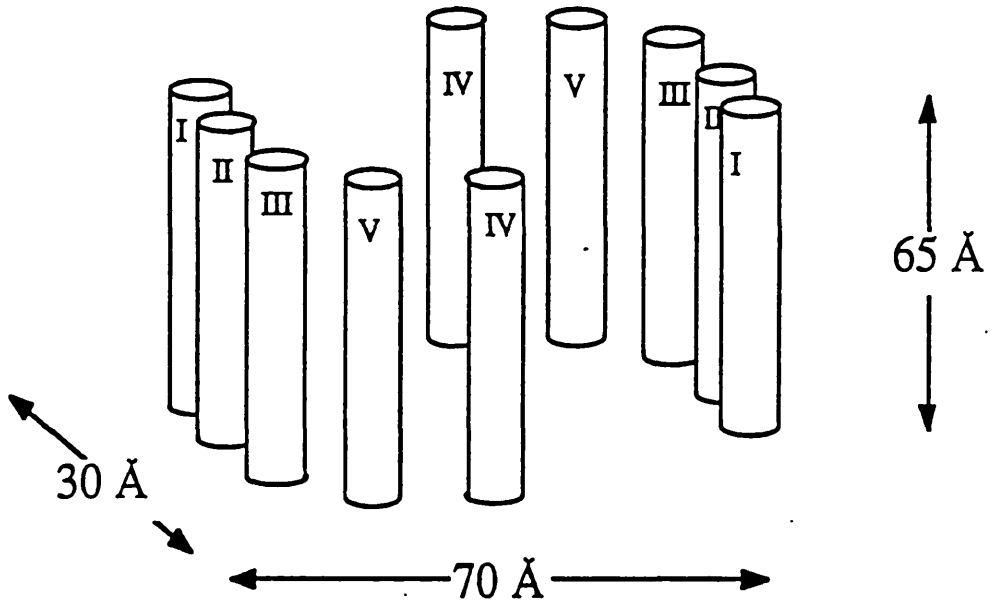


Fig.7.4. Side view of the helices of D1 and D2. The membrane plane is perpendicular to the plane of the paper.



A development of the model of the core complex proposed on the basis of LD spectroscopic data in Chapter 4 is presented below. I include approximate dimensions based on the electron micrographic evidence, and on the dimensions of the bacterial reaction centre.

Fig.7.5. Proposed arrangement of the helices of the dimeric Photosystem 2 core complex, viewed perpendicular to the membrane plane. Car - β-carotene; SP - special pair.

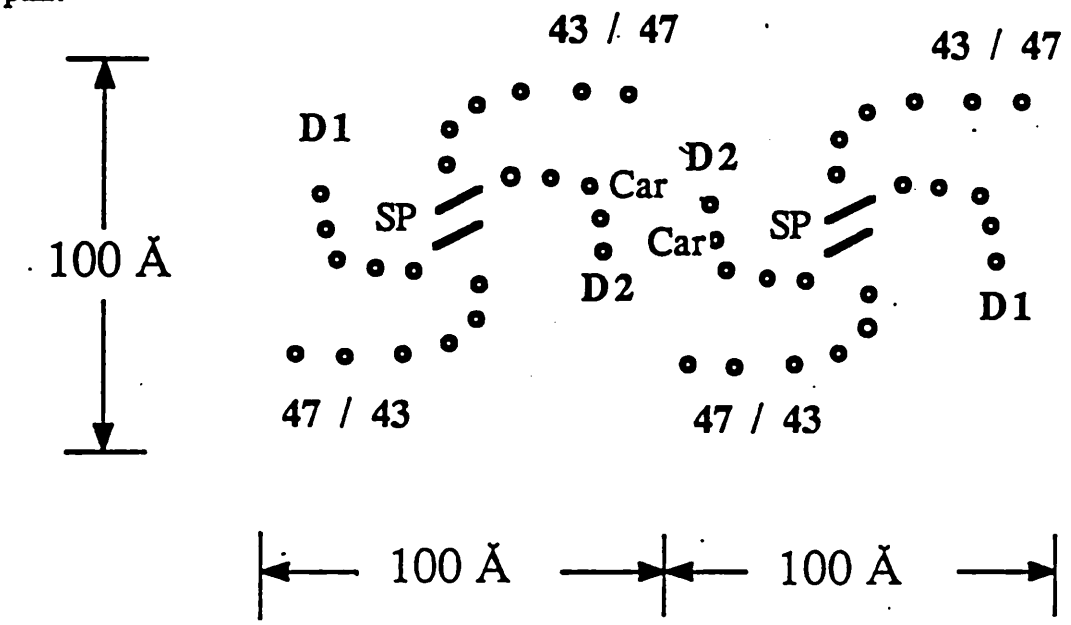
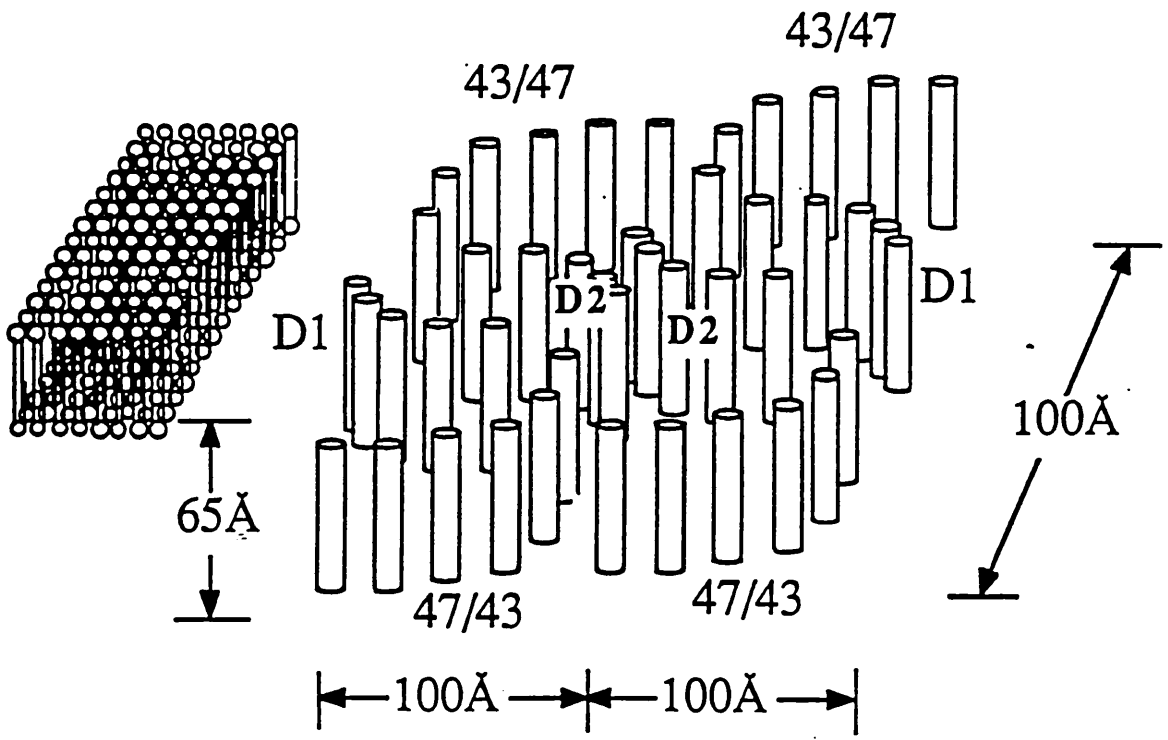


Fig. 7.6. Side-view of the transmembrane helices of the dimeric Photosystem 2 core complex. As discussed below, a possible location of the helices of Cytochrome b_{559} would be at the junction of the two monomeric core units, i.e. near the D2 subunits.



Dekker *et al* (1989, submitted) have recently crystallised a Photosystem 2 core complex from a 43kD subunit-lacking mutant of *Synechococcus* sp. Preliminary low resolution electron micrographs (P.Nixon, DuPont, pers. comm.) show that the longest dimension of this complex is similar to that of the intact PS2 crystals (~20nm), but has a slightly reduced perpendicular dimension, consistent with the placement of the 47 and 43 kD proteins at opposite sides of the D1/D2 heterodimer.

7.5. AGGREGATION OF PHOTOSYSTEM 2 *IN VIVO* AND *IN VITRO*

I now examine the question raised in Chapter 4 concerning the (presumably) different mechanisms involved in the aggregation of hydrophobic proteins *in vitro* at lowered detergent concentrations, and *in vivo* in biological membranes when the aggregating faces of the particles are exposed to hydrophobic lipid molecules. The electron micrographic evidence clearly demonstrates aggregation *in vivo*. The reason for this aggregation has been interpreted as due to the morphology of the phycobilisome antenna, and is therefore a property expected only in cyanobacteria and red algae. However, the likely occurrence of aggregation of PS2 reaction centres and larger core complexes *in vitro*, when isolated from higher plants indicates that this may be a general phenomenon of photosystem 2. Aggregation is proposed by Morschel and Schatz (1987) to confer some evolutionary advantage through an increased efficiency of excitation energy transfer from the phycobilisome antenna, and was presumably acheived by the selection of protein sequences for PS2 which have mutual recognition sites.

The electron micrographic evidence for PS2 dimers relates only to cyanobacteria, and is thought to be necessary for correct coupling of PS2 with the phycobilisome. The results presented in this thesis indicate that aggregation also occurs *in vitro* between PS2 particles derived from higher plants, which do not contain phycobilisomes. If these organisms have a shorter evolutionary history, then aggregation has possibly been retained merely because there has been no selection pressure against it, or because dimerisation confers advantages other than facilitating the correct binding of phycobilisomes. Whether the proposed homodimeric arrangement of the oygen-evolving complex (Millner *et al*, 1987) directly affects the efficiency of the water oxidation reaction has not yet been demonstrated. The implications for the function of $Cytb_{559}$ are discussed below.

Reconsitution of the D1/D2 complex in lipid bilayers may reveal whether the isolated complex aggregates in a comparable way in a hydrophobic environment as in aqueous solution. Haworth et al (1982b) measured the linear dichroic properties of thylakoid membranes from the *Chlorina* Chl*b*-less mutant of barley. Very similar sign changes in the LD of the carotenoid occur in this system as occur in the *in vitro* PS2 core and

aggregated reaction centre complexes. If the interpretation of these sign changes as arising from aggregation of PS2 is correct, then PS2 complexes may also be aggregated in these thylakoid membranes.

7.6. IMPLICATIONS OF PHOTOSYSTEM 2 AGGREGATION

7.6.1. P680 : PS2 stoichiometry

The recent flash absorption study of the D1/D2 complex by Takahashi *et al* (1988) revealed a value for the ratio P680:Chl of 1:20, implying that 75-80% of the complexes were inactive. The authors remark that this interpretation is not satisfactory, since it conflicts with their previous measurements of photochemical activity (Nanba & Satoh, 1987). A possible explanation is that the complexes were aggregated. Depending on the intensity of the actinic flash, exciton annihilations may occur, reducing the number of photons available for initiating the charge separation, and resulting in an underestimate of the concentration of P680 per chlorophyll. Exciton annihilation experiments have been performed on several photosynthetic systems to determine the domain size of coupled pigments in arrays of light-harvesting complexes (Bakker *et al,* 1983; Den Hollander *et al*, 1983). Similar experiments could prove an accurate means of estimating the extent of aggregation of the isolated PS2 reaction centre complex.

7.6.2. Two pools of cytochrome and the stoichiometry of $Cytb_{559}$: PS2

The precise function of $Cytb_{559}$ in active photosystem 2 particles remains unclear. A recent review (Cramer *et al*, 1986) summarises many important results, so I discuss here only a few of its properties in relation to results presented in preceding chapters. Two distiguishable pools of $Cytb_{559}$ with different redox properties were indicated by the biphasic oxidation of two high potential haems (Selak *et al*, 1984). One is of higher mid-point redox potential (+400 mV) than the other (+20 mV). The stoichiometry of $Cytb_{559}$: PS2 is reported by some as 2:1 (Yamamoto *et al*, 1984; Murata *et al,* 1984), and by others as 1:1 (e.g. Sandusky *et al,* 1983). The observation of two pools of cytochrome, and the stoichiometry of 2:1 seem inconsistent with the isolation of a photosystem 2 reaction centre containing only one cytochrome per two pheophytin molecules (Nańba & Satoh, 1987).

I suggest here that the different redox properties of the two pools of cytochrome and the conflicting stoichiometries might both arise as a result of the dimerisation of PS2.

Firstly, redox properties are determined by a number of physical conditions. These

might loosely be called "environmental factors". The two redox-distinguishable pools of Cyt b_{559} might arise from an "asymmetric dimerisation" of two reaction centres. For the aggregation to affect the redox properties of the cytochrome, its location in the monomeric reaction centre should be part of, or very near to, the proposed aggregation site, i.e. closer to D2 than D1. Aggregation might result in a slight change in the conformation of the cytochrome polypeptides, bringing the haem ring into an environment with different electrophilicity, thus altering its redox properties. Babcock *et al* (1985) have suggested that changes in the relative orientation of the imidazole rings from parallel to perpendicular are responsible for the transition from high-potential to low-potential cytochrome. Denaturation of $Cytb_{559}$ has been observed by Rutherford (1985b) to be accompanied by a change in the orientation of the haem plane relative to the membrane plane from perpendicular to an angle of 45°. Other factors correlated with the redox potential of the cytochrome are the hydrophobicity of the environment and in reconstituted systems, the presence of plastoquinone and β-carotene (Okayama & Butler, 1972; Cox & Bendall, 1974).

Secondly, the observed stoichiometry of 2 $Cytb_{559}$: P680, and the isolation of a complex containing 1 $Cytb_{559}$: PS2 reaction centre are mutually inconsistent. This could be due to the method of determining P680 concentrations. As discussed above, quantitative estimates of P680 may be misleading, due to their possible dependence on the extent of aggregation of PS2 complexes. If the unit giving rise to the signals for P680 estimation is a dimer of PS2 complexes, then flash absorption measurements may detect only one of the two component P680 entities. Thus P680 would be underestimated by a factor of two, and the ratio of $Cytb_{559}$: P680 overestimated by a factor of two. It is interesting to note that Klimov *et al* (1980a) measure the stoichiometry of non-haem iron : PS2 as 2:1.

If the two pools of distinguishable cytochrome arise from simple aggregation of two identical reaction centre/cytochrome monomers, then each of the cytochromes in the dimer must have the same vectorial arrangement with respect to the membrane plane. This is contrary to the model of Cramer *et al* (1986) which places the two haem rings at opposite faces of the membrane. However, more recent work (Tae *et al,* 1988) has located the N-terminus of the a subunit exclusively on the stromal side of the membrane. If the monomeric haem is an α/β heterodimer (see below, and discussion in Tae *et al,* 1988), then both haems will lie nearer the stromal face of the thylakoid membrane. This is consistent with the proposals based on aggregation presented above.

7.6.3. Cytochrome b_{559} and photoinhibition

Cramer *et al* (1986) suggest that cytochrome b_{559} serves as part of a stress-response system for photosystem 2, mediating repair to damaged oxygen-evolving complexes caused by heat, chilling, or water stress. A recent report (Thompson & Brudvig, 1988) also assigns a protective role to $Cytb_{559}$. These authors propose that oxidation of a nearby chlorophyll molecule by $P680^+$ is the first event in photoinhibition. Further damage is prevented by re-reduction of this chlorophyll by cytochrome b_{559}. This proposal may be related to the observation of cytochrome oxidation only when the water-splitting complex activity is impaired (Knaff & Arnon, 1969). Thompson & Brudvig assume the presence of two copies of cytochrome b_{559} in Photosystem 2, and explain this as due to the need to rereduce the two photooxidisable monomeric chlorophyll molecules (assumed to be present in PS2 by analogy with the bacterial reaction centre), to protect Photosystem 2 from photoinhibition. It is possible that both proposals are correct in part.

I proposed above that the cytochrome might become distinguishable into two pools with different redox properties only after aggregation of monomeric reaction centres to form dimers in core complexes. Here, I propose further that this dimeric arrangement of $Cytb_{559}$ is necessary for its correct functioning in the prevention of damage to Photosystem 2 by the environment. Then the monomeric form of $Cytb_{559}$ in disassociated Photosystem 2 units in the membrane would not be able to prevent photoinhibition, and monomeric Photosystem 2 units would be more susceptible to damaging treatments. Damaging conditions could then be interpreted as those which cause dissociation of PS2, resulting in disruption of the active $Cytb_{559}$ dimer, and subsequent damage to PS2 components. Heat and chilling treatments could have this effect through changes in the structure of the lipid bilayer surrounding photosystem 2 at higher or lower than "normal" temperatures.

There is evidence connecting the high potential form of the cytochrome with its physiological redox activity. It is possible that the high potential form exists only when the cytochrome exists as the proposed dimer in PS2 aggregates. In agreement with this are the observations of a change in the potential of the cytochrome from high to low following any detergent solubilisation of PS2 membranes in the isolation of PS2 complexes.

7.6.4. The composition of the monomeric (one haem) cytochrome b_{559}

Cramer *et al* (1986) present possible structural models for $Cytb_{559}$ in the membrane. Each of the α and the β subunits contain a twenty-five residue segment which are proposed to constitute a membrane-spanning helix in each subunit. Both subunits also contain a single histidine residue located five residues from the end of the proposed transmembrane helices. Haem binding requires ligation to two histidine residues. Therefore, these authors propose that the simplest model for cytochrome b_{559} is a tetramer comprising a dimer of two haem cross-linked polypeptide dimers. There are two possible arrangements of the tetramer - (1) a homodimer of two (α/β) heterodimers, or (2) a heterodimer comprising one (α/α) dimer and one (β/β) dimer. Arguments for both are presented.

These arrangements are proposed for the cytochrome in a functional oxygen-evolving PS2 complex *in vivo*. With the isolation of a minimal PS2 reaction centre containing one $Cytb_{559}$ per 4-5 Chl molecules, it is relevant to ask what is the monomeric form of $Cytb_{559}$ in this complex - either 50% of the (α/α) homodimer, and 50% of the (β/β) homodimer, or 100% of the (α/β) heterodimer? If it is a heterodimer of an α and a β subunit, there would be one population of identical and indistinguishable monomeric reaction centres. If the other alternative, then there should be two distinguishable pools of monomeric PS2 reaction centres, one containing an (α/α) dimeric Cyt b_{559}, the other containing a (β/β) dimer. These two pools would not be distinguishable by SDS-PAGE without previous separation. Size-exclusion chromatography might resolve these two populations, since they would differ in molecular weight by 10 kD, if the only difference was in the cytochrome. If separable in this way, then their different properties (composition, redox and electron transport properties) could then be investigated, as separate different units, and as a mixture of the two populations.

7.6.5. Photosystem 2 α and β centres

Heterogeneity in Photosystem 2 based on an analysis of chlorophyll fluorescence curves in the presence of the herbicide DCMU was first observed by Melis & Homann (1975). The biphasic rise in the fluorescence was interpreted in terms of two populations of Photosystem 2 differing in their degree of connectivity for energy transfer. One population, called PS2 "α" forms large arrays in the granal membranes, and excitation energy can be transferred between individual units in the array. The other population, called PS2 "β", is proposed to exist as separate units in the stromal membranes. These may be PS2 units undergoing enzymic repair of the D1 protein following damage by exposure to high light intensities. Heterogeneity in Photosystem 2 has been reviewed by

Black *et al* (1986). Here, I propose that the α centres are dimeric or more highly aggregated PS2 complexes, and the β centres are monomeric centres that are more susceptible to photodamage, as discussed above.

7.7. SUMMARY OF PROPOSED PROPERTIES OF THE MONOMERIC AND DIMERIC PHOTOSYSTEM 2 COMPLEX

Below, I present a summary table of the properties proposed for the monomeric and aggregated forms of Photosystem 2, discussed in the preceding sections.

monomer	**dimer**
- low frequency *in vivo*	- high frequency *in vivo*
- low oxygen evolution	- high oxygen evolution
- (a) two distinguishable Cyt b_{559} :	- HP and LP Cytb_{559}
$(\alpha)_2$ and $(\beta)_2$, or	- 1Cyt b_{559} : 2Pheo
(b) one Cyt b_{559} ($\alpha + \beta$).	- ?2Cyt b_{559} : P680
- susceptible to photoinhibition	- protected from photoinhibition
- correct estimation of [P680]	- underestimation of [P680]
- "β" PS2 centre	- "α" PS2 centre

7.8. FUTURE AREAS OF ENQUIRY

The spectroscopic analysis of bacterial pigment-protein complexes is easier than that of higher plant complexes, since the bacteriochlorophylls and bacteriopheophytins have a greater spectral range and wider separation of the energy levels than in the corresponding higher plant pigments. The absorption spectrum of the photosystem 2 reaction centre has only one distinguishable $Q_{y(0\text{-}0)}$ absorption band, which comprises the absorption of possibly six porphyrin pigments. Resolution of these overlapping bands for assignment to specific molecules will require more sophisticated computational analysis of the spectra, possibly by Fourier self-deconvolution, which is used to great effect in infrared spectroscopy.

As discussed above, the stoichiometric relationships of the different molecular components in Photosystem 2 are a source of some confusion. This is most likely a problem concerning techniques, and not due to inherent variability of samples. Techniques should be tested and standardised, so that results from different laboratories are directly comparable.

The relative amounts of the component proteins and cofactors in Photosystem2 preparations are not yet known. Accurate molecular weights of the D1/D2 complex in its various states of aggregation are yet to be measured (using for example the techniques of size exclusion chromatography and density gradient equilibrium ultracentrifugation), and related to the concentration of the other components. The quantitative determination of protein secondary structure from the UVCD data is not possible until this information is obtained.

The precise nature of the damage to photosystem 2 following exposure to light has not yet been revealed. Neither have the exact site of the initial damage, and the subsequent path(s) of the damage through components of PS2, yet been identified. The damage is generally thought (though not yet directly demonstrated) to originate from the highly oxidising potential of $P680^{+}$, which has been estimated to be greater than 1V. Experiments continue into the possible synergistic effects of light and heat in this process. The process might be expected to be dependent on oxygen, if formation of the P680 triplet state is involved. The oxygen-dependence has yet to fully characterised.

A recent study (Chapman *et al*, 1988) has shown that the isolated complex is more stable in detergents other than Triton X-100 (e.g. octyl-glucoside). The properties of these complexes will be investigated, and compared to those of less stable complexes. The reasons for the dependence of the particle's stability on the nature of the detergent are not known, but the existence of a more stable complex makes the prospect of making stable crystals of the D1/D2 complex for X-ray crystallographic analysis much more likely.

Although a great deal of information has accumulated concerning the PS2 reaction centre (pigment content and organisation, electron transport activity, photosensitivity and instability), our knowledge of this system is less than that for the bacterial reaction centre. This is due to the greater number of components and complexity of Photosystem 2, and the only recent isolation of a minimal reaction centre particle. Without doubt, the experiments conducted on the isolated reaction centre will increase our understanding of the larger core complex. Experiments on this larger system may reveal the path of excitation energy transfer from the core antenna polypeptides to the reaction centre. Of particular interest is the path of excitation energy transfer coupling the core antenna to the reaction centre. In bacterial systems, this is thought to involve a pigment absorbing at relatively low energy, denoted "B896", through which all excitations pass before exciting the reaction centre. It will be interesting to see whether this path is similar to that in purple bacterial photosynthesis, and whether general design features have been retained through evolution. Experiments continue in order to determine the extent of the structural similarities between the reaction centres of Photosystem 2 and purple bacteria.

REFERENCES

Abdourakhmanov, I.A., Ganago, A.O., Erokhin, Y.E. Solovev, A.A. & Chugunov, V.A. (1979) "Orientation and linear dichroism of the reaction centres from *Rhodopseudomonas sphaeroides*." *Biochim. Biophys. Acta* 546, 183-186.

Allen, J.P., Feher, G., Yeates, T.O., Komiya, Y. & Rees, D.C. (1987a) "Structure of the reaction centre from *Rhodopseudomonas sphaeroides* R-26: The cofactors." *Proc. Natl. Acad. Sci USA* 84, 5730-5734.

Allen, J.P., Feher, G., Yeates, T.O., Komiya, Y. & Rees, D.C. (1987b) "Structure of the reaction centre from *Rhodopseudomonas sphaeroides* R-26: The protein subunits." *Proc. Natl. Acad. Sci USA* 84, 6162-6166.

Alt, J., Morris, J., Westhoff, P. & Herrman, R.G. (1984) "Nucleotide sequence of the clustered genes for the 44kD chlorophyll *a* apoprotein and the '32 kD'-like protein of the photosystem II reaction centre in the spinach plastid chromosome." *Curr. Genet.* 7, 129-138.

Amesz, J. (ed.) (1987) New Comprehensive Biochemistry, Vol. 15, Photosynthesis. Elsevier, Amsterdam.

Andersson, B., Larsson, C., Jansson, C., Ljungberg, U. & Akerlund, H.-E. (1984) "Immunological studies on the organisation of proteins in photosynthetic oxygen evolution." *Biochim. Biophys. Acta* 766, 21-28.

Andersson, B. & Akerlund, H.-E. (1987) "Proteins of the oxygen-evolving complex." in Topics in Photosynthesis, Vol. 8, "The Light Reactions", Barber, J. ed., Elsevier, Amsterdam.

Argos, P. & Rao, J.K.M. (1986) "Prediction of protein structure." *Meth. Enzymol.* 130, 185-207.

Arnon, D.I. (1949) "Copper enzymes in isolated chloroplasts. Polyphenol oxidase in *Beta vulgaris*." *Pl. Physiol.* 24, 1-15.

Babcock, G.T., Widger, W.R., Cramer, W.A., Oertling, W.A. & Metz, J.G. (1985) "Ligands of chloroplast cytochrome b_{559} - identification and requirement for a heme cross-linked polypeptide structure." *Biochemistry* 24, 3638-3645.

Bakker, J.G.C., van Grondelle, R. & Den Hollander, W.T.F. (1983) " Trapping, loss and annihilation of excitations in a photosynthetic system. II. Experiments with the purple bacteria *Rhodospirillum rubrum* and *Rhodopseudomonas capsulata*." *Biochim. Biophys. Acta* 725, 508-518.

Barber, J. (ed.) (1987a) Topics in Photosynthesis, Vol. 8, "The Light Reactions". Elsevier, Amsterdam.

Barber, J. (1987b) "Composition, organisation, and dynamics of the thylakoid membrane in relation to its function." in: The Biochemistry of Plants, Vol.10, pp. 75-130, eds. M.D. Hatch & N.K. Boardman. Academic Press, New York.

Barber, J. (1987c) "Photosynthetic reaction centres: a common link." *Trends Biochem. Sci.* 12, 321-326.

Barber, J., Chapman, D.J. & Telfer, A. (1987) "Characterisation of a PS II reaction centre isolated from the chloroplasts of *Pisum sativum*." *FEBS Lett.* 220, 67-73.

Bassham, J.A. & Calvin, M. (1957) "The Path of Carbon in Photosynthesis." Prentice-Hall, Englewood Cliffs, New Jersey.

Bensasson, R. & Land, E.J. (1973) "Optical and kinetic properties of semireduced plastoquinone and ubiquinone electron acceptors in photosynthesis." *Biochim. Biophys. Acta* 325, 175-181.

Berthold, D.A., Babcock, G.T. and Yocum, C.F. (1981) "A highly resolved, oxygen-evolving photosystem 2 preparation from spinach thylakoid membranes." *FEBS Lett.* 134, 231-234.

Black, M.T., Brearley, T.H. & Horton, P. (1986) "Heterogeneity in chloroplast photosystem II." *Photosynth. Res.* 8, 193-207.

Blackman, F.F. (1905) "Optima and limiting factors." *Ann. Bot.* 19, 281-295.

Boltzmann, L. (1886) "Der zweite Hauptsatz der mechanischen Warmetheorie." Sitzungsber. Kaiserl. Akad. Wiss. Wien.

Boussac, A. & Etienne, A.L. (1982) "Midpoint potential of Signal II (slow) in Tris-washed Photosystem II particles." *Biochim. Biophys. Acta* 766, 576-581.

Breton, J. (1982) "Hypothesis - the 695nm fluorescence (F_{695}) of chloroplasts at low temperature is emitted from the primary acceptor of photosystem 2." *FEBS Lett.* 147, 16-20.

Breton, J. (1985) "Orientation of the chromophores in the reaction centre of *Rhodopseudomonas viridis*. Comparison of low-temperature linear dichroism spectra with a model derived from X-ray crystallography." *Biochim. Biophys. Acta* 810, 235-245.

Breton, J. & Vermeglio, A. (1982) "Orientation of photosynthetic pigments *in vivo*." In: Photosynthesis: Energy Conversion by Plants and Bacteria. (Govindjee, ed.) Academic Press, New York.

Breton, J. & Katoh, S. (1987) "Orientation of the pigments in Photosystem II: low-temperature linear-dichroism study of a core particle and of its chlorophyll-protein subunits isolated from *Synechococcus* sp." *Biochim. Biophys. Acta* 892, 99-107.

Breton, J. & Nabedryk, E. (1987) "Pigment and protein organisation of in reaction centre and antenna pigments." in: Topics in Photosynthesis, Vol. 8, The Light Reactions (Barber, J., ed.) Elsevier, Amsterdam.

Breton, J. & Duranton, J. (1988) "Orientation of the pigments in the reaction centre and the core antenna of photosystem II." in: "Photosynthetic Light-Harvesting Systems, Structure and Function" Scheer, H. & Scheider, S., eds., W. de Gruyter, West Berlin.

Bricker, T.M., Metz, J.G., Miles, D. & Sherman, L.A. (1983) "Biochemical chracterisation of a highly active oxygen-evolving Photosystem II preparation from maize." *Biochim. Biophys. Acta* 724, 447-455.

Brunisholz, R.A., Wiemken, V., Suter, F. & Bachofen, R. (1984) "The light-harvesting polypeptides of *Rhodospirillum rubrum*. 2. Localisation of the amino-terminal regions of the light-harvesting polypeptides B870-α and B870-β and the reaction centre subunit L at the cytoplasmic side of the photosynthetic membrane of Rhodospirillum rubrum G-9+." *Z. Physiol. Chem.* 365, 689-701.

Cameron, D.G. & Moffatt, D.J. (1987) "A generalised approach to derivative spectroscopy." *Appl. Spectrosc.* 41, 539-544.

Campbell, I.D. & Dwek, R.A. (1984) "Biological Spectroscopy" Benjamin / Cummings, Menlo Park, California.

Canaani, O.D. & Sauer, K. (1978) "Absorption and circular dichroism spectra of chloroplast membrane fragments from spinach, barley, and a barley mutant at room temperature and liquid nitrogen temperature." *Biochim. Biophys. Acta* 501, 545-551.

Cantor, C.R. & Schimmel, P.R. (1980) "Biophysical Chemistry" W.H.Freeman, New York.

Cantor, C.R. & Timasheff, S.N. (1982) "Optical Spectroscopy of Proteins." In: The Proteins (Neurath, H. & Hill, R.L., eds.) Academic Press, New York. pp. 380-385.

Chang, C.T., Wu, C.S.C. & Yang, J.T. (1978) "Circular dichroic analysis of protein conformation: inclusion of the β-turns." *Anal. Biochem.* 91, 13-31.

Chapman, D.J., Gounaris, K. & Barber, J. (1988) "Electron transport properties of the isolated D1-D2-cytochrome b_{559} photosystem II reaction centre." *Biochim. Biophys. Acta* 933, 423-431.

Chapman, D.J., Gounaris, K. & Barber, J. (1989) "The D1/D2/Cytochrome b_{559} photosystem two reaction centre from *Pisum sativum* L.: isolation, characterisation, and damage by light." *Photosynthetica* 29 (in press).

Chen, Y.H., Yang, J.T. & Martinez, H.M. (1972) "Determination of the secondary structure of proteins by circular dichroism and optical rotatory dispersion." *Biochemistry*, 11, 4120-4131.

Chen, Y.H., Yang, J.T. & Chau, K.H. (1974) "Determination of the helix and β form of proteins in aqueous solution by circular dichroism." *Biochemistry* 13, 3350-3359.

Chisholm, D. & Williams, J.G.K. (1988) Nucleotide sequence of psbC, the gene encoding the CP43 chlorophyll *a*-binding protein of photosystem II in the cyanobacterium *Synechocystis* 6803." *Pl. Mol. Biol.* 10, 293-301.

Clayton, R.K. (1963) "Toward the isolation of a photochemical reaction centre in *Rhodopseudomonas sphaeroides*." *Biochim. Biophys. Acta* 75, 312.

Clayton, R.K. (1980) "Photosynthesis : physical mechanisms and chemical patterns" Cambridge University Press.

Clayton, R.K. & Clayton, B.J. (1981) "B850 pigment-protein complex of *Rhodopseudomonas sphaeroides* - extinction coefficients, circular dichroism, and the reversible binding of bacteriochlorophyll." *Proc. Natl. Acad. Sci. USA* 78, 5583-5587

Clayton, R.K. & Sistrom, W.R. (eds.) (1978) "The Photosynthetic Bacteria." Plenum Press, New York.

Clayton, R.K. & Wang, R.T. (1971) "Photochemical reaction centres from *Rhodopseudomonas sphaeroides*." *Meth. Enzymol.* 23, 696-704.

Cogdell, R.J., Monger, T.G. & Parson, W. (1975) "Carotenoid triplet states in reaction centres from *Rhodopseudomonas sphaeroides* and *Rhodospirillum rubrum*." *Biochim. Biophys. Acta* 408, 189-199.

Cogdell, R.J., Parson, W.W. & Kerr, M.A. (1976) "The type, amount, location, and energy transfer properties of the carotenoid in reaction centres from *Rhodospeudomonas sphaeroides*." *Biochim. Biophys. Acta* 430, 83-93.

Cooley, J.W. & Tukey, J.W. (1965) "An algorithm for machine calculation of complex Fourier series." *Math. Comput.* 19, 297-301.

Cox, R.P. & Bendall, D.S. (1974) "Function of plastoquinone and β-carotene in Photosystem II of chloroplasts." Biochim. Biophys. Acta 347, 49-59.

Cramer, W.A., Theg, S.M. & Widger, W.R. (1986) "On the structure and function of cytochrome b_{559}." *Photosynth. Res.* 10, 393-404.

Cramer, W.A., Black, M.T., Widger, W.R. & Girvin, M.E. (1987) "Structure and function of photosynthetic cytochrome b-c_1 and b_6-f complexes." in: Barber, ed. (1987a)

Danielius, R.V., Satoh, K., van Kan, P.J.M., Plijter, J.J., Nuijs, A.M. & van Gorkom, H.J. (1987) "The primary reaction of photosystem II in the D1-D2-cytochrome b_{559} complex." *FEBS Lett.* 213, 241-244.

Debrunner, P.G., Schulz, C.E., Feher,G. & Okamura, M.Y. (1975) "Mossbauer study of reaction centres from *Rhodobacter sphaeroides*." *Biophys. Soc. Abstr.* 15, 226.

Debus, R.J., Feher, G. & Okamura, M.Y. (1986) "Iron-depleted reaction centres from *Rhodopseudomonas sphaeroides* R-26. I. Characterisation and reconstitution with Fe^{2+}, Mn^{2+}, Co^{2+}, Ni^{2+}, Cu^{2+}, and Zn^{2+}." *Biochemistry* 25, 2276-2287.

Debus, R.J., Barry, B.A., Babcock, G.T. & McIntosh, L. (1988a) "Site-directed mutagenesis identifies a tyrosine radical involved in photosynthetic oxygen-evolving system." *Proc. Natl. Acad. Sci. USA* 85, 427-430.

Debus, R.J., Barry, B.A., Sithole, I., Babcock, G.T. & McIntosh, L. (1988b) "Directed mutagenesis indicates that the donor to P_{680}^+ in photosystem 2 is tyrosine-161 of the D1 polypeptide." *Biochemistry* 27, 9071-9074.

Deisenhofer, J., Epp, O., Miki, K., Huber, R. & Michel, H. (1984) "X-ray structure analysis of a membrane protein complex: electron density map at 3Å resolution and a model of the chromophores of the photosynthetic reaction centre from *Rhodopseudomonas viridis*." *J. Mol. Biol.* 180, 385-398.

Deisenhofer, J., Epp, O., Miki, K., Huber, R. & Michel, H. (1985) "Structure of the protein subunits in the photosynthetic reaction centre of *Rhodopseudomonas viridis* at 3Å resolution." *Nature* 318, 618-624.

Den Hollander, W.T.F., Bakker, J.G.C. & van Grondelle (1983) "Trapping, loss and annihilation of excitations in a photosynthetic system. I. Theoretical aspects." *Biochim. Biophys. Acta* 725, 492-507.

DeVitry, C. & Diner, B.A. (1984) "Photoaffinity labelling of the azidoatrazine receptor site in reaction centres of *Rhodopseudomonas sphaeroides*." *FEBS Lett.* 167, 327-331.

Dismukes, G.C. & Siderer, Y. (1981) "EPR spectroscopic observations of a manganese centre associated with water oxidation in spinach chloroplasts." *FEBS Lett.* 121, 78-80.

Doring, G., Renger, G.L., Vater, J. & Witt, H.T. (1969) "Properties of photoactive chlorophyll a_{II} in photosynthesis." *Z. Naturforsch.* B24, 1139-1143.

Drake, A.F. (1986) "Polarisation modulation: the measurement of linear and circular dichroism." *J. Phys. E: Sci. Instrum.* 19, 170-181.

Dutton, P.L., Leigh, J.S. & Seibert, M. (1972) "Primary processes in photosynthesis: *in situ* electron spin resonance studies on the light-induced oxidised and triplet state of reaction centre bacteriochlorophyll." *Biochem. Biophys. Res. Commun.* 46, 406-413.

Dutton, P.L. & Leigh, J.S. (1973) "Electron spin resonance characterisation of *Chromatium vinosum*, strain D: hemes, non-heme irons, and the components involved in primary photochemistry." *Biochim. Biophys. Acta* 314, 178-190.

Dutton, P.L., Leigh, J.S. & Reed, D.W. (1973) "Primary events in the photosynthetic reaction centre from *Rhodopseudomonas sphaeroides*, strain R26. Triplet and oxidised states of bacteriochlorophyll and the identification of the primary electron acceptor." *Biochim. Biophys. Acta* 292, 654-664.

Dutton, P.L., Prince, R.C., Tiede, D.M., Petty, K.M., Kauffman, K.J.,, Netzel, T.L. & Rentzepina, P.M. (1977) "Electron transfer in the photosynthetic reaction centre." *Brookhaven Symp. Biol.* 28, 213-237.

Duysens, L.N.M. (1951) "Transfer of light energy within the pigment systems present in photosynthesising cells." *Nature* 168, 548-550.

Eccles, J., Honig, B. & Schulten, K. (1988) "Spectroscopic determinants in the reaction centre of Rhodopseudomonas sphaeroides." *Biophys. J.* 53, 137-144.

Edelman, M. & Reisfeld, A. (1980) "Synthesis, processing, and functional probing of P-32000, the major membrane-protein translated within the chloroplast." in Genome Organisation and Expression in Plants (C.J. Leaver, ed.) pp. 353-362, Plenum Press, New York.

Eisenberg, D., Weiss, R.M. & Terwilliger, T.C. (1982) "The helical hydrophobic moment - a measure of the amphiphilicity of a helix." *Nature* 299, 371-374.

Eisenberg, D., Schwarz, E., Komarony, M. & Wall, R. (1984) "Analysis of membrane and surface protein sequences with the hydrophobic moment plot." *J. Mol. Biol.* 179, 125-142.

Eisenberg, D. & McLachlan, A.D. (1986) "Solvation energy in protein folding and binding." *Nature* 319, 199-203.

Ellis, R.J. & Baraclough, R. (1978) "Synthesis and transport of chloropast proteins inside and outside the cell." in Chloroplast Development (G. Akoyunoglou & J.H. Argyroudi-Akoyunoglou, eds.) pp.185-194, Elsevier, Amsterdam.

Emerson, R. & Arnold, W.A. (1932a) "A separation of the reactions in photosynthesis by means of intermittent light." *J. Gen. Physiol.* 15, 391-420.

Emerson, R. & Arnold, W.A. (1932b) "The photochemical reaction in photosynthesis." *J. Gen. Physiol.* 16, 191-205.

Evans, M.C.W. & Ford, R.C. (1986) "Evidence for two tightly-bound iron-quinones in the electron-acceptor complex of Photosystem II." *FEBS Lett.* 195, 290-294.

Feher, G. (1971) "Some chemical and physical properties of a bacterial reaction centre particle and its primary photochemical reactants." *Photochem. Photobiol.* 14, 373-387.

Feher, G., Okamura, M.Y. & McElroy, J.D. (1972) "Identification of an electron acceptor in reaction centres of *Rhodopseudomonas sphaeroides* by EPR spectroscopy." *Biochim. Biophys. Acta* 267, 222-229.

Feher, G., Hoff, A.J., Isaacson, R.A. & McElroy, J.D. (1973) "Investigation of the electronic structure of the primary donor in bacterial photosynthesis by the ENDOR technique." *Biophys. J. Abstr.* 13, 61.

Feher, G., Hoff, A.J., Isaacson, R.A. & Ackerson, L.C. (1975) "ENDOR experiments on chlorophyll and bacteriochlorophyll *in vitro* and in the photosynthetic unit." *Ann. N.Y. Acad. Sci.* 244, 239-259.

Feher, G. & Okamura, M.Y. (1978) "Chemical composition and properties of reaction centres." in The Photosynthetic Bacteria (Clayton, R.K. & Sistrom, W.R., eds.) pp. 349-386, Plenum, New York.

Fujita, I., Davis, M.S. & Fajer, J. (1978) "Anion radicals of pheophytin and chlorophyll*a* - their role in primary charge separation of plant photosynthesis." *J. Am. Chem. Soc.* 100, 6280-6282.

Ganago, I.B., Klimov, V.V., Ganago, A.O., Shuvalov, V.A. & Erokhin, Yu. E. (1981) "Linear dichroism of absorption changes in photoreduction of pheophytin in oriented Photosystem II preparations." *Dokl. Akad. Nauk. SSSR* 263, 479-483.

Garewal, H.S. & Wasserman, A.R. (1974) "Triton X-100 - 4M Urea as an extraction medium for membrane proteins. I. Purification of chloroplast cytochrome b_{559}." *Biochemistry* 13, 4063-4071.

Gerwert, K., Hess, B., Michel, H. & Buchanan, S. (1988) "FTIR studies on cystals of photosynthetic reaction centres." *FEBS Lett.* 232, 303-307.

Ghanotakis, D.F. & Babcock, G.T. (1983) "Hydroxylamine as an inhibitor between Z and P680 in Photosystem II." *FEBS Lett.* 153, 231-234.

Gingras, G. & Jolchine, G. (1969) "Isolation of a P870-enriched particle from *Rhodospirillum rubrum.*" *Prog. in Photosynth. Res.* (H. Metzner, ed.) Vol. I, pp. 209-216. H. Laupp, Jr., Tubingen, Germany.

Gingras, G. (1978) "A comparative review of photochemical reaction centre preparations from photosynthetic bacteria." in: The Photosynthetic Bacteria, ed. Clayton, R.K. & Sistrom, W.R., pp. 387-396.

Gounaris, K., Pick, U. & Barber, J. (1987) "Stoichiometry and turnover of Photosystem 2 polypeptides." *FEBS Lett.* 21, 94-98.

Gounaris, K., Chapman, D.J. & Barber, J. (1988a) "The interaction between the 33 kDa manganese-stabilising protein and the D1/D2/ cytochrome b_{559} complex." *Biochim. Biophys. Acta* 234, 374-378.

Gounaris, K., Chapman, D.J. & Barber, J. (1988b) "Reconstitution of plastoquinone in the D1/D2/ cytochrome b_{559} photosystem II reaction centre complex." *FEBS Lett.* 240, 143-147.

Gouterman, M. (1961) "Spectra of porphyrins." *J. Mol. Spectrosc.* 6, 138-163.

Gouterman, M. & Stryer, L. (1962) "Fluorescence polarisation of some porphyrins." *J. Chem. Phys.* 37, 2260-2266.

Greenfield, N. Davidson, B. & Fasman, G.D. (1967) "Use of computed optical rotatory dispersion curves for the evaluation of protein conformation." *Biochemistry* 6, 1630-1635.

Greenfield, N. & Fasman, G.D. (1969) "Computed circular dichroism spectra for the evaluation of protein conformation." *Biochemistry* 8, 4108-4116.

Gregory, R.P.F., Demeter, S. & Faludi-Daniel, A. (1980) "Macromolecular organisation of chlorophyll *a* in aggregated chlorophyll *a/b* protein complex as shown by circular dichroism at room and cryogenic temperatures." *Biochim. Biophys. Acta* 591, 356-360.

Gulen, D., Knox, R. & Breton, J. (1986) "Optical effects of sodium dodecyl sulphate treatment of the isolated light-harvesting complex of higher plants." *Photosynth. Res.* 9, 13-20.

Halliwell, B. & Gutteridge, J.M.C. (1985) "Free radicals in biology and medicine" Oxford Science Publications, Oxford University Press.

Harada, N. & Nakanishi, K. (1983) "Circular Dichroic Spectroscopy - Exciton Coupling in Organic Stereochemistry." University Science Books, Oxford University Press.

Haworth, P., Tapie, P., Arntzen, C.J. & Breton, J. (1982a) "Orientation of pigments in the thylakoid membrane and in the isolated chlorophyll-protein complexes of higher plants. II. Linear dichroism spectra of isolated pigment-protein complexes oriented in polyacylamide gels at 300 and 100K." *Biochim. Biophys. Acta* 682, 152-159.

Haworth, P., Tapie, P., Arntzen, C.J. & Breton, J. (1982b) "Orientation of pigments in the thylakoid membrane and in the isolated chlorophyll-protein complexes of higher plants. IV. The 100K linear dichroism spectra of thylakoids from wild-type and chlorophyll *b*-less barley thylakoids." *Biochim. Biophys. Acta* 682, 504-506.

Hayashi, H., Nozawa, T., Hatono, M. & Morita (1981) "Circular dichroism of bacteriochlorophyll-a in light-harvesting bacteriochlorophyll complexes from *Chromatium vinosum*." *J. Biochem.* 89, 1853-1861.

Hearst, J.E. & Sauer, K. (1984) "Protein sequence homologies between positions of the L and M subunits of reaction centres of *Rhodopseudomonas capsulata* and the Q_b protein of chloroplast membranes: a proposed relation to quinone-binding sites." *Z. Naturforsch.* 39, 421-424.

Hermann, R.G., Alt, J., Schiller, B., Widger, W.R. & Cramer, W.A. (1984) "Nucleotide sequence of the gene for apocytochrome b_{559} on the spinach plastid chromosome." *FEBS Lett.* 176, 239-244.

Hill, R. & Scarisbrook, R. (1940) "Production of oxygen by isolated chloroplasts." *Nature* 146, 61-62.

Hill, R. & Bendall, F. (1960) "Function of the two cytochromes in chloroplasts: a working hypothesis." *Nature* 186, 136-137.

Hopfield, J.J. (1974) "Electron transfer between biological molecules by thermally activated tunneling." *Proc. Natl. Acad. Sci. USA* 71, 3640-3644.

Horton, P. & Croze, E. (1979) "Characterisation of two quenchers with different mid-point oxidation-reduction potentials in chloroplasts." *Biochim. Biophys. Acta* 545, 188-201.

Ikeuchi, M., Yuasa, M. and Inoue, Y. (1985) "Simple and discrete isolation of an O_2-evolving PS II reaction centre complex retaining Mn and the extrinsic 33 kDa protein." *FEBS Lett.* 185, 316-322.

Ikeuchi, M. & Inoue, Y. (1988) "A new photosystem II reaction centre component (4.8 kDa protein) encoded by chloroplast genome." *FEBS Lett.* 241, 99-104.

Jackson, J.B., Cogdell, R.J. & Crofts, A.R. (1973) "Some effects of o-phenanthroline on electron transport in chromatophores from photosynthetic bacteria." *Biochim. Biophys. Acta* 292, 218-225.

Jolchine, G. & Reiss-Husson, F. (1974) "Comparative studies on two reaction centre preparations from *Rhodopseudomonas sphaeroides* Y." *FEBS Lett.* 40, 5-8.

Juszczak, L., Geacintov, N.E., Zilinskas, B.A. & Breton, J. (1988) "Linear dichroism and orientation of pigments in phycobilisomes and their subunits." In: Photosynthetic Light-Harvesting Systems. Walter de Gruyter & Co., Berlin, New York.

Kasha, M. (1963) "Energy transfer mechanisms and the molecular exciton model for molecular aggregates." *Radiation Res.* 20, 55-65.

Kauppinen, J.K., Moffatt, Mantsch, H.H. & Cameron, D.G. (1981) "Fourier self-deconvolution: a method for resolving intrinsically overlapped bands." *Appl. Spectrosc.* 35, 271-276.

Ke, B. & Shuvalov, V.A. (1987) "Picosecond absorption spectroscopy in photosynthesis and primary electron transfer processes." in: Topics in Photosynthesis, Vol. 8 "The Light Reactions" Barber, J. (ed.) Elsevier, Amsterdam.

Kirmaier, C., Holten, D., Debus, R., Feher, G. & Okamura, M.Y. (1986) "Photochemistry of iron-depleted and zinc-reconstituted reaction centres from *Rhodopseudomonas sphaeroides.*" *Proc. Natl. Acad. Sci. USA* 83, 6407-6411.

Klein, P., Kanehisa, M. & DeLisi, C. (1985) "The detection and classification of membrane-spanning helices." *Biochim. Biophys. Acta* 815, 468-476.

Klevanik, A.V., Klimov, V.V., Shuvalov, V.A. & Krasnovskii, A.A. (1977) "Reduction of pheophytin in the light reaction of photosystem II of higher plants." *Dokl. Akad. Nauk. SSSR* 236, 241-244.

Klimov, V.V., Shuvalov, V.A., Krakhmaleva, I.N., Karapetyan, N.V. & Krasnovskii, A.A. (1976) "Changes in yield of fluorescence of bacteriochlorophyll in photoreduction of bacteriopheophytin in chromatophores of purple sulphur bacteria." *Biokhimiya* 41, 1435-1441.

Klimov, V.V., Shuvalov, V.A., Krakhmaleva, I.N., Klevanik, A.V. & Krasnovskii, A.A. (1977a) "Photoreduction of bacteriopheophytin b in the primary light reaction of the chromatophores of *Rhodopseudomonas viridis*." *Biokhimiya* 42, 519-530. (English translation, Plenum Publishing Corporation).

Klimov, V.V., Klevanik, A.V. & Shuvalov, V.A. (1977b) "Reduction of pheophytin in the primary light reaction of Photosystem II." *FEBS Lett.* 82, 183-186

Klimov, V.V., Allakhverdiev, S.I. & Pashchenko, V.Z. (1978) "Measurement of activation energy and lifetime of fluorescence of Photosystem II chlorophyll." *Dokl. Akad. Nauk. SSSR* 242, 1204-1207.

Klimov, V.V., Allakhverdiev, S.I., Demeter, Sh. & Krasnovskii, A.A. (1979a) "Pheophytin reduction in Photosystem II of chloroplasts in relation to oxidation-reduction potential of medium." *Dokl. Akad. Nauk. SSSR* 249, 227-230.

Klimov, V.V., Allakhverdiev, S.I. & Krasnovskii, A.A. (1979b) "EPR signal associated with pheophytin photoreduction in reaction centres of chloroplast Photosystem II." *Dokl. Akad. Nauk. SSSR* 249, 485-488.

Klimov, V.V., Dolan, E. & Ke, B. (1980a) "EPR properties of an intermediary electron acceptor (pheophytin) in Photosystem II reaction centres at cryogenic temperatures." *FEBS Lett.* 112, 97-100.

Klimov, V.V., Dolan, E., Shaw, E.R. & Ke, B. (1980b) "Interaction between the intermediary electron acceptor (pheophytin) and a possible plastoquinone-iron complex in Photosystem II reaction centres." *Proc. Natl. Acad. Sci. USA* 77, 7227-7231.

Klimov, V.V., Ke, B. & Dolan, E. (1980c) "Effect of photoreduction of the photosystem II intermediary electron acceptor (pheophytin) on the triplet state of carotenoids." *FEBS Lett.* 118, 123-126.

Knaff, D.B. & Kampf, C. (1987) "Substrate oxidation and NAD^+ reduction by phototrophic bacteria." in: Amesz, ed., (1987) pp. 199-212.

Kramer, H. & Mathis, P. (1980) "Quantum yield and rate of formation of the carotenoid triplet state in photosynthetic structures." *Biochim. Biophys. Acta* 593, 319-329.

Kyte, J. & Doolittle, R.F. (1982) "A simple method for displaying the hydrophobic character of a protein." *J. Mol. Biol.* 157, 105-132.

Laemmli, U.K. (1970) "Cleavage of structural proteins during the assembly of the bacteriophage T4." *Nature* 227, 680-685.

Leigh, J.S. & Dutton, P.L. (1974) "Reaction centre bacteriochlorophyll triplet states: redox potential dependence and kinetics." *Biochim. Biophys. Acta* 357, 67-77.

Lichtenhaler, H.K. (1987) "Chlorophylls and carotenoids: pigments of photosynthetic biomembranes." *Meth. Enzymol.* 148 (Packer, L. & Douce, R., eds.) pp 350-382.

Loach, P.A. & Walsh, K. (1969) "Quantum yield for the photoproduced electron paramagnetic resonance signal in chromatophores from *Rhodospirillum rubrum.*" *Biochemistry* 8, 1908.

Loach, P.A., Androes, G.M., Maksim, A.F. & Calvin, M. (1963) "Variation of electron paramagnetic resonance signals of photosynthetic systems with the redox level of their environment." *Photochem. Photobiol.* 2, 443-454.

MacKinney, G. (1941) "Absorption of light by chlorophyll solutions." *J. Biol. Chem.* 140, 315-322.

Manodori, A. & Melis, A. (1985) "Phycobilisome-photosystem II association in *Synechococcus* 6301." *FEBS Lett.* 181, 79-82.

Mantele, W., Nabedryk, E., Tavitian, B.A., Kreutz, W. & Breton, J. (1985) "Light-induced Fourier transform infrared (FTIR) spectroscopic investigations of the primary donor oxidation in bacterial photosynthesis." *FEBS Lett.* 187, 227-232.

Mantele, W., Wollenweber, A., Nabedryk, E., Breton, J., Rashwan, F., Heinze, J. & Kreutz, W. (1987) "Fourier transform infrared (FTIR) spectroelectrochemistry of bacterio-chlorophylls." in: *Progress in Photosynthesis Research*, Vol. I, (Biggins, J., ed.).

Mathis, P., Breton, J., Vermeglio, A. & Yates, M. (1976) "Orientation of the primary donor chlorophyll of Photosystem II in chloroplast membranes." *FEBS Lett.* 63, 171-173.

McCrea, P.D., Engelman, D.M. & Popot, J.L. (1988) "Topography of integral membrane proteins : hydrophobicity analysis vs. immunolocalisation." *Trends Biochem. Sci.* 13, 289-290.

McElroy, J.D., Feher, G. & Mauzerall, D. (1970) "Observation of a second light-induced EPR signal from reaction cantres of photosynthetic bacteria." *Biophys. Soc. Abstr.* 10, 204.

McElroy, J.D., Feher, G. & Mauzerall, D.C. (1972) " Characterisation of primary reactants in bacterial photosynthesis. I.Comparison of the light-induced signal (g=2.0026) with that of a bacteriochlorophyll radical." *Biochim. Biophys. Acta* 267, 363.

Meiburg, R.F. (1985) "Orientation of components and vectorial properties of photosynthetic reaction centres." Thesis, State University of Leiden, The Netherlands.

Melis, A. & Homann, P.H. (1975) "Kinetic analysis of the fluorescence induction in 3-(3,4-dichlorophenyl)-1,1-dimethylurea poisoned chloroplasts." *Photochem. Photobiol.* 21, 431-437.

Michel, H. & Deisenhofer, J. (1986) "X-ray diffraction studies on a crystalline bacterial photosynthetic reaction centre: A progress report and conclusions on the structure of photosystem II reaction centres." in Encycl. of Pl. Physiol., Vol. 19, (Staehelin, L.A. & Arntzen, C.J., eds.), pp. 371-381, Springer-Verlag, Berlin.

Michel, H., Epp, O. & Deisenhofer, J. (1986) "Pigment-protein interactions in the photosynthetic reaction centre from *Rhodopseudomonas viridis*." *EMBO J.* 5, 2445-2451.

Michel, H. & Deisenhofer, J. (1988) "Relevance of the photosynthetic reaction centre from purple bacteria to the structure of photosystem II." *Biochemistry* 27, 1-7.

Michel, H.P., Hunt, D.F., Shabanowitz, J. & Bennett, J. (1988) "Tandem mass spectrometry reveals that three photosystem II proteins of spinach chloroplasts contain N-acetyl-O-phosphothreonine at their NH_2 termini." *J. Biol. Chem.* 263, 1123-1130.

Michel-Beyerle, M.E., Plato, M., Deisenhofer, J., Michel, H., Bixon, M. & Jortner, J. (1988) "Unidirectionality of charge separation in reaction centres of photosynthetic bacteria." *Biochim. Biophys. Acta* 932, 52-70.

Millner, P.A., Gogel, G. & Barber, J. (1987) "Investigation of the spatial relationships between photosystem 2 polypeptides by reversible crosslinking and diagonal electrophoresis." *Photosynth. Res.* 13, 185-198.

Miyazaki, A., Shina, T., Toyoshima, Y., Gounaris, K. & Barber, J. (1989) "Stoichiometry of cytochrome b_{559} in photosystem 2." *Biochim. Biophys. Acta* (in press).

Morita, S., Hayashi, H., Miyazaki, T. & Takaichi, S. (1977) "Hyperchromicity of bacteriochlorophyll in organella of photosynthetic bacteria." *Pl. Cell Physiol.* 3, 97-99.

Morschel, E. & Schatz, H.G. (1987) "Correlation of photosystem-II complexes with exoplasmic freeze-fracture particles of thylakoids of the cyanobacterium *Synechococcus* sp." *Planta* 172, 145-154.

Morschel, E. & Schatz, H.G. (1988) "On the structure of photosystem II-phycobilisome complexes of cynobacteria." In:Photosynthetic Light-Harvesting Systems (Scheer, H. & Schneider, S., eds.) Walter de Gruyter & Co., Berlin.

Murata, N., Miyao, M. & Kuwabara, T. (1983) "Organisation of the photosynthetic oxygen evolution system. " In: Inoue, Y., Crofts, A.R., Govindjee, Murata, N., Renger, G. & Satoh, K. (eds.) The Oxygen Evolving System of Photosynthesis, pp. 213-222. Academic Press, Tokyo.

Murata, N., Miyao, M., Omata, T., Matsunami, H. & Kuwabara, T. (1984) "Stoichiometry of components in the photosynthetic oxygen-evolution system of Photosystem II particles prepared with Triton X-100 from spinach chloroplasts." *Biochim. Biophys. Acta* 765, 363-369.

Nabedryk, E., Tiede, D.M., Dutton, P.L. & Breton, J. (1982) "Conformation and orientation of the protein in the bacterial photosynthetic reaction centre." *Biochim. Biophys. Acta* 682, 273-280.

Nabedryk, E., Andrianambinintsoa, S. & Breton, J. (1984a) "Transmembrane orientation of α-helices in the thylakoid membrane and in the light-harvesting complex. A polarised infrared spectroscopic study." *Biochim. Biophys. Acta* 765, 380-387.

Nabedryk, E., Biaudet, P., Darr, S., Arntzen, C.J. & Breton, J. (1984b) "Conformation and orientation of chlorophyll-proteins in photosystem I by circular dichroism and polarised infrared spectroscopies." *Biochim. Biophys. Acta* 767, 640-647.

Nabedryk, E., Berger, G., Andrianambinintsoa, S. and Breton, J. (1985) "Comparison of α-helix orientation in the chromatophore, quantasome and reaction centre of *Rhodopseudomonas viridis* by circular dichroism and polarised infrared spectroscopy" *Biochim. Biophys. Acta* 809, 271-276.

Nabedryk, E., Mantele, W., Tavitian, B.A. & Breton, J. (1986) "Light-induced Fourier transform infrared spectroscopic investigations of the intermediary electron acceptor reduction in bacterial photosynthesis." *Photochem. Photobiol.* 43, 461-465.

Nakatani, H.Y. & Barber, J. (1977) "An improved method for isolating chloroplasts retaining their outer membranes." *Biochim. Biophys. Acta* 461, 510-512.

Nakatani, H.Y., Ke, B., Dolan, E. & Arntzen, C.J. (1984) "Identity of the photosystem 2 reaction centre polypeptide." *Biochim. Biophys. Acta* 765, 347-352.

Nanba, O. & Satoh, K. (1987) "Isolation of a photosystem II reaction centre containing D1 and D2 polypeptides and cytochrome b_{559}." *Proc. Natl. Acad. Sci. USA* 84, 109-112.

Netzell, T.L., Rentzepis, P.M. & Leigh, J.S. (1973) "Picosecond kinetics of reaction centres containing bacteriochlorophyll." *Science* 182, 238-241.

Newell, W.R., van Amerongen, H., van Grondelle, R., Drake, A.F., Udvarhelyi, P. & Barber, J. (1988) "Spectroscopic characterisation of the reaction centre of photosystem II from higher plants." *FEBS Lett.* 228, 162-166.

Norris, J.R., Uphaus, R.A., Crespi, H.L. & Katz, J.J. (1971) "Electron spin resonance of chlorophyll and the origin of signal II in photosynthesis." *Proc. Natl. Acad. Sci. USA* 68, 625-628.

Norris, J.R., Druyan, M.E. & Katz, J.J. (1973) "Electron nuclear double resonance of bacteriochlorophyll free radical *in vitro* and *in vivo*." *J. Am. Chem. Soc.* 95, 1680-1687.

Nugent, J.H.A., Diner, B.A. & Evans, M.C.W. (1981) "Direct detection of the electron-acceptor of Photosystem II - evidence that Q is an iron-quinone complex." *FEBS Lett.* 124, 241-244.

Ohno, T., Satoh, K. & Katoh, S. (1986) "Chemical composition of purified oxygen-evolving complexes from the thermophilic cyanobacterium Synechococcus sp." *Biochim. Biophys. Acta* 825, 1-8.

Okamura, M.Y., Isaacson, R.A. & Feher, G. (1975) "The primary acceptor in bacterial photosynthesis: Obligatory role of ubiquinone in photoactive reaction centres of *Rhodopseudomonas sphaeroides*." *Proc. Natl. Acad. Sci. USA* 72, 3491-3495.

Okamura, M.Y., Satoh, K., Isaacson, R.A. & Feher, G. (1987) "Evidence of the primary charge separation in the D1/D2 complex of photosystem II from spinach: EPR of the triplet state." In: *Progress in Photosynthesis Research* (Biggins, J., ed.) Vol. 1, pp. 379-381, Martinus Nijhoff publ., Dordrecht.

Okayama, S. & Butler, W.L. (1972) "Extraction and reconstitution of Photosystem II." *Plant Physiol.* 49, 769-774.

O'Malley, P.J. & Babcock, G.T. (1984) "Electron paramagnetic resonance properties of immobilised quinone cation radicals and the molecular origin of Signal II in spinach chloroplasts." *Biochim. Biophys. Acta* 765, 370-379.

Otten, H.A. (1971) "Absorption changes in the reaction centre of photosynthetic bacteria and π-electron calculations on bacteriochlorophyll, its mono cation and anion." *Photochem. Photobiol.* 14, 589-596.

Ovchinnikov, Y.A., Abdulaev, N.G., Zolotarev, A.S., Shmuckler, B.E., Zargarov, A.A., Kutuzov, M.A., Telezhinskaya, I.N., Levina, N.B. & (1988a) "Photosynthetic reaction centre of *Chloroflexus aurantiacus*: I. Primary structure of L-subunit." *FEBS Lett.* 231, 237-242.

Ovchinnikov, Y.A., Abdulaev, N.G., Shmuckler, B.E., Zargarov, A.A., Kutuzov, M.A., Telezhinskaya, I.N., Levina, N.B. & Zolotarev, A.S. (1988b) "Photosynthetic reaction centre of *Chloroflexus aurantiacus*: II. Primary structure of M-subunit." *FEBS Lett.* 232, 364-368.

Packham, N.K. & Barber, J. (1987) "Structural and functional comparison of anoxygenic and oxygenic organisms." in: Barber (1987a).

Parson, W.W. (1987) "The bacterial reaction centre." in: Photosynthesis, Amesz, J. (ed.)

Parson, W.W. & Monger, T.G. (1977) "Interrelationships among excited states in bacterial reaction centres." *Brookhaven Symp. Biol.* 28, 195-212.

Pearlstein, R.M. (1982) "Chlorophyll singlet excitons." in Photosynthesis: Energy Conversion by Bacteria and Plants (Govindjee, ed.) Academic Press, New York.

Petrouleas, V. & Diner, B.A. (1982) "Investigation of the iron components in Photosystem II by Mossbauer spectroscopy." *FEBS Lett.* 147, 111-114.

Pfister, K., Steinback, K.E., Gardner, G. & Arntzen, C.J. (1981) "Photoaffinity labelling of an herbicide receptor protein in chloroplast membranes." *Proc. Natl. Acad. Sci. USA* 78, 981-985.

Philipson, K.D. & Sauer, K. (1972) "Exciton interaction in a bacteriochlorophyll-protein from *Chloropseudomonas ethylica*. Absorption and circular dichroism at 77K." *Biochemistry* 11, 1880-1885.

Philipson, K.D. & Sauer, K. (1973) "Comparative study of circular dichroism spectra of reaction centres from several photosynthetic bacteria." *Biochemistry* 12, 535-539.

Pierson, B.K. & Olson, J.M. (1987) "Photosynthetic Bacteria." In "Photosynthesis", Amesz, J. (ed.), pp. 21-42.

Plijter, J.J. (1988) "Photosystem II and the oxygen-evolving complex." Thesis, State University of Leiden, The Netherlands.

Prince, R.C. (1988) "Tyrosine radicals." *Trends Biochem. Sci.* 13, 286-288.

Pucheu, N.L., Kerber, N.L. & Garcia, A.F. (1976) "Isolation and purification of the reaction centre from *Rhodopseudomonas viridis* NHTC 133 by means of LDAO." *Arch. Microbiol.* 109, 301-305.

Pulles, M.P.J., van Gorkom, H.J. & Verschoor, G.A.M. (1976) "Primary reactions of Photosystem II at low pH. 2. Light-induced changes of absorbance and electron-spin resonance in spinach chloroplasts." *Biochim. Biophys. Acta* 440, 98-106.

Raman, R. & Tollin, G. (1971) "Chloropyll one-electron photochemistry - flash-photolysis studies of chlorophyll-quinone reactions in pyridine." *Photochem. Photobiol.* 13, 135-145.

Rao, J.K.M. & Argos, P. (1986) "A conformational preference parameter to predict helices in integral membrane proteins." *Biochim. Biophys. Acta* 869, 197-214.

Rasmussen, O.F., Bookjans, G., Stummann, B.M. & Henningsen, K.W. (1984) "Localisation and nucleotide sequence of the gene for the membrane polypeptide D2 from pea chloroplast DNA." *Plant Mol. Biol.* 3, 191-199.

Reed, D.W. & Clayton, R.K. (1968) "Isolation of a reaction centre fraction from *Rhodopseudomonas sphaeroides*." *Biochem. Biophys. Res. Comm.* 30, 471-

Reed, D.W. & Ke, B. (1973) "Spectral properties of reaction centre preparations from *Rhodopseudomonas sphaeroides.*" *J. Biol. Chem.* 248, 3041-3045.

Reed, D.W. & Peters, G.A. (1977) "Characterisation of pigments in reaction centre preparations from Rhodopseudomonas sphaeroides." *J. Biol. Chem.* 247, 7148-7152.

Rich, P.R. & Moss, D.A. (1987) "The reactions of quinones in higher plant photosynthesis." in: Barber (1987a), pp.421-446.

Robinson, S.P. & Walker, D.A. (1981) "Photosynthetic carbon reduction cycle." in The Biochemistry of Plants, Vol. 8, eds. M.D. Hatch & N.K. Boardman, pp.193-236, Academic Press, New York.

Rochaix, J.-D., Dron, M., Rahire, M. & Malnoe, P. (1984) Sequence homology between the 32 kD and the D2 chloroplast membrane polypeptides of *Chlamydomonas reinhardtii.*" *Plant Mol. Biol.* 3, 363-370.

Rogner, M., Dekker, J.P., Boekema, E.J. & Witt, H.T. (1987) "Size, shape and mass of the oxygen-evolving complex from the thermophilic cyanobacterium *Synechococcus* sp." *FEBS Lett.* 219, 207-211.

Rosenfeld, L. (1928) "Quantenmechanische theorie der naturlichen optiscen aktivitat von flussigkeiten und gasen." *Z. Phys.* 52, 161-174.

Rutherford, A.W. (1985a) "How close is the analogy between the reaction centre of photosystem II and that of purple bacteria?" *Biochem. Soc. Trans.* 14, 15-17.

Rutherford, A.W. (1985b) "Orientation of EPR signals arising from components in Photosystem II membranes." *Biochim. Biophys. Acta* 807, 189-201.

Rutherford, A.W. & Heathcote, P. (1985) "Primary photochemistry in photosystem I." *Photosynth. Res.* 6, 295-316.

Sandusky, P.O., Selvius De Roo, C.L., Hicks, D.B., Yocum, C.F., Ghanotakis, D.F. & Babcock, G.T. (1983) in: The Oxygen-Evolving System of Photosynthesis (Inoue, Y., Crofts, A.R., Govindjee, Murata, N., Renger, G. & Satoh, K., eds.) pp.189-199. Academic Press, Tokyo.

Satoh, K. & Nanba, O. (1987) "Isolation of a photosystem II reaction centre consisting of γ and δ subunits (D-1 and D-2) and cytochrome b_{559}." *Progr. Photosynth. Res.* Biggins, J., ed., Vol. II, pp. 69-72, Martinus Nijhoff, Dordrecht, The Netherlands.

Sauer, K. (1975) "Primary events and the trapping of energy." In: Bioenergetics of Photosynthesis" ed. Govindjee. Academic Press, New York.

Sauer, K., Dratz, E.A. & Coyne, L. (1968) "Circular dichroism spectra and the molecular arrangement of bacteriochlorophylls in the reaction centers of photosynthetic bacteria." *Proc. Natl. Acad. Sci. USA* 61, 17-24.

Saxena, V.P. & Wetlaufer, D.B. (1971) "A new basis for interpreting circular dichroism spectra of proteins." *Proc. Natl. Acad. Sci. USA* 68, 969-972.

Sayre, R.T., Andersson, B. & Bogorad, L. (1986) "The topology of a membrane protein : the orientation of the 32kD Qb-binding chloroplast thylakoid membrane protein." *Cell* 47, 601-608.

Schatz, G.H. & Witt, H.T. (1984) "Extraction and characterisation of oxygen-evolving Photosystem II complexes from a thermophilic cyanobacterium *Synechococcus* sp." *Photobiochem. Photobiophys.* 7, 1-14.

Schellman, J. & Jensen, H.P. (1987) "Optical spectroscopy of oriented molecules." *Chem. Rev.* 87, 1359-1399.

Scherz, A. & Parson, W.W. (1984a) "Oligomers of bacteriochlorophyll and bacteriopheophytin with spectroscopic properties resembling those found in photosynthetic bacteria." *Biochim. Biophys. Acta* 766, 653-665.

Scherz, A. & Parson, W.W. (1984b) "Exciton interactions in dimers of bacteriochlorophyll and related molecules." *Biochim. Biophys. Acta* 766, 666-678.

Scherz, A., Brown, P., Greenberg, B.M., Marder, J.B. & Barber, J. (1989) "An analysis of the optical spectra of the isolated Photosystem II reaction centre indicates that the primary donor is probably a special pair of chlorophyll *a* molecules." Submitted to *Proc. Natl. Acad. Sci. USA.*

Selak, M.E., Koch-Whitmarsh, B.E. & Whitmarsh, J. (1984) *Adv. Photosyn. Res*, Sybesma, C., ed., pp. 493-496. Martinus Nijhoff / Dr. W. Junk, The Hague.

Shuvalov, V.A., Klimov, V.V., Krakhmaleva, I.N., Moskalenko, A.A. & Krasnovskii, A.A. (1976) "Photoconversion of bacteriopheophytin in reaction centres of *Rhodospirillum rubrum* and *Chromatium minutissimum.*" *Dokl. Akad. Nauk. SSSR* 227, 984-987. (English translation).

Shuvalov, V.A. & Asadov, A.A. (1978) "Organisation and interaction of pigment molecules in reaction centres of *Rhodopseudomonas viridis.*" *Dokl. Akad. Nauk. SSSR* 242, 1208-1211 (English translation).

Shuvalov, V.A. & Asadov, A.A. (1979) "Arrangement and interaction of pigment molecules in reaction centres of *Rhodopseudomonas viridis*. Photodichroism and circular dichroism of reaction centres at 100K." *Biochim. Biophys. Acta* 545, 296-308.

Sistrom, W.R. (1977) "Transfer of chromosomal genes mediated by plasmid R68.45 in *Rhodopseudomonas sphaeroides.*" *J. Bacteriol.* 131, 526-532.

Sistrom, W.R. & Clayton, R.K. (1964) "Studies on a mutant of *Rhodopseudomonas sphaeroides* unable to grow photosynthetically" *Biochim. Biophys. Acta* 88, 61-73.

Straley, S.C. & Clayton, R.K. (1973) "Extraction of oxidised bacteriochlorophyll from photosynthetic reaction centre particles." *Biochim. Biophys. Acta* 292, 685-691.

Surewicz, W.K. & Mantsch, H.M. (1988) "New insight into protein secondary structure from resolution-enhanced infrared spectra." *Biochim. Biophys. Acta* 952, 115-130.

Susi, H. & Byler, D.M, (1986) "Resolution-enhanced Fourier transform infrared spectroscopy of enzymes" *Meth. Enzymol.* 130, 290-311.

Tae, G.S., Black, M.T., Cramer, W.A., Vallon, O. & Bogorad, L. (1988) "Thylakoid membrane topography: transmembrane orientation of the chloroplast cytochrome b-559 psbE gene product." Biochemistry 27, 9075-9080.

Takahashi, Y., Hansson, O., Mathis, P. & Satoh, K. (1987) "Primary radical pair in the photosystem II reaction centre." *Biochim. Biophys. Acta* 893, 49-59.

Tang, X.-S. & Satoh, K. (1984) "Characterisation of a 47 kD chlorophyll-binding polypeptide (CP47) isolated from a photosystem 2 core complex." *Plant and Cell Physiol.* 25, 935-945.

Tapie, P., Haworth, P., Hervo, G. & Breton, J. (1982) "Orientation of pigments in the thylakoid membrane and in the isolated chlorophyll-protein complexes of higher plants. III. A quantitative comparison of the low-temperature linear dichroism spectra of thylakoids and isolated pigment-protein complexes." *Biochim. Biophys. Acta* 682, 339-344.

Tapie, P., Choquet, Y., Wollman, F.-A., Diner, B. & Breton, J. (1986) "Orientation of the pigments in Photosystem II: a low-temperature linear dichroism and polarised fluorescence emission study of chlorophyll-protein complexes isolated from *Chlamydomonas reinhardtii*." *Biochim. Biophys. Acta* 850, 156-161.

Tavitian, B.A., Nabedryk, E., Mantele, W. & Breton, J. (1986) "Light-induced Fourier transform infrared (FTIR) spectroscopic investigations of primary reactions in photosystem I and photosystem II." *FEBS Lett.* 201, 151-157.

Telfer, A., Barber, J. & Evans, M.C.W. (1988) "Oxidation-reduction potential dependence of reaction centre triplet formation in the isolated D1/D2/cytochrome b_{559} Photosystem II complex." *FEBS Lett.* 232, 209-213.

Thompson, L.K. & Brudvig, G.W. (1988) "Cytochrome b_{559} may function to protect photosystem II from photoinhibition." *Biochemistry* 27, 6653-6658.

Thurnauer, M.C., Katz., J.J. & Norris, J.R. (1975) "The triplet state in bacterial photosynthesis: possible mechanisms of the primary photo-act." *Proc. Natl. Acad. Sci. USA* 72, 3270-3274.

Tiede, D.M., Prince, R.C. & Dutton, P.L. (1976) "EPR and optical spectroscopic properties of the electron carrier intermediate between the reaction centre bacteriochlorophylls and the primary acceptor in *Chromatium vinosum.*" *Biochim. Biophys. Acta* 449, 447-467.

Tinoco, I. (1963) "The exciton contribution to the optical rotation of polymers." *Radiation Res.* 20, 133-139.

Trebst, A. (1986) "The topology of the plastoquinone and herbicide binding peptides of photosystem II in the thylakoid membrane." *Z. Naturforsch.* 41c, 240-245.

Uphaus, R.A., Norris, J.R. & Katz, J.J. (1975) "Triplet states in photosynthesis." *Biochem. Biophys. Res. Commun.* 61, 1057-1063.

Van Dorssen, R.J., Plijter, J.J., Dekker, J.P., den Ouden, A., Amesz, J. & van Gorkom, H.J. (1987a) "Spectroscopic properties of chloroplast grana membranes and of the core of Photosystem II." *Biochim. Biophys. Acta* 890,134-143.

Van Dorssen, R. Breton, J., Plijter, J.J., Satoh, K., van Gorkom, H.J. & Amesz, J. (1987b) "Spectroscopic properties of the reaction centre and of the 47 kDa chlorophyll protein of photosystem 2." *Biochim. Biophys. Acta* 893, 267-274.

Van Gorkom, H.J. (1974) "Identification of the reduced primary electron acceptor of Photosystem II as a bound semiquinone anion." *Biochim. Biophys. Acta* 347, 439-442.

Van Gorkom, H.J. (1985) "Electron transfer in photosystem II." *Photosynth. Res.* 6, 97-112.

Van Gorkom, H.J. (1987) "Evolution of Photosynthesis." In "Photosynthesis", Amesz, J. (ed.) pp. 343-350.

Van Grondelle, R. (1985) "Excitation energy transfer, trapping and annihilation in photosynthetic systems." *Biochim. Biophys. Acta* 811, 147-195.

Van Grondelle, R., Romijn, J.C. & Holmes, N.G. (1976) "Photoreduction of the long wavelength bacteriopheophytin in reaction centres and chromatophores of the photosynthetic bacterium *Chromatium vinosum* strain D." *FEBS Lett.* 72, 187-192.

Van Metter, R.L. (1977) "Excitation energy transfer in the light-harvesting chlorophyll *a/b* protein." *Biochim. Biophys. Acta* 462, 642-658.

Van Niel, C. B. (1941) "The bacterial photosyntheses and their importance for the general problem of photosynthesis." *Adv. Enzymol.* 1, 263-328.

Velthuys, B.R. (1987) "The photosystem II reaction centre." in Topics in Photosynthesis, Vol. 8, "The Light Reactions" Barber, J., ed., Elsevier, Amsterdam.

Velthuys, B.R. & Visser, J.W.M. (1975) "Reactivation of EPR Signal II in chloroplasts treated with reduced dichlorophenol-indophenol - evidence against a dark equilibrium between two oxidation states of the oxygen-evolving system." *FEBS Lett.* 55, 109-112.

Vermaas, W.F.J. (1989) "The structure and function of Photosystem II." in Techniques and New Developments in Photosynthesis Research (J. Barber, ed.) Plenum Press, in press.

Vermaas, W.F.J., Williams, J.G.K. & Arntzen, C.J. (1987) "Sequencing and modification of psbB, the gene encoding the CP47 protein of photosystem 2, in the cyanobacterium *Synechocystis* 6803." *Plant Mol. Biol.* 8, 317-326.

Vermaas, W.F.J., Rutherford, A.W. & Hansson, O. (1989) "Site-directed mutagenesis in photosystem II of the cyanobacterium *Synechocystis* sp. PCC 6803: Donor D is a tyrosyl residue in the D2 protein." *Proc. Natl. Acad. Sci. USA* (in press).

Vermeglio, A., Breton, J., Paillotin, G. & Cogdell, R. (1978) "Orientation of chromophores in reaction centres of *Rhodopseudomonas sphaeroides* - a photoselection study." *Biochim. Biophys. Acta* 501, 514-530.

Visser, J.W.M., Rijgersberg, C.P. & Gast, P. (1977) "Photooxidation of chlorophyll in spinach chloroplasts between 10K and 180K." *Biochim. Biophys. Acta* 460, 36-46.

Webber, A.N., Packman, L., Chapman, D.J., Barber, J. & Gray. J.C. (1989) "A fifth chloroplast-encoded polypeptide is present in the Photosystem II reaction centre complex." *FEBS Lett.* (in press).

Weiss, C. Jr. (1972) "The π electron structure and absorption spectra of chlorophylls in solution." *J. Mol. Spectrosc.* 44, 37-80.

Wellburn, A.R. & Lichtenhaler, H. (1984) "Formulae and program to determine total carotenoids and chlorophylls *a* and *b* of leaf extracts in different solvents." *Adv. Photosynth. Res.* (ed. Sybesma, C.) Vol.II, 9-12, Martinus Nijhoff, The Hague.

Williams, J.C., Steiner, L.A., Ogden, R.C., Simon, M.I. & Feher, G. (1983) "Primary structure of the M subunit of the reaction centre from *Rhodopseudomonas sphaeroides*." *Proc. Natl. Acad. Sci. USA* 80, 6505-6509.

Williams, J.C., Steiner, L.A., Feher, G. and Simon, M.I. (1984) "Primary structure of the L subunit of the reaction centre from *Rhodopseudomonas sphaeroides*." *Proc. Natl. Acad Sci. USA* 81, 7303-7307.

Williams, J.C., Steiner, L.A. &Feher, G. (1986) "Primary structure of the reaction centre from *Rhodopseudomonas sphaeroides*." *Proteins: Structure, Function and Genetics* 1, 312-325.

Wraight, C. (1977) "Electron acceptors of photosynthetic bacterial reaction centres. Direct observation of oscillatory behaviour suggesting two closely equivalent ubiquinones." *Biochim. Biophys. Acta* 459, 525-531.

Yamagishi, A. & Katoh, S. (1984) "A photoactive photosystem 2 reaction centre complex lacking a chlorophyll-binding 40 kD subunit from the thermophilic cyanobacterium *Synechococcus* sp." *Biochim. Biophys. Acta* 765, 118-124.

Yamagishi, A. & Katoh, S. (1985) "Further characterisation of the two photosystem 2 reaction centre complex preparations from the thermophilic cyanobacterium *Synechococcus* sp." *Biochim. Biophys. Acta* 807, 74-80.

Yamamoto, Y., Tabata, K., Isogai, Y., Nishimura, M., Okayama, S., Matsuura, K. & Itoh, S. (1984) "Quantitative analysis of membrane components in a highly active oxygen-evolving Photosystem II preparation from spinach chloroplasts." *Biochim. Biophys. Acta* 767, 493-500.

Yang, J.T., Wu, C.-S.C. & Martinez, H.M. (1986) "Calculation of protein conformation from circular dichroism." *Meth. Enzymol.* 130, pp. 208-269.

Yang, W.J., Griffiths, P.R., Byler, D.M. & Susi, H. (1985) "Protein conformation by infrared spectroscopy: resolution enhancement by Fourier self-deconvolution." *Appl. Spectrosc.* 39, 282-287.

Yeates, T.O., Komiya, H., Rees, D.C., Allen, J.P. & Feher, G. (1987) "Structure of the reaction centre from *Rhodopseudomonas sphaeroides* R-26: Membrane-protein interactions." *Proc. Natl. Acad. Sci USA* 84, 6438-6442.

Yeates, T.O., Komiya, H., Chirino, A., Rees, D.C., Allen, J.P. & Feher, G. (1988) "Structure of the reaction centre from *Rhodopseudomonas sphaeroides* R-26 and 2.4.1: Protein-cofactor (bacteriochlorophyll, bacteriopheophytin, and carotenoid) interactions." *Proc. Natl. Acad. Sci. USA* 85, 7993-7997.

Youvan, D.C., Bylina, E.J., Alberti, M., Begusch, H. & Hearst, J.E. (1984) "Nucleotide and deduced polypeptide sequences of the photosynthetic reaction centre, B870 antennae and flanking polypeptides from *Rhodopseudomonas capsulata.*" *Cell* 37, 949-957.

Zimmerman, J.L. & Rutherford, A.W. (1984) *Biochim. Biophys. Acta* 767, 160-167.

Zuber, H., Brunisholz, R. & Sidler, W. (1987) "Structure and function of light-harvesting pigment-protein complexes." In Amesz, J., ed. (1987).

Zurawski, G., Bohnert, H.J., Whitfeld, P.R. & Bottomley, W. (1982) "Nucleotide sequence of the gene for the M_r 32,000 thylakoid membrane protein from *Spinacia oleracea* and *Nictiana debneyi* predicts a totally conserved primary translation product of M_r 38,950." *Proc. Natl. Acad. Sci. USA* 79, 7699-7703.